

Copyright

by

JIN-YONG CHOI

2014

**The Dissertation Committee for JIN-YONG CHOI Certifies that this is the  
approved version of the following dissertation:**

**pH-Induced Flocculation/Deflocculation Process for Harvesting  
Microalgae from Water**

**Committee:**

---

Kerry A. Kinney, Co-Supervisor

---

Lynn E. Katz , Co-Supervisor

---

Desmond F. Lawler

---

Albert Frank Seibert

---

Halil Berberoglu

**pH-Induced Flocculation/Deflocculation Process for Harvesting  
Microalgae from Water**

**by**

**JIN-YONG CHOI, B.E.; M.S.E.**

**Dissertation**

Presented to the Faculty of the Graduate School of

The University of Texas at Austin

in Partial Fulfillment

of the Requirements

for the Degree of

**Doctor of Philosophy**

**The University of Texas at Austin**

**August 2014**

## **Dedication**

*To Sunmi Han, my wife and best friend,  
for her patient, support, and love*

## **Acknowledgements**

First and foremost, I would like to thank my advisors, Drs. Kerry Kinney and Lynn Katz. I cannot begin to recount all that I have learned from you; you have provided insight to look at from the details to the big picture of research, have impressed upon me your exuberance, brightness, and passion for both life and science, have touched a string in my heart by your endless care and support throughout my time at the University of Texas at Austin. All accomplishments that I have achieved would not have been possible without your help. I am forever indebted to you for the influence you have had on me during my time at UT.

I would like to thank the members of my PhD committee, Drs. Desmond Lawler, Halil Berberoglu, and Frank Seibert for their academic support, wonderful guidance, and thoughtful comments regarding my research. Their scientific advice and knowledge and expertise in engineering have added value on my research. Thank you.

I would like to thank Dr. Eric Chen his valuable perspective on field work and support from beginning to end of the pilot-scale work. Dr. Schonna Manning and her colleague and staff for sharing the ideas and providing algae for completion of this research work. I would like to thank Algae research team (EWRE) Allison Osborne, Aurore Mercelat, Altan Oezkan, and Fernando Almada for their friendship, all of the help, and the great conversations about research. I would like to thank Algae research team (CEM) Dr. Rhykka Connelly, Mr. Michael Werst, Mr. Bruce Morrison, and Dr. Robert

Pearsall for major support for the pilot-scale work through the use of equipment and cost-sharing with other projects.

Finally, I would like thank to my family (Sikyung Choi, Hosook Oh, Jungyou Choi, Sunmi Han, and Siyeon Choi), the people most important to me, for kindly love and support during my academic endeavors. I would like to thank my wife, Sunmi Han, for trust, patient, and many sacrifices. I promise her that I will keep in shape so that I can repay your love for good.

# **pH-Induced Flocculation/Deflocculation Process for Harvesting Microalgae from Water**

JIN-YONG CHOI, Ph.D.

The University of Texas at Austin, 2014

Supervisors: Kerry A. Kinney and Lynn E. Katz

Historically, the presence of microalgae (algae hereafter) in natural waters has been viewed as a nuisance due to its adverse impact on water quality. More recently, however, algae are being investigated as potential sources of biofuel and a range of natural products. These applications require the development of large-scale cultivation systems for mass production that include growth, harvesting, concentration, and product recovery components. While challenges still remain with respect to many of the processes involved in mass production, one of the most technically and economically challenging steps is harvesting the algae from dilute growth cultures, especially in systems where chemical additives are of concern either within the algae concentrate or the effluent water. For this reason, a pH-induced flocculation/deflocculation method using the hydroxides of alkali or alkaline earth metals (e.g., lime, caustic soda) is of particular interest for algae harvesting as Na, Ca and Mg are typically present in natural waters. The goal of this research was to determine the underlying mechanisms responsible for algae coagulation by magnesium and calcium and to evaluate the potential

of these mechanisms for harvesting algae for a range of synthetic and field source water chemistries.

In the first two phases of this research, the mechanisms for coagulation with magnesium and calcium were studied independently. A series of bench-scale experiments were designed to isolate the potential mechanisms of algae destabilization associated with each of these cations as a function of water chemistry, and microscopic analyses were performed to characterize the flocculated algae/precipitate mixtures. In the third phase of this research, removal of algae in field source waters was evaluated with respect to the underlying science elucidated in the previous phases.

The results indicate that the dominant algae destabilization mechanism associated with magnesium shifts from Mg adsorption/charge neutralization to  $\text{Mg}(\text{OH})_{2(\text{s})}$  precipitation-enhanced coagulation with increasing pH. Moreover, dissolved  $\text{Mg}^{2+}$  adsorption to the algae surface led to effective algae coagulation, while minimizing the mass of precipitated  $\text{Mg}(\text{OH})_{2(\text{s})}$ . For Ca, this research identified the importance of the nucleation process (heterogeneous vs. homogeneous nucleation) on algae removal efficiency. Heterogeneous nucleation is a key factor for optimizing algae removal; thus, the degree of oversaturation with respect to  $\text{CaCO}_{3(\text{s})}$  is a crucial operating parameter. This research demonstrated that the algae harvesting process using pH-induced flocculation/deflocculation method can be optimized for a wide range of source waters if the water chemistry (e.g. pH, ion concentration, alkalinity, ionic strength) is properly incorporated into the system design.

## Table of Contents

List of Tables .....	xii
List of Figures .....	xiii
Chapter 1: Introduction .....	1
1.1. Background .....	1
1.2. Problem Statement .....	4
1.3. Objectives .....	6
1.4. Approach .....	7
Chapter 2: Background .....	9
2.1. Introduction .....	9
2.2. Characteristics of algae .....	14
2.3. Algae destabilization mechanisms .....	18
2.3.1. Compression of the diffuse layer .....	19
2.3.2. Adsorption and Precipitation .....	21
2.3.2.1. Adsorption and Charge neutralization .....	22
2.3.2.2. Precipitation and sweep flocculation .....	25
2.3.3. Adsorption and interparticle bridging .....	27
2.4. pH induced Coagulation using hydroxide .....	29
2.5. Chemical reactions involving calcium and magnesium in water .....	32
2.6. Kinetics of precipitation reactions .....	36
2.6.1. Nucleation .....	36
2.6.2. Crystal growth .....	39
2.7. Factors affecting precipitation reactions .....	43
2.7.1. Saturation ratio .....	44
2.7.2. Ion activity ratio .....	45
2.7.3. pH .....	46
2.7.4. Type/concentration of foreign particles .....	47
2.7.5. Inhibitory species .....	48

2.8. Characteristics of reaction products .....	50
2.8.1. $\text{CaCO}_3(\text{s})$ .....	50
2.8.2. $\text{Mg}(\text{OH})_2(\text{s})$ .....	53
2.9. Summary .....	55
Chapter 3: Research Approach .....	58
3.1. Introduction .....	58
3.2. Experimental approach: The purpose of the different types of tests .....	60
Chapter 4: The role of magnesium on algae removal mechanisms and practical implications on algae harvesting process .....	67
4.1. Introduction .....	67
4.2. Materials and Methods .....	69
4.2.1. Preparation of the algae sample solution .....	69
4.2.2. Adsorption experiments .....	70
4.2.3. Jar tests .....	71
4.2.4. Deflocculation tests .....	73
4.2.5. Analytical methods .....	73
4.3. Results and discussion .....	75
4.3.1. Adsorption isotherms .....	75
4.3.2. Algae removal via heterocoagulation vs adsorption and/or precipitation .....	77
4.3.3. Algae removal via adsorption/ charge neutralization vs precipitation-enhanced coagulation .....	81
4.3.4. Deflocculation tests .....	92
4.4. Conclusions .....	94
Chapter 5: The role of calcium in harvesting algae in alkaline water .....	96
5.1. Introduction .....	96
5.2. Materials and Methods .....	99
5.2.1. Preparation of algae sample solutions .....	99
5.2.2. Adsorption experiments .....	100
5.2.3. Jar tests .....	101

5.2.4. Deflocculation tests.....	104
5.2.5. Analytical methods .....	104
5.3. Results and discussion .....	106
5.3.1. Adsorption isotherm.....	106
5.3.2. Algae Removal in Heterocoagulation Experiments.....	110
5.3.3. Algae Removal via Direct Addition of Calcium to Algae Slurries .....	113
5.3.4. Impacts of Homonucelation vs. Heterocoagulation.....	120
5.3.4.1. Effect of the mode of nucleation on algae removal .....	120
5.3.4.2. Effect of algae cell density on algae removal .....	132
5.3.4.3. Extensibility to a different algal species .....	134
5.3.5. Potential for acid deflocculation of algae flocculated with Ca	137
5.4. Conclusions.....	139
Chapter 6: Evaluation of pH Induced Flocculation for a Range of Source Waters	141
6.1. Introduction.....	141
6.2. Materials and Methods.....	143
6.2.1. Algae source waters .....	143
6.2.2. Jar tests.....	144
6.2.3. Pilot-scale tests.....	145
6.2.4. Analytical methods .....	147
6.3. Results and discussion .....	149
6.3.1. Examination of jar test results and strategies for process optimization .....	149
6.3.2. Examination of pilot-scale results and strategies for process optimization .....	163
6.4. Conclusions.....	167
Chapter 7: Conclusions.....	169
References.....	174

Vita 187

## List of Tables

Table 2-1	Comparison of algae harvesting technologies.....	11
Table 3-1	Experimental approach.....	60
Table 4-1	The concentrations of the major ions in the softened water .....	70
Table 4-2	EDX analysis of the flocculated solids before and after the deflocculation test .....	94
Table 5-1	Impact of atmospheric CO <sub>2</sub> exchange on algae removal and Ca <sup>2+</sup> removal for varying ion activity ratios ( $\{Ca^{2+}\}/\{CO_3^{2-}\}$ ). .....	104
Table 5-2	Langmuir parameters, q <sub>max</sub> and k <sub>a</sub> , obtained for two different ionic strength levels in solution .....	108
Table 5-3	Characteristics of two algal species studied in this research ( <i>Chlorella</i> sp. and <i>Scenedesmus</i> sp.). .....	136
Table 6-1	Algae species and site descriptions for the range of algae source water tested in this research. ....	144
Table 6-2	Characteristics of algae source waters from various sites .....	149
Table 6-3	Water parameters at pH 9.7 for two different synthetic waters tested in Chapter 5 and source water G.....	162
Table 6-4	Operating conditions and performance of pilot-scale tests for source waters D-G .....	164

## List of Figures

- Figure 2-1 Dry cell weight concentration and temperature profiles (on the left) and zeta potential profile (on the right) for 100 L outdoor cultivation of microalgae in a bag photobioreactor (Source: Danqueh et al., 2009).17
- Figure 2-2 Compression of the diffuse layer (dotted line) at high ionic strength. The particle is assumed to be negatively charged (Benjamin and Lawler, 2013). .....20
- Figure 2-3 Effect of solution ionic strength on the energy of interaction as one particle is approaching another (Benjamin and Lawler, 2013).....21
- Figure 2-4 Schematic diagram of charge neutralization for particle destabilization at two different particle concentrations (Benjamin and Lawler, 2013).24
- Figure 2-5 Schematic of a charge balance used in alkalinity calculations. “a” represents the sum of concentrations (meq/L) of strong base cations and “b” represents the sum of concentrations (meq/L) of strong acid anions. ....35
- Figure 2-6 Scanning electron microscopic images of  $\text{CaCO}_3(\text{s})$  formed for different lime doses and initial  $\text{Mg}^{2+}$  concentrations (A) 100 mg/L CaO, 0 mg/L  $\text{Mg}^{2+}$  (B) 100 mg/L CaO, 38 mg/L  $\text{Mg}^{2+}$  (C) 189 mg/L CaO, 0 mg/L  $\text{Mg}^{2+}$  (D) 189 mg/L CaO, 38 mg/L  $\text{Mg}^{2+}$  (Russell et. al., 2009) and transmission electron micrographs of nano-size magnesium hydroxides at different temperature (E) 20 °C (F) 40 °C (G) 60 °C (H) 80 °C (Wang et al., 2011). .....42
- Figure 2-7 Schematics of crystal habit of  $\text{CaCO}_3(\text{s})$  as a function of  $\text{Mg}^{2+}$  incorporation (Source: Folk, 1974).....53

Figure 3-1	Schematic diagram of potential mechanisms of algae destabilization	62
Figure 3-2	Schematic diagram of a series of batch reactor adsorption tests (e.g., adsorption kinetics, isotherms, and jar tests).	63
Figure 3-3	Schematic diagrams of a series of batch reactor jar test procedures (e.g., seeded test, unseeded test, and variable pH test). Typical jar test procedures were employed.	64
Figure 3-4	Schematic diagram of a series of batch reactor deflocculation tests. The variable pH test preceded the deflocculation test for the preparation of the sample solution.	66
Figure 4-1	Adsorption isotherms and Langmuir model fits of $Mg^{2+}$ sorption to <i>Scenedesmus</i> sp. at $pH = 9.6 \pm 1$ at varying ionic strength (0.01 M and 0.1 M). Langmuir isotherm model fits (solid lines) were obtained using non-linear regression.	76
Figure 4-2	Magnesium addition required to achieve an algae removal efficiency of 90% as a function of algae cell density. Dissolved magnesium ions and pre-precipitated $Mg(OH)_{2(s)}$ were added for unseeded and seeded tests, respectively. The pH of the sample solutions were maintained at 10.6 for all tests.	78
Figure 4-3	SEM images for preformed $Mg(OH)_{2(s)}$ precipitated solids (A), flocs in $Mg(OH)_{2(s)}$ seeded algae slurries (B, C), and $Mg(OH)_{2(s)}$ flocs formed within the algae slurry (unseeded tests) (D) for an algae cell density and pH of 0.26 g/L and 10.6, respectively. The quantity of $Mg^{2+}$ added in the unseeded tests was 25 mg/L (D). The amorphous structure of preformed $Mg(OH)_{2(s)}$ precipitated solids is evident in panels A, B, and C.	80

Figure 4-4	Algae removal as a function of pH for a range of initial $Mg^{2+}$ concentrations (25-200 mg/L as $Mg^{2+}$ ) and algae cell densities (A: 0.26 g/L, B: 0.64 g/L, C: 1.42 g/L) in unseeded algae slurries.....	82
Figure 4-5	Algae removal as a function of pH for initial $Mg^{2+}$ concentrations of 25 and 100 mg/L as $Mg^{2+}$ and algae cell densities (A: 0.26 g/L, B: 0.64 g/L, C: 1.42 g/L) in unseeded algae slurries.....	83
Figure 4-6	$Mg^{2+}$ removal (symbols) and Minteq model (lines) predicted removal (due to $Mg(OH)_{2(active)}$ precipitation) as a function of pH for a range of initial $Mg^{2+}$ concentrations and algae cell densities (A: 0.26 g/L, B: 0.64 g/L, C: 1.42 g/L). ....	84
Figure 4-7	$Mg^{2+}$ removal as a function of pH for low Mg percent removal and varying algae cell densities: (A) 0.26 g/L; (B) 0.64 g/L; (C) 1.42 g/L respectively. ....	86
Figure 4-8	SEM images for flocs under adsorption/charge neutralization (A, B) and precipitation-enhanced coagulation (C, D) for an algae cell density of 0.26 g/L and varied pH and initial $Mg^{2+}$ concentration: (A) pH 9.97, ionic strength adjusted with NaCl in the absence of $Mg^{2+}$ (B) pH 9.97, 25 mg/L as $Mg^{2+}$ (C) pH 10.6, 25 mg/L as $Mg^{2+}$ (D) pH 10.6, 200 mg/L as $Mg^{2+}$ . C-1 and D-1 are enlarged images of C and D, respectively. ....	89

Figure 4-9 Algae removal efficiency as a function  $Mg^{2+}$  consumption normalized by algae cell density. A range of initial  $Mg^{2+}$  concentrations (25-200 mg/L) and algae cell density (0.26, 0.64, and 1.42 g/L) were tested. To indicate the removal mechanism responsible for algae removal, open (adsorption) and close (precipitation) figures were sorted based on the mechanism transition zone at pH near 10. The dotted lines are only a guide to the eye, not theoretical curves.....90

Figure 4-10 Operating pH necessary to achieve target algae percent removals as a function of initial  $Mg^{2+}$  concentration for an algae cell density of 0.26 g/L .....91

Figure 4-11 SEM images for flocs before deflocculation (panel A) and after flocculation (panel B) for the flocculated solids generated from a solution containing an algae cell density of 0.26 g/L and initial  $Mg^{2+}$  concentration of 200 mg/L as  $Mg^{2+}$ . The pH of the algae concentrates were acidified from 10.6 to 7.5 by bubbling the  $CO_2$ . The cross marks indicate the spot on which EDX analyses were conducted.....93

Figure 5-1 Adsorption isotherms for calcium and magnesium at fixed pH of  $9.6 \pm 1$ . The experimental data (symbols) were fit to the Langmuir isotherm using non-linear regression.....107

Figure 5-2 Comparison of algae removal at constant ionic strength (0.01 M) and fixed pH ( $9.6 \pm 1$ ) in the absence of carbonate. The target ionic strength for each jar test was achieved only by the addition of NaCl and  $\text{CaCl}_2$  salts. 0.01 M  $\text{CaCl}_2$  is equivalent to 120 mg  $\text{Ca}^{2+}/\text{L}$ . The algae cell density was 0.5 g/L. For comparison, algae removal associated adsorption of  $\text{Mg}^{2+}$  described in Chapter 4 is embedded (initial  $\text{Mg}^{2+}$  concentration ranging from 50 to 100 mg/L as  $\text{Mg}^{2+}$  at algae cell density of 0.64 g/L at pH 9.7).....109

Figure 5-3 Effect of pH on algae removal efficiency for varying ionic strengths in solutions containing NaCl as the background electrolyte. Jar tests were conducted in a  $\text{CO}_2$  free glove box in the absence of calcium. Only NaCl was added to deionized water to adjust the target electrolyte concentration. The algae cell density was 0.5 g/L.....110

Figure 5-4 Effect of calcium carbonate dose (pre-precipitated  $\text{CaCO}_{3(s)}$ ) addition on algae removal efficiency for a range of algae cell densities (panel A). The pH of the solutions was maintained at 10.6. The image (panel B) represents the test results after sedimentation for an algae cell density of 2.0 g/L. “Raw” represents the untreated original solution and the numbers represent doses of 0, 7000, 14000, 28000, and 57000 mg  $\text{Ca}^{2+}/\text{L}$ , respectively from 1 to 5. ....112

Figure 5-5 Effect of Ca addition (dissolved  $\text{Ca}^{2+}$ ) on algae removal for a range of initial alkalinity (1.41, 3.0, 10.0 meq/L) and for (A) 0.5 g/L and (B) 1.0 g/L algae cell density. (C) Algae removal for 1.0 g/L algae cell density is plotted as a function of calcium consumed. The pH of the solutions was adjusted to 10.6 thus, *in situ* precipitation of  $\text{CaCO}_{3(s)}$  was allowed during the experiments.....114

Figure 5-6 Calcium consumption normalized by the amount of algae that has removed (settled) in unseeded experiments for varying ion activity ratios ( $\{\text{Ca}^{2+}\}/\{\text{CO}_3^{2-}\}$ ). The algae cell density was 1.0 g/L.....115

Figure 5-7 Impact of the degree of supersaturation on enhanced calcium removal in the presence of algae (algae cell density of 1.0 g/L). The percent difference plotted on the y-axis is the difference in removal of Ca in the presence and absence of algae. The supersaturation ratio with respect to  $\text{CaCO}_{3(s)}$  was calculated based on the initial calcium concentration and carbonate concentration at target pH 10.6.....118

Figure 5-8 Effect of pH on algae removal and  $\text{Ca}^{2+}$  removal for two different initial calcium ion concentrations, 120 mg/L as  $\text{Ca}^{2+}$  (A) and 320 mg/L as  $\text{Ca}^{2+}$  (B), respectively. Initial alkalinity was 3.0 meq/L for both tests. The algae cell density was 0.5 g/L.....122

Figure 5-9 Comparison of algae removal in the presence and absence of magnesium. Percent algae removal on the left axis and  $\text{Me}^{2+}$  ( $\text{Ca}^{2+}$  or  $\text{Mg}^{2+}$ ) removal on the right axis were plotted as a function of pH. Initial concentrations of calcium, magnesium, algae and alkalinity were 120, 100 mg/L (when present) and 3.0 meq/L, respectively. The algae cell density was 0.5 g/L.....123

- Figure 5-10 Effect of calcium on algae and magnesium removal. Percent algae removal on the left axis and  $Me^{2+}$  ( $Ca^{2+}$  or  $Mg^{2+}$ ) removal on the right axis were plotted as a function of pH. In the absence of calcium, initial concentrations of magnesium, alkalinity, and algae cell density were 100 mg/L, 0.98 meq/L, and 0.64 g/L, respectively. In the presence of calcium, initial concentrations of magnesium ion, calcium ion, initial alkalinity, and algae cell density were 100 mg/L, 120 mg/L, 3.0 meq/L, and 0.5 g/L, respectively. ....126
- Figure 5-11 Scanning electron microscopic (SEM) images of flocculated solids formed at the pH 9.7 (panel A-D) and 10.6 (panel E-H) during the variable pH tests. Initial concentration of calcium and initial alkalinity were 120 mg/L and 3.0 meq/L, respectively. ....129
- Figure 5-12 Effect of ionic strength on algae removal efficiency and percent  $Ca^{2+}$  removal. Algae removal efficiency (A) and percent calcium removal (B) at three levels of ionic strength were plotted as a function of supersaturation ratio. The experimental condition in the previous variable pH test (e.g., initial  $Ca^{2+}$  concentration of 120 mg/L as  $Ca^{2+}$  and 3.0 meq/L of alkalinity) was carried out in three levels of ionic strength of the solution. Initial activities of calcium and bicarbonate ions for all the cases of ionic strength were set equal. ....131
- Figure 5-13 Effect of algae cell density on algae removal. Percent  $Ca^{2+}$  removal (A) and algae removal efficiency (B) were plotted as a function of pH. The experimental condition in the previous variable pH test (e.g., initial  $Ca^{2+}$  concentration of 120 mg/L as  $Ca^{2+}$  and 3.0 meq/L of alkalinity) was carried out algae cell densities of 0.25, 0.5, 1.0, and 3.0 g/L. ....133

Figure 5-14 Effect of the modes of nucleation for  $\text{CaCO}_3(\text{s})$  on algae removal for the two common algae species, *Scenedesmus* sp. and *Chlorella* sp. Algae removal efficiency (A) and percent calcium removal (B) for two different algae species were plotted as a function of pH. Initial calcium ion concentration and initial alkalinity were 120 mg/L and 3.0 meq/L, respectively. Algae cell density was 0.5 g/L for two algae species. Colored and black lines are assigned to *Scenedesmus* sp. and *Chlorella* sp., respectively.....135

Figure 5-15 Effect of the initial water composition on the deflocculation process. Flocculated solids for a range of initial  $\text{Ca}^{2+}$  concentrations and pH of 10.6 were acidified to pH 6.0 by bubbling the  $\text{CO}_2$ . The error bars indicate the standard deviation calculated from each experiment (n=3). .....139

Figure 6-1 Schematic of the pilot-scale system for the algae harvesting process utilized in this research. Samples were collected from the incoming water (1), effluent (2), flocculated solids (3), and acidified algae concentrate (4) for analysis.....146

Figure 6-2 Pilot-scale units for harvesting algae from source water. Plate settlers (60° inclined) were used for effective solid/liquid separation. The range of operating feed flow rates were 0.2 – 1.0 gpm (A), 1.0 – 10 gph (B), and 1.0 – 5.0 gpm (C). .....146

Figure 6-3 Jar test results for a range of algae source waters. The pH was adjusted by the addition of lime or NaOH. ....150

Figure 6-4	Effect of Mg salt on the optimum pH for algae recovery for source water A (AlgaEternal). The Mg ion concentration was increased to 200 mg/L as Mg <sup>2+</sup> with supplementary salt addition prior to the Mg supplement jar test.....	152
Figure 6-5	Effect of pH on solid production in a synthetic water for an algae cell density of 0.26 g/L (from experiments presented in Chapter 4). Mg consumption was directly related to mass precipitated above pH 10.	153
Figure 6-6	Effect of pH on algae removal efficiency and percent metal ion removal for source water D (Hornsby). The increase in initial Ca <sup>2+</sup> concentration via the addition of lime was taken into account for the calculation of percent metal ion removal with the assumption of complete dissolution of lime. Mg removal tested in synthetics waters with similar water quality as water source D (initial Mg <sup>2+</sup> concentration: 50 mg/L, algae cell density: 0.64 g/L in Figure 4-4) is shown for comparison. The dotted line represents the model prediction for percent Mg <sup>2+</sup> removal due to precipitation as Mg(OH) <sub>2(s)</sub> active in Minteq for an initial Mg <sup>2+</sup> concentration of 43.7 mg/L.....	157
Figure 6-7	Effect of pH on algae removal efficiency and percent metal ion removal for source water G (CEM). The increase in initial Ca <sup>2+</sup> concentration via the addition of lime was taken into account for the calculation of percent metal ion removal with the assumption of complete dissolution of lime.....	161
Figure 6-8	Algae removal efficiency during the pilot-scale test. Time zero represents the time at which the first samples of influent and effluent were collected right after the reactor was filled up with treated water.	165

Figure 6-9 X-ray diffraction analysis to determine the chemical composition of precipitated solids before (algae-laden flocculated solids) and after deflocculation (inorganic solid residue) for source water G. CO<sub>2</sub> was bubbled through the flocculated solids until the target pH (6.0 – 6.5) was reached. ....167

## **Chapter 1: Introduction**

### **1.1.BACKGROUND**

Historically, the presence of algae in natural waters has been viewed as a nuisance. The adverse effects of algae are numerous and include eutrophication of surface waters, taste and odor problems, harmful algal toxins, and increased chlorine demand in drinking water plants. Treatment processes for the removal of algae from natural waters were designed to either prevent the formation of algal blooms or to remove algae from water for aesthetic or health related issues. More recently, however, algae are being produced for a variety of beneficial uses including animal feed, fertilizers, cosmetics, biodiesel, pigments or high-value bioactive compounds and nutraceuticals (Becker, 1986; Lee et al., 1998; Li et al., 2001; Banerjee et al., 2002; Khan et al., 2005; Chisti, 2007; Chen et al., 2008; Zamalloa et al., 2011). All of these benefits lead to a new definition of microalgae by Chisti (2007) as “sunlight-driven cell factories that convert carbon dioxide to potential biofuels, foods, feeds and high-value bioactives.”

The mass production of algae for commercial purposes requires optimization of each step in the process from growth of the algae through recovery of the components of interest. Harvesting the algae from either open pond systems or photobioreactors is one of the most technically and economically challenging steps for several reasons. Growth conditions typically yield dilute algae cell densities (less than 1 g/L in open systems and 3 g/L in closed bioreactors) which implies that a significant amount of water needs to be managed. According to a 2007 study by NREL, 16 to 120 trillion gallons of water

would need to be treated per year to yield an annual production of 60 billion gallons of biodiesel from algae biomass (e.g., 260-2000 liter water/liter biodiesel). The large range in water needs reflects the variation in productivity across different climates, growth systems, and water composition. More recently, an estimated fresh water requirement of 1,000 liters of freshwater per liter of algae biodiesel, with a range of 200-2,000 liters was reported (Vasudevan et al., 2012). Sustainable management of this volume of water presents one of the most significant challenges associated with large scale growth systems. In addition, the small size of microalgae typically used for oil production (e.g., 3 to 30  $\mu\text{m}$ ) presents additional challenges with respect to developing an economically feasible technology. Typical particle removal processes are often not technically or economically viable for these micron-sized particles. For instance, typical membrane filtration processes would be energy intensive for harvesting algae without significant pre-treatment. Due to their low density which is similar to water, metal coagulants (e.g., aluminum  $[\text{Al}_2(\text{SO}_4)_3]$  or iron  $[\text{FeCl}_3, \text{Fe}_2(\text{SO}_4)_3]$ ) or synthetic polymers could be employed. However, the coagulant metals or polymers will accumulate with the algae, and this can impact subsequent downstream processing and product value. Also, it is often desirable to prevent the algal cells from lysing during the harvesting process since releasing the cell contents could negatively impact product recovery. Finally, generating an algae concentrate that has properties consistent with downstream transport and processing must also be considered for full-scale design. For example, the concentrated algae slurry should have rheological properties conducive to pumping to downstream processing (Grima et al., 2003; Uduman et al., 2010). Electromechanical lysing of the

algae concentrate is less efficient as the conductivity of the solution containing algae increases, and oil extraction via a membrane process requires de-flocculated algae to prevent clogging.

A number of methods routinely utilized in water and wastewater treatment have been suggested for algae harvesting including centrifugation, filtration, chemical flocculation, flotation, gravity sedimentation, and electrophoresis. One attractive option for harvesting algae for commercial applications is a pH-induced flocculation and deflocculation process which utilizes Ca and/or Mg to coagulate the algae into a settleable mass. Features of this technology include: addition of the hydroxides of alkali or alkaline earth metals (e.g., lime, caustic soda) to induce particle destabilization and coagulation followed by flocculation, sedimentation, and acidification of both effluent and algae slurry concentrate to produce a homogeneous and pumpable algae concentrate and dischargeable effluent water. Traditionally, lime or caustic soda has been used to remove hardness in softening processes or to accomplish chemical clarification of wastewater. Such processes have been implemented successfully in large scale systems. In addition, pH adjustment using lime or caustic has been shown to effectively remove algae from suspensions for tertiary treatment applications (Folkman and Wachs, 1973; Friedman, 1977; Ayoub and Koopman, 1986; Elmaleh et al., 1996) as well as for algae harvesting applications (McCaousland et al., 1999; D'Souza et al., 2002; Knucky et al., 2006).

## 1.2. PROBLEM STATEMENT

The addition of lime or caustic soda to a natural water leads to precipitation of  $\text{CaCO}_3(\text{s})$  and  $\text{Mg}(\text{OH})_2(\text{s})$ . For both solids, increasing pH yields higher degrees of supersaturation; however, typically  $\text{CaCO}_3(\text{s})$  precipitates at lower pH than  $\text{Mg}(\text{OH})_2(\text{s})$ . Vandamme et al (2012) and Wu et al (2012) argued that charge neutralization and sweep flocculation are the primary mechanisms of algae flocculation, which is in a good agreement with the mechanisms proposed previously using other coagulation agents such as metal salts and polymers (Tenney et al., 1969; Edzwald and Wingler, 1990; Bernhardt and Clasen, 1991; Duan and Gregory, 2003). Recent investigations support the idea that  $\text{Mg}(\text{OH})_2(\text{s})$  precipitation is far more effective in algae removal than the formation of  $\text{CaCO}_3(\text{s})$  precipitates (Vandamme et al., 2012; Wu et al., 2012). It has been postulated that the large adsorptive surface area and positive superficial charge of the  $\text{Mg}(\text{OH})_2(\text{s})$  precipitate attracts negatively charged colloidal particles, including the  $\text{CaCO}_3(\text{s})$  flocs, thus inducing adsorption and agglomeration. This might explain the effective algae removal achieved when  $\text{Mg}(\text{OH})_2(\text{s})$  precipitation occurs (Semerjian and Ayoub, 2003). Moreover, the importance of  $\text{Mg}(\text{OH})_2(\text{s})$  highlights the charge neutralization component of this process as the surface charge of microalgae is typically negative, and  $\text{Mg}(\text{OH})_2(\text{s})$  has a more positive surface charge than calcite or aragonite at high pH values. Indeed, the pH of the point of zero charge for  $\text{Mg}(\text{OH})_2(\text{s})$  is 12.4 compared to 8-9 for calcite.

While the importance of  $\text{Mg}(\text{OH})_2(\text{s})$  for microalgae removal is evident in the literature, few studies have clearly elucidated the specific algae removal mechanisms associated with the dissolved magnesium ion and its solid phases as a function of pH,

algae concentration and Mg concentration. The impact of these variables is not only important for optimizing removal of algae, but also essential for minimizing the production of excess solid that is removed from solution along with the algae. Moreover, most algae suspensions contain both calcium and magnesium unless the growth medium is synthesized to specifically remove one or more of these ions. However, the specific role of calcium in algae removal is not yet clearly understood. Given that Ca is often present in natural waters at significantly higher concentrations than Mg and that  $\text{CaCO}_{3(s)}$  precipitation typically occurs at lower pH than  $\text{Mg(OH)}_{2(s)}$ , it is important to evaluate specific removal mechanisms for Ca as well.

A fundamental understanding of the algae removal mechanisms is essential if the design and operation of the process is to be optimized to meet site-specific water quality conditions and downstream requirements. The performance of algae harvesting processes in terms of algae removal efficiency, quality of effluent, and composition of algae slurry concentrates is a function of the operating mechanism responsible for algae removal during the harvesting process. Moreover, developing an effective harvesting process is highly interdependent on both upstream and downstream processes. Therefore, understanding the removal mechanisms during the algae harvesting process is critical to the success of the overall end to end process from algae growth to product recovery.

### **1.3.OBJECTIVES**

The primary goal of this research was to investigate the algae removal mechanisms associated with alkaline earth metals, calcium and magnesium, in the algae harvesting process. The scope of this research was narrowed to focus on one particular algae harvesting method, the pH-induced flocculation/deflocculation process. This research was divided into three phases to allow for a quantitative discussion of the role of calcium and magnesium in this process and the implications of the various algae removal mechanisms on the viability of the pH induced flocculation/deflocculation process for algae harvesting as well as overall biomass production. These three phases are:

- Phase I: Investigate the role of magnesium in the pH induced flocculation/deflocculation process in the absence of calcium
- Phase II: Investigate the role of calcium in the pH induced flocculation/deflocculation process in the absence of magnesium
- Phase III: Apply the mechanistic understanding of algae removal in the pH induced flocculation/deflocculation process to representative field source waters with varying water chemistries.

#### **1.4.APPROACH**

The role of calcium and magnesium in the algae harvesting process was studied independently (Phase I and II). A series of controlled batch reactor tests (e.g., adsorption tests, jar tests, deflocculation tests) were conducted to quantify algae removal, characterize precipitate formation, assess deflocculation potential and identify the mechanisms of algae removal. The microalgae, *Scenedesmus* sp., was used as a model species in this research, and a second species, *Chlorella* sp., was selected to validate that the results could be extended to a different algae system. Experimental conditions were designed to isolate several potential mechanisms of algae destabilization including: (1) heterocoagulation in which two dissimilar particles (e.g., algae and  $\text{CaCO}_{3(s)}$ ) are attracted to each other (2) adsorption and charge neutralization and (3) precipitation-enhanced coagulation. Tests were conducted in the presence and absence of carbonate, and in the presence and absence of Mg (for Phase II) to provide additional mechanistic insight into the systems. Microscopy and spectroscopy were used to characterize the algae-laden flocculated mixtures and deflocculated algae. The underlying science elucidated in Phases I and II was tested by evaluating performance of jar and pilot tests for a range of field source waters (Phase III).

The remainder of this dissertation is divided as follows: Chapter 2 contains general background regarding the characteristics of microalgae and particle destabilization mechanisms related to algae removal processes. This chapter also discusses the pH-induced coagulation process that utilizes lime or caustic soda in water and wastewater treatment and the characteristics of the common reaction products,

$\text{CaCO}_3(\text{s})$  and  $\text{Mg}(\text{OH})_2(\text{s})$ . Chapter 3 provides the rationale for the experimental approaches and the purpose of each of the experiments employed in this research. Chapter 4 and 5 present experimental results to delineate the role of magnesium and calcium in the algae removal process. Chapter 6 presents lab and pilot scale experimental results to verify the effectiveness of algae harvesting process mechanisms identified in previous chapters for a range of algae source waters. Finally, Chapter 7 outlines the conclusions of this work and provides recommendations for future work.

## Chapter 2: Background

### 2.1. INTRODUCTION

The present work focuses on microalgae which are microscopic (1 to 50  $\mu\text{m}$  in size) photosynthetic organisms that contain chlorophyll. Microalgae (hereafter referred to as algae in this study) have been a public concern for many years for a variety of reasons. Algae can have a significant impact on water quality, including the creation of unpleasant tastes and odors, the release of toxins from cyanobacteria and the formation of disinfection byproducts (DBPs) in drinking water treatment plants. Moreover, algae are known to interfere with water treatment processes by shortening filter run times, increasing coagulant demand, and even contributing to microbial re-growth in distribution systems (Suffet et al., 1995; Schmidt et al., 1998; Plummer and Edzwald, 2001). At municipal wastewater treatment plants, algae can increase the TSS and BOD levels in the effluent which can impact downstream pumps and receiving waters (Toms et al., 1975). More recently, algae have attracted positive attention for their potential to provide an alternative energy source and a range of valuable natural products (Greenwell et al., 2010). Regardless of whether algae are being removed from water to mitigate detrimental impacts or to generate valuable products, the separation of algae from water is of great concern.

A variety of methods have been developed to remove algae from aqueous solutions, as shown in Table 2-1. Many of these processes used extensively in water and wastewater treatment plants are being adapted for use in harvesting algae biomass to

recover valuable products. Successful algae harvesting can be accomplished through a variety of coagulation/flocculation methods. Each coagulation/flocculation method is often coupled to a downstream water treatment operation to yield more efficient solid/liquid separation than can be achieved in a single step process.

The objective of this study was to investigate a pH-induced flocculation process that is followed by sedimentation; this harvesting technology is hereafter referred to as the “*pH-induced flocculation/deflocculation process*”. Features of this technology include: addition of the hydroxides of alkali or alkaline earth metals (e.g., lime, caustic soda) to induce particle (i.e., algae) destabilization and coagulation/flocculation followed by sedimentation and acidification of the algae slurry concentrate to produce a homogeneous and pumpable algae concentrate. The effectiveness of this process is expected to be a function of various factors such as the characteristics of the algae being recovered and the composition of the water.

This chapter begins with an overview of algae characteristics that are relevant to assessing and optimizing treatability using chemical-induced flocculation. The potential coagulation mechanisms responsible for algae removal in these systems are then discussed. A brief discussion of chemical flocculation processes that rely on calcium and magnesium ions is provided. A summary of the relevant equilibrium reactions that drive Ca and Mg precipitation and a characterization of potential reaction products are also discussed.

Table 2-1 Comparison of algae harvesting technologies (MolinaGrima et al., 2003; Uduman et al., 2010; Greenwell et al., 2010; Pragya et al., 2013; Milledge and Heaven, 2013; Vandamme et al., 2013; Kim et al., 2013)

**Coagulation methods**

<b>Coagulation Method</b>	<b>Examples</b>	<b>Factors affecting efficiency</b>	<b>Salient features</b>	<b>Limitations</b>
Polymer	Natural and synthetic polymer; Cationic, anionic, and neutral polymer  Purifloc, Zetag 51, Chitosan	Molecular weight of polymer, pH and electrolyte concentration of the medium, Surface charge density, The total cell surface area, Charge density of flocculant	A number of types of polymer are commercially available  Effective for a wide range of algae species	High salinity may inhibit flocculation
Chemical flocculation	Ferric chloride (FeCl <sub>3</sub> ), Aluminum sulfate (Al <sub>2</sub> (SO <sub>4</sub> ) <sub>3</sub> ), Ferric sulfate (Fe <sub>2</sub> (SO <sub>4</sub> ) <sub>3</sub> )	pH of the solution, surface charge of the algae	Commonly used in water treatment	Risk of potential contamination of the biomass and medium  pH sensitive
pH-induced flocculation	NaOH Lime	pH of the solution, Ca and Mg ion concentrations	Simple pH adjustment; A wide range of source waters can be treated	Extreme pH may damage algae cells
Autoflocculation	Photosynthetic CO <sub>2</sub> depletion	pH of the solution, Phosphate concentration	Natural process, Environmentally friendly	May not be reliable

Table 2-1 continued.

<b>Coagulation Method</b>	<b>Examples</b>	<b>Factors affecting efficiency</b>	<b>Salient features</b>	<b>Limitations</b>
Electro coagulation	Sacrificial aluminium or iron electrodes	Current intensity, Power input, Potential difference, Surface area of plates, Distance between electrodes	Lower energy consumption in salt water	Increased temperature may damage the process, Negative effects of chlorine production, Electrodes need to be replaced periodically
Electrolytic flocculation		Power input, Distance between electrodes, Surface area of the electrodes, Numbers of electrodes	No flocculants are required; Does not involve the use of sacrificial electrodes	Cathodes are prone to fouling; Electrodes need to be replaced periodically
Ultrasound		Ingoing flow rate, Biomass concentration	Can be used to improve performance of other methods, A small footprint, No cell damage, Chemical free process	Limited demonstrated potential at field scale, High energy input and low separation efficiency

Table 2-1 continued.

**Separation techniques**

<b>Separation Techniques</b>	<b>Examples</b>	<b>Factors affecting efficiency</b>	<b>Salient features</b>	<b>Limitations</b>
Centrifugation	Disc-stack, Nozzle discharge, Decanter bowl, Hydrocyclones, Spiral plate	Exposure time (duration), Volume of medium	Can handle most types of algae, Commercially used for high-value algae product	Energy intensive, Cost-prohibitive for large scale use, Damage to cell structure
Sedimentation	Lamella separator, Sedimentation tank	Density of algae and floc; Sedimentation velocity	Implemented at large-scale; Simple and inexpensive process	The reliability is low without the addition of flocculants
Flotation	Dispersed air flotation, Dissolved air flotation, Electrolytic air flotation, Autoflotation, Electrolytic Flotation	Size of the bubble created, Size of the particles, Concentration of air, The diameter of the bubbles, Pressure of the air tank, recycling rate, Dissolved oxygen concentration (autoflotation)	Proven method at large scale, Suitable for harvesting small and unicellular algae	Oversized bubbles break up the floc, Energy intensity due to the high pressure required
Filtration	Packed bed filters, Tangential flow filtration, Membrane vacuum filter, Microstrainer, Filter press, Belt filter, Vibrating screen	Size of algae, Pore size of the filter; concentration of microalgae, Ionic strength, Colloidal fouling, Hydrodynamic condition, Concentration and properties of the algae	Minimal impact on water, A number of types of filter are commercially available, High separation efficiency	Continuous fouling and subsequent replacement

Table 2-1 continued.

<b>Separation Techniques</b>	<b>Examples</b>	<b>Factors affecting efficiency</b>	<b>Salient features</b>	<b>Limitations</b>
Magnetic separation	Use of magnetic particles and an external magnetic field	Applied pH, Composition of the culture medium (concentration of di- and trivalent ions)	The completion of algae harvesting within a few minutes	Regeneration of the magnetic particles can be species dependent, Emerging technology, Requires further research

## **2.2. CHARACTERISTICS OF ALGAE**

### **Algae characteristics relevant to destabilization**

There are over 50,000 types of algae that vary with respect to their growth conditions, shape, types of pigments in chloroplasts, and cellular type, *etc.* Three of these characteristics (morphology, surface charge, and density) are expected to have the greatest impact on the separation of algae from the water especially for processes that include coagulation/flocculation followed by sedimentation.

Cell morphology is characterized by the shape, size, and presence of appendages. Morphology is an initial algae feature that can be used to screen out non-viable harvesting options (e.g., standard membrane filtration is not appropriate for small algae with dimensions similar to bacterial dimensions). Similarly, cells with flagella can escape from flocs (Pieterse and Cloot, 1997). Also, close contact among cells can

be impeded by the presence of spinal appendages such as those found in *Scenedesmus* sp. and the diatom *Stephanodiscus* sp. (Bernhardt and Clasen, 1991).

Algae cell densities vary from 1070 to 1140 kg m<sup>-3</sup> (Edzwald and Wingler, 1990). This density range is a function of cell structure; diatoms are heavier than the other species as a result of their silica-rich hard outer wall while cyanobacteria cells can have a density less than water due to their ability to adjust the water content within their cells using gas vacuoles (John et al., 2002). While higher cell density is preferable for sedimentation processes, flotation is an option for cells with low density. The settling velocity of a particle in laminar flow regime is described by Stokes's law:

$$v_p = \left( \frac{d^2(\rho_s - \rho)g}{18\mu_c} \right) \quad (2-1)$$

where  $v_p$  is sedimentation velocity of the particle (m s<sup>-1</sup>),  $d$  is particle diameter (m),  $\rho_s$  is particle density (kg m<sup>-3</sup>),  $\rho$  is the density of the fluid (kg m<sup>-3</sup>),  $g$  is the acceleration due to gravity (m s<sup>-2</sup>) and  $\mu_c$  is the viscosity of the suspension (Ns m<sup>-2</sup>).

Although the assumptions used to develop Equation 2-1 limit its application to ideal dilute conditions, this equation is still useful for illustrating the impacts of particle density on sedimentation velocities. If an algae particle with a diameter of 30 µm diameter and density of 1200 kg m<sup>-3</sup> is in water, the settling velocity would be 0.35 m hr<sup>-1</sup>. These calculations are consistent with observations that microalgae do not typically settle fast enough to be removed in a typical flow through treatment processes

(e.g., up to 4-6 hours). Modification of particle density ( $\rho_s$ ) or particle diameter resulting from interactions between particles (e.g., algae-algae and/or algae-inorganic precipitates) increases the settling velocity which could enhance the efficiency of the sedimentation process. By adding chemicals that assist in particle destabilization, growth in particle size can lead to significant removal of algae from solution (Elmaleh et al., 1996; Wyatt et al., 2011).

Algae cells carry a net negative surface charge as do many other particles encountered in water and wastewater treatment systems. Electrostatic effects resulting from repulsive forces between algae cells and interactions between cells and surrounding water contribute to the stability of algae suspensions (Tenney et al., 1969). In general, the isoelectric point of algae species (i.e., the pH at which the surface carries no net electrical charge as a result of interactions with other ions in addition to protons and hydroxide ions) occurs at approximately pH 3-4 (Stumm and Morgan, 1996; Liu et al., 1999; Clasen et al., 2000; Phoochinda and White, 2003). In other words, most algae cells exhibit a negative charge under the conditions encountered in natural water sources. This arises as a result of the dissociation of functional groups at the cell surface, particularly carboxylic acid groups (Northcote et al., 1958). The presence of extracellular organic molecules (EOM) attached at the cell surface can also yield a negative charge (Bernhardt et al., 1985). More negative charges are observed at higher pH due to the contribution of amino groups which have pKa values between 9 and 11 (Lehninger, 1970). Moreover, the degree of charge on the algae surface varies with algae growth phase. Edzwald and Wingler (1990) measured less negative values

(from -19.6 to -17.4mV) when *Chlorella vulgaris* transitioned from log growth phase to stationary phase. Konno (1993) also measured the zeta potential of the diatom *Nitzschia* during the initial growth phase, (-30mV), the log growth phase (-35mV), and the stationary phase (-28mV). Henderson et al (2008) collected zeta potential measurements during their coagulation tests, and initial testing solutions were taken periodically to minimize the effect of growth phase on the efficiency of the process. Figure 2-1 shows the zeta potential profile determined by Danquah et al (2009). The zeta potential trends they observed are in good agreement with previous studies.

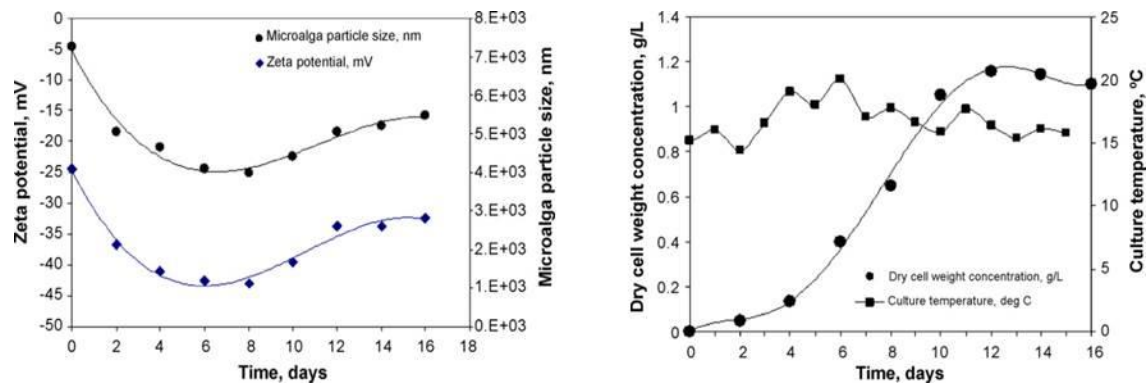


Figure 2-1 Dry cell weight concentration and temperature profiles (on the left) and zeta potential profile (on the right) for 100 L outdoor cultivation of microalgae in a bag photobioreactor (Source: Danquah et al., 2009).

Algae, like other microorganisms, secrete extracellular polymeric substances (EPS) that are composed of different substances including protein, nucleic acids, lipids, carbohydrates and small molecules of many different kinds (Myklestad, 1995). EPS can form multiple complexes with many heavy metal ions (Selck et al., 1999). In addition,

divalent cations, such as  $\text{Ca}^{2+}$  and  $\text{Mg}^{2+}$  bound to the negatively charged EPS can form a cation bridge between the negatively charged sites which improves bioflocculation (Higgins and Novak, 1997). EPS is assumed to be responsible for the spontaneous bioflocculation observed during natural algal blooms (Vandamme et al., 2013). However, the underlying mechanism is poorly understood and additional research is needed to optimize this additive-free method of algae flocculation (Vandamme et al., 2013).

### **2.3. ALGAE DESTABILIZATION MECHANISMS**

Previous research has shown that coagulation and algae removal is effectively achieved using coagulants such as alum (Jiang et al., 1993), ferric chloride (Jun et al., 2001), cationic polymers (Tenney et al., 1969), and chitosan (Divakaran and Pillai, 2002). However, several problems also have been reported in the application of this treatment scheme for algae removal. For instance, the high salinity of a marine environment can inhibit flocculation by polymers (Bilanovic et al., 1988) for marine algae growth systems. Also, metal salts can cause cell lysis, which may render this approach inappropriate in some cases (Papazi et al., 2010). In addition to the use of metal salts and polymers, pH adjustment using lime or caustic soda (and subsequent precipitation of  $\text{CaCO}_{3(s)}$  and/or  $\text{Mg(OH)}_{2(s)}$ ) has been shown to effectively remove algae from suspensions in tertiary treatment (Folkman and Wachs, 1973; Friedman, 1977; Ayoub and Koopman, 1986; Elmaleh et al., 1996) and during the production of algae biomass (McCaousland et al., 1999; D'Souza et al., 2002; Knucky et al., 2006).

The mechanisms of particle destabilization for algae depend on the type and dose of coagulant used and the cause of algae stability. Edzwald (1993) explained the stability of suspended particles, including algae, by (1) electrostatic repulsive forces between similarly charged particles, (2) steric effects caused by adsorption of molecules such as humic substances or extracellular organic matter (EOM) on the surface of particles, and (3) hydrophilic effects as a result of adsorbed water on the surface of particles. Successful algae harvesting efforts depend initially on destabilizing the algae particles to allow subsequent aggregation and floc formation. Sedimentation is often employed to remove the flocs formed. This section reviews possible algae destabilization mechanisms.

### **2.3.1. Compression of the diffuse layer**

Particle destabilization via *compression of the diffuse layer* surrounding algae particles is illustrated in Figure 2-2. As the ionic strength of a solution increases, the diffuse layer of the particle is compressed which reduces the distance over which repulsion between the particles extends. According to DLVO theory (named after the Russian scientists B. Derjaguin and L. Landau, and Dutch scientists E. Verwey and J. Overbeek), compression of the double layer leads to a sufficient reduction in the repulsive forces between particles such that the attractive forces dominate and particle aggregation occurs; in other words, the energy barrier for particles to aggregate is reduced (Verwey and Overbeek, 1947). The reduction in the energy barrier with increasing ionic strength of a solution is schematically described in Figure 2-3. This

mechanism may not be practical for harvesting algae from natural waters where ionic strength adjustment is often impractical. However, a variety of water sources (e.g., fresh, brackish, salt) are expected to be encountered in the algae harvesting processes; thus, the ionic strength of the source water itself is an important parameter that is expected to affect algae harvesting processes. In addition, precipitation reactions can be catalyzed or increased in solutions of higher ionic strength (Bischoff, 1968; Zhang and Dawe, 1998; Zuddas and Mucci, 1998).

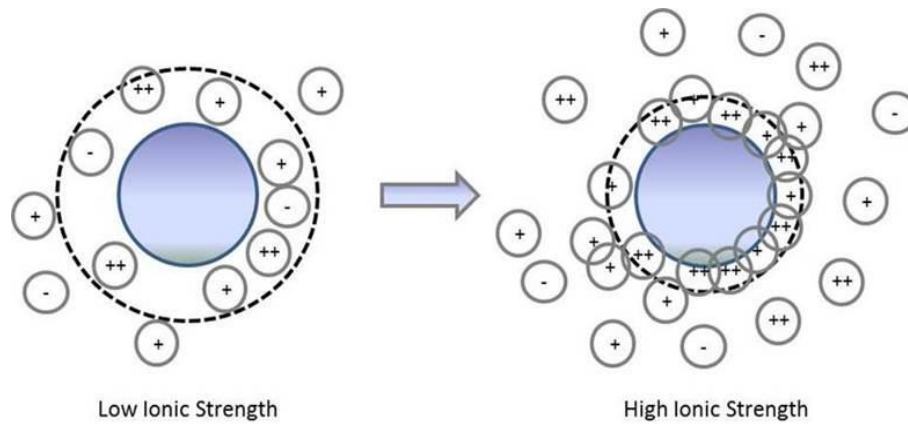


Figure 2-2 Compression of the diffuse layer (dotted line) at high ionic strength. The particle is assumed to be negatively charged (Benjamin and Lawler, 2013).

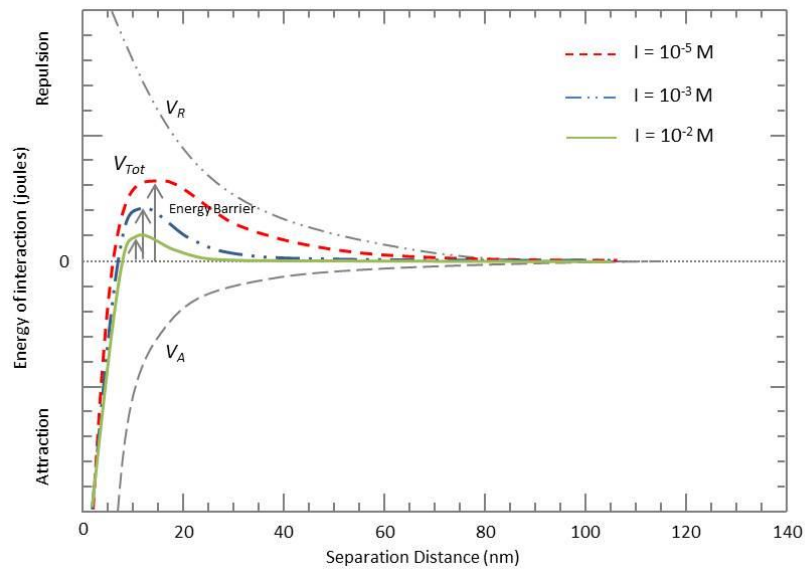


Figure 2-3 Effect of solution ionic strength on the energy of interaction as one particle is approaching another (Benjamin and Lawler, 2013)

### 2.3.2. Adsorption and Precipitation

Particles typically encountered in water and wastewater treatment plants are negatively charged, including algae. These particles can be destabilized by the accumulation of either ions of opposite charge that are dissolved in the water or through interaction with positively charged surfaces in the water.

The first of these mechanisms is referred to as *adsorption and charge neutralization*. The second mechanism for coagulation of particles is often induced in engineered systems by exceeding the solubility of constituent or added ions in solution and is commonly referred to as *precipitation and sweep flocculation* because sufficient particles are generated to ensure that the negatively charged particles are attracted to and

fully entrained or enmeshed within the newly formed solid phase. These mechanisms can occur simultaneously and/or dominate over the other depending on the specific coagulant selected and operating conditions such as pH, chemical dose, and source water composition.

#### **2.3.2.1. Adsorption and Charge neutralization**

Adsorption of ions of opposite charge onto particles can be induced physically (electrostatic force), chemically (covalent forces, surface complexation), or via hydrophobic interactions for molecules that prefer to attach onto the surface rather than remain in the bulk aqueous solution. Algae have been investigated in the past as potential biosorbents to remove heavy metals from solution due to their low cost, high adsorption capacity, and the fact that they do not generate secondary pollution (Tsezos et al., 1988; Trujillo et al., 1991). The principle mechanism of metallic cation sequestration involves the formation of complexes between a metal ion and functional group present on the surface or inside the porous structure of biological materials (Fourest and Volesky, 1997). Folsom et al (1986) suggested that relatively weak electrostatic bonding exhibited by alkali and alkaline earth metals and stronger coordination bonding for certain transition metals can be responsible for the metal interactions with algae. Adsorption of alkali, alkaline earth, and transition metal ions on algae by electrostatic attraction to negative sites was quantitatively represented via the Langmuir adsorption isotherm (Crist et al., 1988). Thus, if sufficient positively charged metal ions are

adsorbed to the negatively charged algae surface, electrostatic repulsion can be reduced and destabilized particles can aggregate with each other.

Ives (1959) first suggested that coagulation of algae can be achieved by charge neutralization in processes that utilize iron or aluminum salts as chemical agents. Also, the chemical requirements for charge neutralization and effective coagulation can be determined based on algae concentration, size, and surface charge density. Effective charge neutralization occurs when the cationic hydrolysis products of aluminum or iron react with the negatively charged surface of the algae and are able to destabilize the algae particles (Bernhardt and Clasen 1994). In addition to the addition of aluminum and iron salts, effective charge neutralization has been observed in electro-coagulation-flocculation (ECF) processes that used aluminum or iron anodes (Gao et al., 2010, Vandamme et al., 2011). Similar results were obtained in our laboratories using iron anodes.

Since the initial concentration of metal ions is an important driving force for adsorption onto an adsorbent, the charge neutralization mechanism for particle destabilization is often observed in the coagulation processes in which abundant metallic cations are available as a result of chemical addition. A stoichiometric relationship has been observed between algae or microorganism concentration and coagulant dose required for charge neutralization (Tenney and Stumm, 1965; Tilton et al., 1972). This relationship has been the basis for explaining algae removal via the adsorption and charge neutralization mechanism. For instance, Wyatt et al (2011) posited charge neutralization

as the algae removal mechanism after they observed that the amount of  $\text{FeCl}_3$  required for effective coagulation increases linearly with increasing algae cell concentration.

In Figure 2-4, surface charge density and fraction remaining are plotted as a function of dose of destabilizing chemical for two different particle concentrations. High removal efficiency is achieved when the negatively charged surface is neutralized with increasing dose. With further increase in destabilizing chemical dose, the surface charge reverses and removal efficiency declines. Since the driving force for adsorption (e.g., destabilizing chemical onto surface of the particle) is not primarily electrostatic, charge reversal can be induced by a destabilizing chemical overdose (Benjamin and Lawler, 2013).

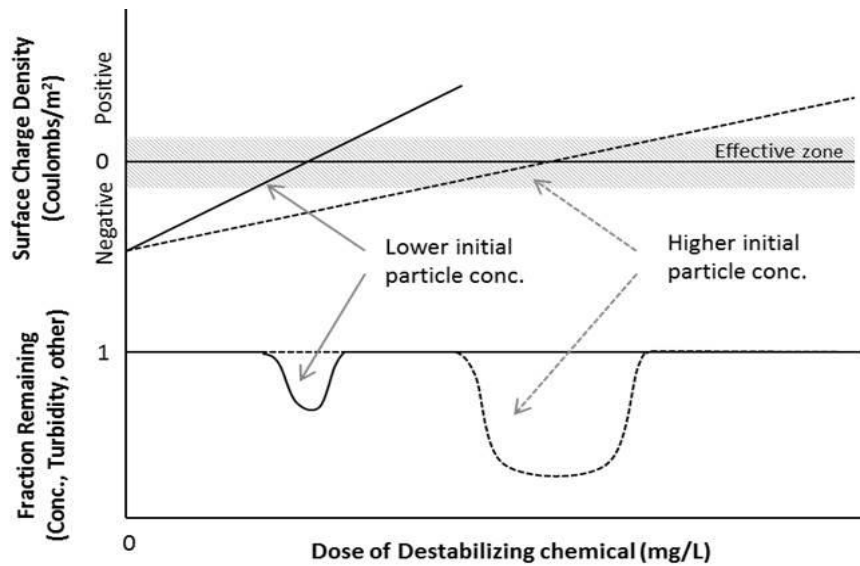


Figure 2-4 Schematic diagram of charge neutralization for particle destabilization at two different particle concentrations (Benjamin and Lawler, 2013).

### 2.3.2.2. Precipitation and sweep flocculation

As the dose of coagulant is increased, the ion concentration product or ion activity product (IAP) of potential solid phases often exceeds the solubility product ( $K_{SP}$ ). Under these conditions the solution is over or supersaturated and precipitation is thermodynamically favorable. Commonly observed forms of precipitates in water and wastewater treatment processes are aluminum hydroxide ( $\text{Al}(\text{OH})_{3(\text{s})}$ ) and ferric hydroxide ( $\text{Fe}(\text{OH})_{3(\text{s})}$ ). Often, precipitation of calcium carbonate ( $\text{CaCO}_{3(\text{s})}$ ) and magnesium hydroxide ( $\text{Mg}(\text{OH})_{2(\text{s})}$ ) occurs in pH-induced processes that utilize lime or caustic soda. Contaminants including suspended particles can be effectively removed via a *precipitation and sweep flocculation mechanism*. In this mechanism, precipitation of the newly formed particles entrap or enmesh the particles already present in solution and/or the particles present in the solution serve as an initial surface for nucleation of the newly formed precipitate. In this latter process, enmeshment and sweep flocculation are really misnomers as the particle removal process may be due to the precipitate acting as a bridge between particles. In this work, this process is referred to as precipitation-enhanced coagulation rather than sweep floc or enmeshment.

In the presence of foreign particles such as algae, heterogeneous nucleation should precede homogeneous nucleation due to the lower energy required for the formation of  $\text{CaCO}_{3(\text{s})}$  nuclei on the existing surface (Nason, 2006). Although homogeneous nucleation for the formation of  $\text{CaCO}_{3(\text{s})}$  nuclei often requires higher energy (i.e., higher IAP), homogeneous nucleation can occur at higher supersaturated conditions. In this case, the constituent ions of the precipitate tend to accumulate on the

newly formed nuclei rather than on foreign particles already present in the solution. This tendency is the result of structural similarity between the constituent ions and precipitating solids. Then, the two dissimilar types of particles (e.g., algae and precipitates) can interact with each other via electrostatic attraction and/or hydrophobic interactions. This mechanism in which two dissimilar particles coagulate is termed *heterocoagulation*.

It is likely that *adsorption and charge neutralization, precipitation and sweep flocculation (or precipitation-enhanced coagulation)* as well as *heterocoagulation* could exist simultaneously and/or dominate in a given system depending on operating conditions such as pH, coagulant dose, and initial ion concentration. Several researchers have observed the shift in the dominant mechanism from *adsorption and charge neutralization* to *precipitation and sweep flocculation* in coagulation processes. For instance, Duan and Gregory (2003) studied the mechanisms involved in water treatment using alum as a coagulant. They observed that the removal efficiency of colloidal particles in kaolin suspensions did not decrease even at a relatively high dose sufficient to instigate charge reversal. This was attributed to a shift in the dominant mechanisms from charge neutralization to sweep coagulation. A similar shift in the removal mechanism with ferric chloride as a coagulant was reported by Wyatt et al (2011). They observed the transition from a stoichiometric relationship between the required dose for high removal efficiency and algae cell density to a relationship independent of algae cell density that exhibits increasing removal efficiency with increasing dose.

Wu et al (2012) explored algae removal mechanisms in a pH-induced coagulation process in which precipitation of magnesium hydroxide occurred due to addition of strong base. The trend in the zeta potential of the particles in solution as a function of pH was employed to explain the shift in the dominant algae removal mechanism. They observed an increase in the zeta potential (toward less negative values) with increasing pH. They suggested that this trend indicated that precipitation of  $\text{Mg}(\text{OH})_{2(s)}$  with a large adsorptive surface area and positive surface charge attracts negatively charged algae particles. Even higher removal efficiency was observed as the zeta potential decreased (toward more negative values) with increasing pH which was attributed to deprotonation of functional groups on the surface of algae. They suggested that sweep flocculation was the dominant mechanism in this region of pH.

However, few researchers have focused on isolating each of these mechanisms to better understand the algae removal process. For example, heterocoagulation has not been investigated as an algae removal mechanism nor has it been distinguished from precipitation-enhanced coagulation under highly supersaturated conditions.

### **2.3.3. Adsorption and interparticle bridging**

Adsorption and inter-particle bridging for particle destabilization is often observed in processes that utilize polyelectrolytes such as ionic, nonionic, natural or synthetic polymers. For this destabilization mechanism, the polymer molecule is thought to be attached to two or more particles forming a so-called bridge between them. The

driving force of polymer adsorption on the surface of the particles is not only electrostatic, but also chemical in nature.

Tenney et al (1969) observed that algae flocculation was only successful with the addition of cationic polyelectrolytes. They proposed that the bridging mechanism occurs between discrete algal cells and the linearly extended cationic polymer chains, forming a three dimensional matrix that is capable of settling under quiescent conditions.

Recently, Salim et al (2011) studied bio-flocculation in which polymers excreted from one flocculating microalgae are effective for concentrating the non-flocculating microalgae of interest. They proposed two different sub-mechanisms under the polymer-induced flocculation process. The bridging model is one of the mechanisms in which unoccupied parts of the polymers can bind to other microalgae cells, thereby bridging them and resulting in a network of polymers and microalgae cells. For example, *Chlorella vulgaris* (target) was entrapped within the network of *Ankistrodesmus falcatus* (agent) based on their microscopic observations. Another mechanism proposed was a “patching” model in which adsorption of polymer creates uneven charge distribution on the surface. This resulted in flocculation between *Tetraselmis suecica* and *Scenedesmus obliquus*.

A stoichiometric relationship between the particle concentration and optimum dose is unlikely for adsorption and inter-particle bridging mechanisms as the polymer may attach to multiple sites on the same particle, especially at conditions in which the optimum dose is exceeded. Indeed, overdosing can lead to re-stabilization of the particles

as the polymer coats the surfaces and fully occupies adsorption sites that prevent one end of the polymer from forming a bridge with another particle.

While extracellular polymeric material produced by the algae, may lead to coagulation in algal systems without the addition of a coagulant, it is expected that *adsorption and charge neutralization*, *precipitation-enhanced coagulation*, and *heterocoagulation* mechanisms are mainly responsible for algae removal in the pH-induced flocculation process studied in this research.

#### **2.4. PH INDUCED COAGULATION USING HYDROXIDE**

Treatment trains involving coagulation, flocculation and sedimentation are common in water treatment operations. The coagulation step is initiated via the addition of a chemical followed by mixing to destabilize the suspended particles and induce particle agglomeration. In the case of particle removal (e.g., algae), the success of the process depends on an effective destabilization mechanism which is the focus of the current study. Moreover, in harvesting processes, the goal is not simply to produce an effluent water that meets water quality requirements. Rather, the primary objective is to concentrate the algae particles to form a pumpable, concentrated algal suspension that can be conveyed to downstream processes that may involve cell lysing and lipid extraction. This transport step may require that the flocculated solid removed in the sedimentation process be deflocculated or restabilized. The previous section reviewed the potential destabilization mechanisms for algae particles in solution, and identified several potential coagulants. The application of lime or sodium hydroxide for algae removal

offers several advantages over other coagulants because the ions associated with these solids are already present in most source waters and deflocculation does not add heavy metals to the residual biomass or recycle streams.

Traditionally, sodium and calcium hydroxide have been employed to raise pH to levels sufficient for hardness removal (i.e., softening) from drinking water through precipitation of  $\text{CaCO}_{3(s)}$  and  $\text{Mg}(\text{OH})_{2(s)}$  as well as chemical clarification of wastewaters via the so-called sweep flocculation mechanism. The purpose of the softening process is to reduce the hardness that is contributed mostly by Ca and Mg compounds. In enhanced softening, the purpose has been expanded to include removal of natural organic matter (NOM) to avoid human exposure to disinfection byproducts (DBPs) of which NOM is considered to be a precursor. Thus, NOM is removed with the precipitating solids, a factor which should eventually be considered if this process is used for algae harvesting.

In many lime softening treatment systems, a “recarbonation” step is provided for the clarified, softened effluent in which carbon dioxide is bubbled into the water prior to discharge to reduce the pH and stabilize the water. A similar concept is adapted in the “pH-induced flocculation/deflocculation” method investigated in this research; however,  $\text{CO}_2$  is bubbled into the algae concentrate produced in the flocculation step to dissolve the precipitate and release the algae to produce a homogeneous and pumpable algae concentrate.

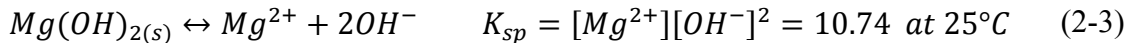
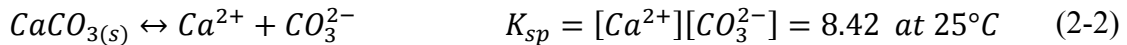
The softening process has been implemented successfully at large scale and many researchers have focused on optimization of the process for hardness and NOM

removal. Although the treatment goal is different (e.g., water treatment vs. algae harvesting), the fundamentals of water treatment processes that use the hydroxides of alkali or alkaline earth metals (e.g., lime, caustic soda) provide useful insight into the process mechanisms and factors that will affect the success of this process for algae removal in waters of varying composition.

The selection of the particular hydroxide chemical employed in water treatment operations has primarily been based on cost and ease of use. Lime and caustic soda (sodium hydroxide-NaOH) are the most common alkaline chemicals employed. Lime generally includes quicklime (CaO) and its hydrated form, hydrated lime (Ca(OH)<sub>2</sub>). Lime has been widely used in water and wastewater treatment to raise pH because it is abundant and cost effective. It also has the inherent advantage of not contributing to an increase in salinity, as in the case of alum or iron salts addition (Dziubek and Kowal, 1984). Caustic soda can be used as a source of hydroxyl ions to raise the pH to levels at which precipitation of calcium carbonate and magnesium hydroxide is induced. NaOH is approximately 100 times more soluble in water than lime (at 25°C). It is easier to handle, store, and feed than lime (Edward, 1990). However, it is significantly more expensive. Mg(OH)<sub>2</sub> is an alternative that has not been used extensively in the softening field, but offers benefits for algae removal. Vandamme et al (2012) compared the effects of different bases including Mg(OH)<sub>2</sub> on algae flocculation. Mg(OH)<sub>2</sub> induced flocculation at a lower pH (9.7) than the other bases; however, the quantity required was relatively high.

## 2.5. CHEMICAL REACTIONS INVOLVING CALCIUM AND MAGNESIUM IN WATER

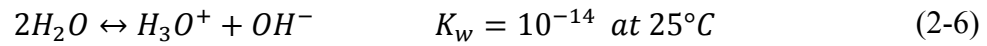
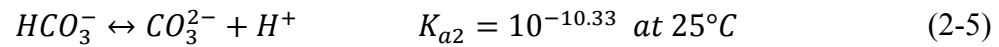
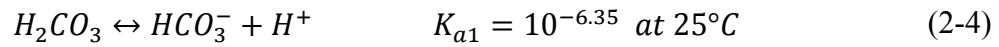
When lime, caustic soda or other strong base is introduced to water, the pH becomes elevated. Consequently, precipitation reactions of calcium, as calcium carbonate ( $\text{CaCO}_{3(s)}$ ), and magnesium, as magnesium hydroxide ( $\text{Mg(OH)}_{2(s)}$ ), can be initiated depending on water composition and chemical dose. Reaction products of calcium carbonate and magnesium hydroxide are governed by the equilibrium expressions shown below.



where  $K_{sp}$  is the equilibrium constant which is dependent on temperature.

As the concentration of constituent ions of the precipitates increase via chemical addition or speciation, the ion concentration product or the ion activity product (IAP) exceeds the solubility product ( $K_{sp}$ ) and a thermodynamically favorable condition for precipitation of each mineral solid is achieved. Even if the solubility product has been exceeded, additional chemical doses are frequently required to overcome the activation energy to initiate actual precipitation. Thermodynamic aspects of precipitation reactions and their kinetics are discussed in detail in the following subsection. Chemical reactions based on equilibrium are discussed in this subsection.

As the equilibrium expressions (2-2) and (2-3) indicate, the extent of  $\text{CaCO}_{3(s)}$  and  $\text{Mg(OH)}_{2(s)}$  precipitation depends on the concentration of its constituent ions: calcium and carbonate ions for  $\text{CaCO}_{3(s)}$  and magnesium and hydroxide ions for  $\text{Mg(OH)}_{2(s)}$ . Chemicals such as  $\text{Ca(OH)}_2$  or  $\text{NaOH}$  provide hydroxide ion, affecting the concentration of hydroxide ion as well as the distribution of carbonate species described in equations (2-4) - (2-6):



The equilibrium carbonate concentration can be determined when the pH and total carbonate concentration of the source water are known:

$$C_T = [\text{H}_2\text{CO}_3] + [\text{HCO}_3^-] + [\text{CO}_3^{2-}] \quad (2-7)$$

$$[\text{CO}_3^{2-}] = \alpha_2 \times C_T \quad (2-8)$$

$$\alpha_2 = K_{a1}K_{a2}/[\text{H}^+]^2 + K_{a1}[\text{H}^+] + K_{a1}K_{a2} \quad (2-9)$$

The total carbonate concentration is directly related to alkalinity which is one of the most important parameters in water treatment processes where mineral precipitation occurs. Alkalinity can be defined as “*capacity of the water to neutralize a strong acid*” and is often expressed as one of the following equations:

$$\text{Alkalinity} = [\text{HCO}_3^-] + 2[\text{CO}_3^{2-}] + [\text{OH}^-] - [\text{H}^+] \quad (2-10)$$

$$\begin{aligned} \text{Alkalinity} = & [\text{HCO}_3^-] + 2[\text{CO}_3^{2-}] + [\text{OH}^-] - [\text{H}^+] \quad (2-11) \\ & + \{ \text{terms for other weak acid/base systems} \} \end{aligned}$$

$$\text{Alkalinity} = [\Sigma \text{ strong base cations}] - [\Sigma \text{ strong acid anions}] \quad (2-12)$$

Equation 2-10 was derived for systems with no other weak acid/base other than those associated with the carbonate system. Equation 2-11 includes other possible weak bases (e.g.,  $\text{HPO}_4^{2-}$ ,  $\text{H}_2\text{PO}_4^-$ ,  $\text{NH}_3$ ,  $\text{CH}_3\text{COO}^-$ , etc.) in the water together with the carbonate system since they have the ability to accept protons within the same pH range as the carbonate system. Equation 2-12 can be translated to the diagram shown in Figure 2-5 below which illustrates that an alternative definition of alkalinity can be derived from the difference between the equivalent concentration of strong base cations and strong acid anions.

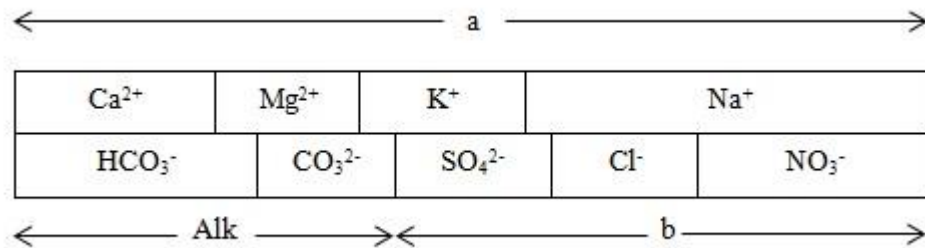


Figure 2-5 Schematic of a charge balance used in alkalinity calculations. “a” represents the sum of concentrations (meq/L) of strong base cations and “b” represents the sum of concentrations (meq/L) of strong acid anions.

Analogous to its acid neutralizing capacity, water also exhibits a base neutralizing capacity. Because the acid neutralizing capacity (alkalinity) and base neutralizing capacity (acidity) are quantitatively related through the proton and charge balances, more base is often required to raise the pH in source waters with high alkalinity. On the other hand, solutions with low alkalinity may limit the precipitation of calcium carbonate since carbonate is typically the main source of alkalinity in natural waters. Soda ash (sodium carbonate- $\text{Na}_2\text{CO}_3$ ) is usually added to waters with low alkalinity in traditional softening processes. Thus, the alkalinity as well as the cation composition of the water (e.g., concentration of calcium and magnesium) are important factors affecting the operational requirements. The quantity and types of chemical additives needed to achieve specific treatment goals such as the removal of hardness or algae will be a function of water chemistry.

The reactions described above are based on the assumption of equilibrium. Equilibrium relationships provide useful information regarding whether a reaction is

thermodynamically favorable and for predicting the extent of reaction at equilibrium. However, engineered processes with finite retention times may not achieve equilibrium, and thus, the relationships described above have limited utility in such situations.

## **2.6. KINETICS OF PRECIPITATION REACTIONS**

Typical chemical processes in water treatment operations are kinetically-controlled and are not at equilibrium. The kinetics of precipitation reactions must be considered when the hydraulic retention time is insufficient for a system to reach equilibrium. The primary objective of most engineering systems is to achieve treatment as quickly as possible at the shortest hydraulic retention time. Therefore, delineating the kinetics of the precipitation process as well as characterizing the reaction products is necessary to optimize the design and operation of precipitation systems.

### **2.6.1. Nucleation**

When lime or caustic soda is introduced into an aqueous solution, the concentration of the constituent ions of the associated precipitates changes. Once the degree of oversaturation is sufficient to overcome the energy barrier for crystallization, precipitation can occur. The following equation is the thermodynamic driving force for precipitation.

$$\Delta G = -\eta RT \ln S \quad (2-13)$$

where  $\Delta G$  is the free energy associated with making bonds between constituent ions,  $S$  is the saturation ratio and  $\eta$  is the number ions in the formula unit of the mineral (e.g.,  $\alpha+\beta=2$  in  $\text{CaCO}_{3(s)}$ ).

The saturation ratio is defined as:

$$S = \left( \frac{IAP}{K_{s0}} \right)^{1/\eta} \quad (2-14)$$

$$S = \left( \frac{\{Ca^{2+}\}\{CO_3^{2-}\}}{K_{sp,CaCO_3}} \right)^{1/2} \quad (2-15)$$

$$S = \left( \frac{\{Mg^{2+}\}\{OH^{-}\}^2}{K_{sp,Mg(OH)_2}} \right)^{1/3} \quad (2-16)$$

where  $IAP$  is the ion activity product (of the precipitating ions in the supersaturated solution) and  $K_{sp}$  is the solubility product.

Equations (2-15) and (2-16) provide the saturation ratios for  $\text{CaCO}_{3(s)}$  and  $\text{Mg(OH)}_{2(s)}$ , respectively. The ion activity product is often replaced by the ion concentration product (e.g.,  $[Ca^{2+}][CO_3^{2-}]$ ) with the assumption that the activity coefficient,  $\gamma$ , is near 1 in dilute solutions.

When the solubility product is exceeded, conditions are favorable for precipitation; however, formation of the new phase will not be initiated when the energy consumption to create a surface is greater than the free energy available from making bonds between constituent ions. The overall free energy term to form a nucleus is described in Equation 2-17.

$$\Delta G_j = \Delta G_{bulk} + \Delta G_{surface} \quad (2-17)$$

where  $\Delta G_j$  is the free energy of the formation of a nucleus,  $\Delta G_{bulk}$  is consistent with  $\Delta G$  in equation 2-13, and  $\Delta G_{surface}$  is the free energy term that requires work to create a surface (cluster-solution interface or cluster-substrate interface).

Usually, the energy required to create a surface in a pure bulk solution (i.e., *homogeneous nucleation*) is higher than that required to create one on a pre-existing surface or substrate as occurs in *heterogeneous nucleation*. The degree of energy required for heterogeneous nucleation is dependent on how similar the substrate surface is to that of the cluster of interest (Nason, 2006). In practice, precipitates in lime softening are recycled back to the head of the treatment plant to provide seed (i.e., initial surface) to increase the rate of precipitation via heterogeneous nucleation (Lawrence, 1963). The following rate expression describes the rate of formation of supercritical nuclei as a function of the critical work for nucleation as well as the saturation ratio.

$$J = AS^2 \exp\left(\frac{-W^*}{K_B T}\right) = AS \exp\left(\frac{-B}{\ln^2 S}\right) \quad (2-18)$$

where  $J$  is the rate of formation of supercritical nuclei ( $\text{m}^{-3} \text{s}^{-1}$  or  $\text{m}^{-2} \text{s}^{-1}$ ),  $W^*$  is the critical work for nucleation,  $K_B$  is the Boltzmann constant (J/K),  $B$  is a dimensionless thermodynamic parameter,  $S$  is a saturation ratio, and  $A$  is a kinetic parameter that depends on the type of nucleation ( $\text{m}^{-3} \text{s}^{-1}$  for homogeneous and  $\text{m}^{-2} \text{s}^{-1}$  for 2-D surface nucleation, Kashchiev and van Rosmalen, 2003).

As seen in Equation 2-18, the rate of formation of nuclei is a function of  $S$  and increases with increasing  $S$  by reducing the critical work required for nucleation. Due to the lower energy barrier, heterogeneous nucleation often prevails over homogeneous nucleation in the presence of particles. However, homogeneous nucleation can occur or dominate in highly supersaturated conditions.

The rate and extent of nucleation is an important consideration with respect to the algae harvesting process because the algae itself can serve as the substrate or initial surface for precipitation and the algae removal mechanism can be affected by the mode of nucleation.

### **2.6.2. Crystal growth**

Once a surface is created either by homogeneous or heterogeneous nucleation, the constituent ions of the precipitate undergo a series of sequential processes for crystal growth. These processes include: diffusion from the bulk solution to the surface, adsorption onto the surface, surface diffusion, partial dehydration, step nucleation, and

expansion of its two and three dimensional crystal structure. Nancollas and Reddy (1971) and Liu and Nancollas (1973) described the kinetically-controlled crystal growth rate ( $r$ ) of the precipitates of  $\text{CaCO}_{3(s)}$  and  $\text{Mg(OH)}_{2(s)}$ .

$$r = ks \left( [\text{Ca}^{2+}][\text{CO}_3^{2-}] - \frac{K_{s0,\text{CaCO}_3}}{\gamma_2^2} \right) \quad (2-19)$$

$$r = ks \left( ([\text{Mg}^{2+}][\text{OH}^-]^2)^{1/3} - \left( \frac{K_{s0,\text{Mg(OH)}_2}}{\gamma_2^2} \right)^{1/3} \right) \quad (2-20)$$

where  $[\text{Ca}^{2+}]_T$ ,  $[\text{Mg}^{2+}]_T$  are the total concentration of dissolved calcium and magnesium,  $k$  is a temperature dependent precipitation rate constant,  $s$  is the surface area of the crystals in suspension,  $[ ]$  denotes molar concentration,  $\gamma_2$  is the divalent cation activity coefficient.

The rate expression for calcium carbonate is based on the loss of  $\text{Ca}^{2+}$  ions in the solution. Wiechers et al (1975) studied precipitation kinetics for softening processes and validated the rate expression for higher supersaturation conditions. Moreover, the rate expression has been well fitted to seawater solutions and other strong electrolyte solutions (Zhang and Dawe, 1998; Zuddas et al., 2003). These results imply that the rate expression applies to a variety of source waters (e.g., fresh, brackish, salt water) that are expected to be encountered in algae harvesting systems. It is beneficial to examine how the kinetic models that describe the crystal growth mechanism affect the

morphology of calcium carbonate as this will affect particle interaction with algae.

Nielson (1984) outlined the rate expression for each step in crystal growth:

Bulk transport (diffusion)/surface adsorption:

$$K_G = k_1(S - 1) \quad (2-21)$$

Spiral growth on surface:

$$K_G = k_2(S - 1)^2 \quad (2-22)$$

Surface nucleation:

$$K_G = k_e S^{7/6} (S - 1)^{1/6} \exp\left(\frac{-k_e}{\ln S}\right) \quad (2-23)$$

where  $K_G$  is the overall linear growth rate ( $L T^{-1}$ ),  $k$  is a temperature dependent rate constant,  $n$  is the empirical reaction order.

Nielsen believed that the incorporation of ions at kink sites is the rate-limiting step for spiral growth on the crystal surface. This has been supported by atomic force microscopy studies that showed spiral growth during calcite precipitation (Gratz et al., 1993; Teng et al., 2000; Larsen et al., 2010). As a result of crystal growth, a highly structured rhombohedral shape for the calcite was formed as shown in the Figure 2-6 (Panel A).

The kinetics of magnesium hydroxide formation has not been as carefully studied compared to calcium carbonate. One difficulty associated with measuring the kinetics of magnesium hydroxide is the induction period for nucleation (i.e., the time required for the formation of critical nuclei) is much smaller than that for  $\text{CaCO}_3$ . As a result, the accuracy of measurement of the induction period is lower (Myasnikov et al., 2013). Difficulties also arise for experimentally investigating the growth mechanism of rapidly growing structures which include needle-like and disk-like morphologies shown in Figure 2-6 (Panel E-H) for  $\text{Mg}(\text{OH})_{2(\text{s})}$ .

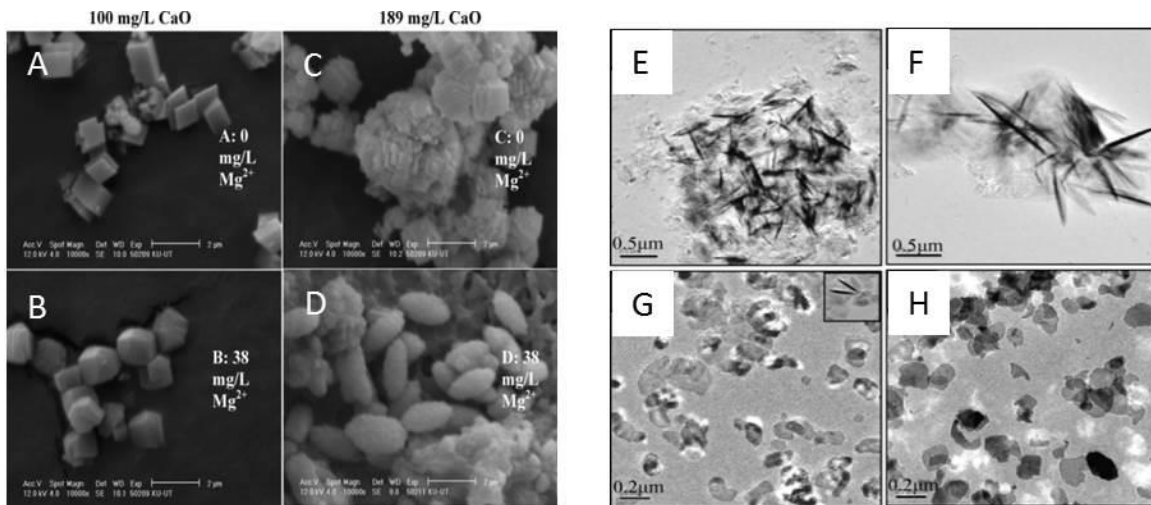


Figure 2-6 Scanning electron microscopic images of  $\text{CaCO}_3(\text{s})$  formed for different lime doses and initial  $\text{Mg}^{2+}$  concentrations (A) 100 mg/L CaO, 0 mg/L  $\text{Mg}^{2+}$  (B) 100 mg/L CaO, 38 mg/L  $\text{Mg}^{2+}$  (C) 189 mg/L CaO, 0 mg/L  $\text{Mg}^{2+}$  (D) 189 mg/L CaO, 38 mg/L  $\text{Mg}^{2+}$  (Russell et. al., 2009) and transmission electron micrographs of nano-size magnesium hydroxides at different temperature (E) 20 °C (F) 40 °C (G) 60 °C (H) 80 °C (Wang et al., 2011).

Nevertheless, kinetic models have been developed to investigate the kinetics of magnesium hydroxide precipitation as a function of different operating variables. Dabir et al (1982) studied the precipitation kinetics of magnesium hydroxide in a softening process as a function of operating parameters such as the NaOH/Mg<sup>2+</sup> feed ratio. Excellent Mg<sup>2+</sup> removal in the presence of excess NaOH was observed; however, low growth rates and a high nucleation rate resulted in small crystals which make the subsequent settling and filtration steps more difficult. More recently, Alamdari et al (2008) also showed similar production of particles with poor settlability with similar kinetic trends for the sea bittern (i.e., the residual rich in magnesium from salt production unit upon the solar evaporation of seawater) that contained impurities. They suggested a higher nucleation rate and a lower particle growth rate for precipitation due to the adsorption of impurities onto the active growth site of magnesium hydroxide particles. This is consistent with the results of Turek and Gnot (1995) who observed a lower sedimentation rate for the precipitation of Mg(OH)<sub>2(s)</sub> in the presence of excess OH<sup>-</sup> than was observed in the presence of excess Mg<sup>2+</sup>.

## **2.7. FACTORS AFFECTING PRECIPITATION REACTIONS**

The rate and extent of precipitation reactions are affected by many factors. This subsection summarizes a number of factors that can be important during precipitation processes that rely on pH adjustment (i.e., higher pH). In addition, the implications of factors affecting precipitation reactions are discussed with respect to algae harvesting processes.

### 2.7.1. Saturation ratio

The saturation ratio ( $S$ ) is an important variable controlling the rate of precipitation since rate expressions for nucleation and crystal growth are a strong functions of  $S$ . In water treatment plants, the  $S$  of calcium carbonate and magnesium hydroxide can be controlled by adding base during the rapid mixing stage.

Depending on the type of agents,  $S$  can be increased in several different ways. The addition of hydrated lime ( $\text{Ca}(\text{OH})_2$ ) increases the  $S$  of calcium carbonate by raising the concentration of calcium and carbonate ions (the increased  $\text{OH}^-$  ion concentration shifts the carbonate system in the direction of increased carbonate ions). The addition of sodium hydroxide, on the other hand, increases only the concentration of hydroxide ions. The  $S$  of magnesium hydroxide can be increased by the addition of both lime and sodium hydroxide by providing additional hydroxide ions. In addition to the pH adjustment using strong base (e.g., hydroxide), the  $S$  in high-pH water treatment processes can be increased by adding supplements such as magnesium chloride, magnesium carbonate, magnesium hydroxide, processed dolomite, seawater, seawater liquid bittern and marine dried bittern to induce magnesium hydroxide formation (Semerjian and Ayoub, 2003).

The mode of precipitation that occurs in a system is a function of the level of saturation. In other words, homogeneous nucleation can occur or dominate in highly supersaturated conditions. If that is the case, algae can not only serve as a surface for precipitation but also interact with precipitates inducing particle-particle aggregation.

### 2.7.2. Ion activity ratio

The saturation ratio is calculated from the product of the activities of the constituent ions (e.g.,  $\{Ca^{2+}\}\{CO_3^{2-}\}$  and  $\{Mg^{2+}\}\{OH^{-}\}^2$ ). Thus, the same saturation ratio can be achieved with numerous combinations of constituent ion concentrations. The kinetics of precipitation of calcium carbonate and magnesium hydroxide are affected by these ratios.

Nehrke et al (2007) conducted calcite growth experiments at a constant degree of supersaturation ( $\Omega = IAP/K_{sp} = \{Ca^{2+}\}\{CO_3^{2-}\}/K_{sp} = 5$  and 16); the highest growth rate was observed at an ion concentration ratio,  $r = [CO_3^{2-}]/[Ca^{2+}]$  near 1 and decreased symmetrically with either an increase or a decrease of the ratio from 1. In the work of Gebrehiwet et al (2012), similar trends were observed with the highest rate observed at a lower ratio ( $r = 0.306$ ) for a fixed supersaturation level ( $\Omega = 9.4$ ). Atomic force microscopy (AFM) was employed to examine the effect of  $Ca^{2+}:CO_3^{2-}$  activity ratio on growth kinetics at constant supersaturation. Changes in growth velocity were attributed to ion incorporation that is affected by the dissimilar dehydration properties of  $Ca^{2+}$  and  $CO_3^{2-}$  (Larsen et al., 2010) since dehydration of the ions is required prior to incorporation into the crystal lattice.

As stated previously, the precipitation of  $Mg(OH)_{2(s)}$  in the presence of excess  $OH^{-}$  results in high nucleation rates and a low growth rate which yields crystals which are difficult to settle. In contrast, excess  $Mg^{2+}$  produces coarse particles with better settlability (Alamdari et al., 2008). This tendency is consistent with the results of Turek and Gnot (1995) who observed a lower sedimentation rate for the precipitation of

$\text{Mg(OH)}_{2(s)}$  in the presence of excess  $\text{OH}^-$  than that observed in the presence of excess  $\text{Mg}^{2+}$ . These results indicate that the ion activity ratio is an important parameter to control if the algae harvesting process includes sedimentation after the flocculation step to separate the algae-laden precipitates/flocs from the suspension.

### 2.7.3. pH

pH is one of the most important factors affecting precipitation reactions. pH is coupled with the saturation ratio and the ion activity ratio since pH governs the carbonate system and hydroxyl ion concentrations. Thus, isolating the effect of pH on the precipitation reactions independent of its effect on saturation ratio and ion activity ratio is difficult.

As the pH increases, supersaturation with respect to  $\text{CaCO}_{3(s)}$  increases. This results in an increase in the rate of precipitation including nucleation and crystal growth. Ion activity ratio,  $\text{CO}_3^{2-}/\text{Ca}^{2+}$ , also increases with increasing pH. This could increase the rate of crystal growth due to the increased number of carbonate active sites (i.e.,  $\equiv \text{CaCO}_3^-$ ) at the surface of  $\text{CaCO}_{3(s)}$  (Nisson and Sternbeck, 1999; Zeppenfeld, 2010).

In addition to the surface species, solute species in the solution can affect the rate of crystal growth. It is worth restating that cation dehydration is required for the crystal growth prior to the incorporation into the crystal lattice (Ruiz-Agudo et al., 2011). Hydrated calcium ions in the solution can replace their water molecule with carbonate ligands, forming partially dehydrated  $\text{CaCO}_3^0$  species. This ligand exchange promotes the rate of crystal growth because the water exchange rate of  $\text{CaCO}_3^0$  is higher than that

of  $\text{Ca}^{2+}$  (Nillson and Sternbeck, 1999; Zeppenfeld, 2010; Ruiz-Agudo et al., 2011). Furthermore, the water exchange rate of  $\text{Ca}^{2+}$  increases in the presence of abundant hydroxyl ions, facilitating their incorporation into the crystal lattice (Ruiz-Agudo et al., 2011).

As with the kinetics of precipitation, the performance of the coagulation process of interest in this research for algae harvesting is expected to be dependent on the pH of the solution.

#### **2.7.4. Type/concentration of foreign particles**

In the absence of particles, precipitation is initiated by homogeneous nucleation, after which crystal growth can occur. In the presence of particles, heterogeneous nucleation and crystal growth can dominate the process due to the lower energy barrier that must be overcome relative to that of homogeneous nucleation. In practice, sludge is often recycled back to the head of the treatment plant to provide seed particles to increase the rate of precipitation. Although heterogeneous nucleation and crystal growth are more likely to occur on particles that are chemically similar to the precipitating solids, certain algae species actually promote calcium carbonate precipitation by heterogeneous nucleation (Stabel, 1986). Currently, various types of algae with different cell characteristics and biomass concentrations are being cultivated in algae growth systems. Precipitation reactions and the associated algae removal efficiency are likely affected by the types and concentration of algae present. It is desirable to develop an algae harvesting process to be able to recover a variety of algae.

### 2.7.5. Inhibitory species

Many researchers have determined that the kinetics of precipitation can be influenced by the presence of ions and molecules such as divalent cations, orthophosphate, and natural organic matter (Reddy and Nancollas, 1976; Xu and Higgins, 2011; Gutjahr et al., 1996; Giannimaras and Koutsoukos, 1987; Plant and House, 2002; Lebron and Suarez, 1996; Lin et al., 2005). In many natural environments, magnesium is considered as one of the principal inhibitors of calcite formation and is known to exhibit an inhibitory effect on the growth rate of calcite. (Reddy and Nancollas, 1976; Gutjahr et al., 1996). The rate expression for the growth of calcite in the presence of impurities can be modified as follows:

$$r_i = r(1 - \theta_i) \quad (2-24)$$

$$\theta_i = \frac{k_i c_i}{(k_i c_i + 1)} \quad (2-25)$$

where  $r_i$  is the modified rate of calcite growth rate,  $r$  is the calcite growth rate without impurities,  $\theta_i$  is the fraction of surface sites covered by the impurities based on the adsorption via a Langmuir isotherm,  $k_i$  is the constant, and  $c_i$  is the concentration of impurity in the solution.

Reddy and Nancollas, (1976) observed that inhibition of calcite growth depends on the magnesium concentration in the solution. The concentration of  $\text{Mg}^{2+}$  ions below

$10^{-4}$  M L<sup>-1</sup> did not affect calcite growth, however, more than  $10^{-3}$  M L<sup>-1</sup> retarded its growth rate (Gutjahr et al., 1996; Xu and Higgins, 2011). It has been proposed that inhibition of calcite growth can be induced either by adsorption of Mg<sup>2+</sup> ions onto the surface of calcite or by incorporation into its crystal lattice (Davis et al., 2000; Gutjahr et al., 1996). This adsorption or incorporation of Mg<sup>2+</sup> ions leads to the formation of magnesium-rich calcite with enhanced solubility (Berner, 1975) and results in the formation of calcium and magnesium carbonates of the general formula (Ca<sub>1-x</sub>Mg<sub>x</sub>)CO<sub>3</sub> (Gutjahr et al., 1996; Lopez et al., 2009; Xu and Higgins, 2011). Observation via atomic force microscopy supports the hypothesis that enhanced mineral solubility through magnesium incorporation inhibits calcite growth (Davis et al., 2000). It is likely that a defect in lattice structure induced by either adsorption or incorporation of Mg<sup>2+</sup> ions results in a higher activation energy that must be overcome for particle growth. This is not a favorable condition for the growth of the most stable and highly structured form of calcite. Inhibition of calcite precipitation induced by magnesium may be inevitable in situations in which the source water contains a sufficient amount of Mg<sup>2+</sup> ions. This inhibition might affect the characteristics of CaCO<sub>3(s)</sub> (e.g., morphology, surface charge) and yield more favorable conditions for algae harvesting processes. The inhibitory effects of magnesium on the characteristics of CaCO<sub>3(s)</sub> are discussed in the following subsection.

## 2.8. CHARACTERISTICS OF REACTION PRODUCTS

### 2.8.1. $\text{CaCO}_{3(s)}$

Calcium carbonate is one of the most abundant mineral species on the surface of the earth (Smyth and Ahrens, 1997). Precipitation of  $\text{CaCO}_{3(s)}$  is responsible for biomineralization (often termed calcification) that plays an important role in the global carbon cycle. Calcium carbonate can be precipitated in three common forms, calcite, aragonite, and vaterite depending on parameters such as solution pH, temperature, concentration ratio of components, supersaturation, ionic strength, and type and concentration of additives (Tai and Chen, 1998). A number of precursor phases are formed during the formation of the most stable form of calcite. Many researchers studied the crystallization of amorphous calcium carbonate (ACC) to calcite in both abiotic and biotic systems (Ogino et al., 1987; Pontoni et al., 2003; Radha et al., 2010; Rodriguez-Blanco et al., 2011; Bots et al., 2012). With the aid of previous research, Bots et al (2012) suggested the full abiotic transformation pathway from ACC via vaterite to calcite as follows: hydrated and disordered ACC, more ordered and dehydrated ACC, anhydrous ACC, vaterite, and calcite. In addition, it was proposed that the transformation mechanism from vaterite to calcite (i.e., dissolution of vaterite and reprecipitation of calcite) is dependent on the surface area of calcite present (Ogino et al., 1990). These conclusions were supported by high temporal resolution *in situ* and time-resolved analysis conducted by Rodriguez-Blanco et al (2011).

Calcite is the most thermodynamically stable form of the three phases and is most commonly formed during the softening processes (Liao and Randtke, 1985; Mercer et al., 2005). Calcite exhibits a highly-structured rhombohedral shape formed from six-fold coordination between the calcium cations and the oxygen atoms (Reeder, 1983). Calcite precipitates out of the solution in a pH range of 9.1–9.5 depending on the composition of the solution and operating conditions. The pH of the point-of-zero-charge was estimated to be between pH 8 and 9 (Parks, 1967). With respect to algae harvesting processes, it is likely that the highly structured shape and negatively charged calcium carbonate particles produce unfavorable conditions for attracting negatively charged algae particles.

Many researchers have studied how the characteristics of calcium carbonate depend on water composition. It is likely the characteristics of highly structured and negatively charged calcium carbonate particles are subject to change. Black and Christman (1961) observed negatively charged  $\text{CaCO}_{3(s)}$  produced in lime softening processes throughout the entire pH (9-11) range tested. This result was consistent with the electrophoretic analysis from Folkman and Wachs (1973) who found that the charge of  $\text{CaCO}_{3(s)}$  was negative and ranged from -15 to -40 depending on the calcium and carbonate concentrations. Stipp (1999) stated that  $\text{Ca}^{2+}$  and  $\text{CO}_3^{2-}$  are the potential charge determining ions which control the electrophoretic mobility of calcite particles. Further study showed positive zeta potentials (15mV) of precipitated  $\text{CaCO}_{3(s)}$  under excess  $\text{Ca}^{2+}$  conditions and negative values (-10 to -25mV) in the presence of excess  $\text{CO}_3^{2-}$  (Chibowski et al., 2003). More recently, a charge reversal from negative to more

positive values was observed in softening experiments under carbonate limited conditions (Russell et al, 2009). In fact, it was suggested that timing and exposure to CO<sub>2</sub> can also influence the measurement of surface charge of CaCO<sub>3(s)</sub> (Wolthers et al., 2008).

Magnesium also affects the surface charge of CaCO<sub>3(s)</sub>. Black and Christman (1961) observed that the surface charge of CaCO<sub>3(s)</sub> increased in the direction of more positive values with increasing aqueous Mg<sup>2+</sup> concentration. They attributed the associated changes to adsorption of magnesium on the surface of CaCO<sub>3(s)</sub> in a pH range at which precipitation of Mg(OH)<sub>2(s)</sub> is not expected based on bulk thermodynamics. A positive electrophoretic value of CaCO<sub>3(s)</sub> solids was observed with increasing Mg<sup>2+</sup> concentration (Cicerone et al., 1992). They suggested that Mg<sup>2+</sup>, Ca<sup>2+</sup>, and CO<sub>3</sub><sup>2-</sup> become potential determining ions in the presence of magnesium ions. Russell et al (2009) observed a more positive surface charge with increasing Mg<sup>2+</sup> concentration, which they attributed to incorporation of Mg<sup>2+</sup> into the calcite crystal lattice. Due to the association with magnesium, they also observed a change in morphology from highly structured to a rounded and elongated shape as previously shown in Figure 2-6 (A-D). This shift in morphology is consistent with the classical study by Folk (1974) that showed that incorporation of magnesium ions into the crystal lattice impedes sideward growth and results in an elongated crystal structure. This idea was supported by AFM observations that showed that the step growth direction is altered by strains at the intersection of steps resulting from Mg incorporation into non-equivalent step-types (Davis et al., 2004). The effect of Mg<sup>2+</sup> incorporation into the crystal lattice on CaCO<sub>3(s)</sub> morphology is schematically illustrated in Figure 2-7.

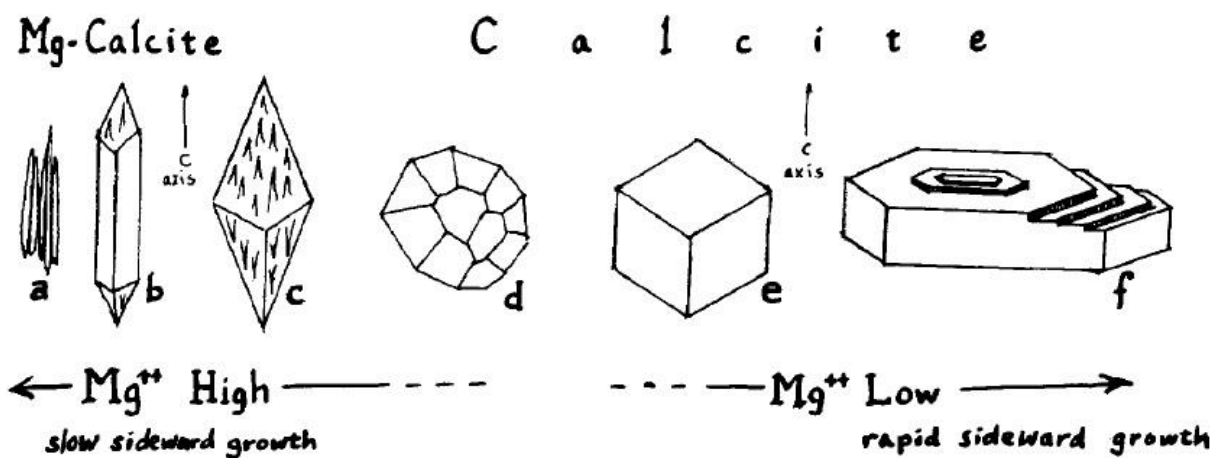


Figure 2-7 Schematics of crystal habit of  $\text{CaCO}_3(\text{s})$  as a function of  $\text{Mg}^{2+}$  incorporation (Source: Folk, 1974)

Moreover with respect to surface area and crystallite size, Busenberg and Plummer (1989) utilized BET analyses to show that the surface area increased with increasing magnesium incorporation. These results indicate that favorable conditions for precipitated calcium carbonate to attract negatively charged algae particles can be induced depending on the water composition such as activity ratio between calcium and carbonate ions and magnesium concentration

### 2.8.2. $\text{Mg}(\text{OH})_2(\text{s})$

$\text{Mg}(\text{OH})_2(\text{s})$  provides a more favorable surface for interacting with algae particles than  $\text{CaCO}_3(\text{s})$  due to its morphological and surface charge characteristics. Significant magnesium hydroxide precipitation can be expected at higher pH (10.5) levels

than precipitation of calcium carbonate depending on the composition of the water and operating conditions. High pH conditions are often adopted to achieve effective removals of particles, dissolved contaminants, and natural organic matter present in water and wastewater.

Primary crystals of magnesium hydroxide have a layer structure characteristic of brucite, the mineral form in which  $\text{Mg}(\text{OH})_{2(\text{s})}$  occurs in nature (Turek and Gnot, 1995). Depending on the conditions (e.g., type of base or temperature) used to synthesize  $\text{Mg}(\text{OH})_{2(\text{s})}$ , a globular-shape or platelet-shape morphology (Henrist et al., 2003), as well as a needle-like or disk-like morphology have been observed (Wang et al., 2011).  $\text{Mg}(\text{OH})_{2(\text{s})}$  floc is strongly hydrophilic and gelatinous in contrast to the crystalline  $\text{CaCO}_{3(\text{s})}$  (Faust et al., 1998). In fact, lyosorption can occur as the  $\text{Mg}(\text{OH})_{2(\text{s})}$  crystals adsorb the liquid (e.g., water), form aggregates with pores filled with water. These aggregates have a low specific gravity and, therefore, a low sedimentation rate (Turek and Gnot, 1995).

With respect to the surface charge of  $\text{Mg}(\text{OH})_{2(\text{s})}$ , a positive zeta potential (+11.3mV) was measured at a pH 10.9 (Folkman and Wachs, 1973). The point of zero charge was measured at a pH of approximately 12.4 (Parks, 1967) and at even higher values of 13.2 (McLaughlin et al., 1993). The positively charged and fluffy structural features of  $\text{Mg}(\text{OH})_{2(\text{s})}$  floc have ensured better removal efficiency of contaminants encountered in water and wastewater when the  $\text{Mg}(\text{OH})_{2(\text{s})}$  precipitates along with  $\text{CaCO}_{3(\text{s})}$ . For instance, additional removal of suspended solids and total organic carbon (TOC) was observed when the pH was raised high enough to induce precipitation of

magnesium hydroxide along with  $\text{CaCO}_{3(s)}$  (Leetvaar and Rebhun, 1982). The positively charged  $\text{Mg}(\text{OH})_{2(s)}$  floc is large and fluffy, providing a large surface area that enables NOM removal above and beyond that provided by removal of calcium carbonate (Liao and Randtke, 1985). Even  $\text{CaCO}_{3(s)}$ , which normally tends to remain in suspension in lime softening processes can be adsorbed onto the  $\text{Mg}(\text{OH})_{2(s)}$  floc (Van Vuuren et al., 1967). In addition, high pH conditions as a result of  $\text{Mg}(\text{OH})_{2(s)}$  precipitation can be beneficial to the reduction or deactivation of viruses (Wolf, et. al., 1974 and Rao, et. al., 1988) and the alkaline conditions can be toxic to bacteria (Brock, et. al., 1994). Moreover, previous research has determined that precipitation of magnesium hydroxide is the principal factor needed for algae removal (Folkman and Wachs, 1973; Friedman, 1977; Ayoub and Koopman, 1986; Elmaleh et al., 1996, Knucky et al., 2006, Vandamme et al., 2012; Wu et al., 2012). However, these studies have not provided a detailed understanding of the role of the various algae removal mechanisms associated with dissolved ions and solid phases of calcium and magnesium. Gaps in existing literature are discussed in the following section along with a summary of what has been discussed in this chapter.

## **2.9. SUMMARY**

Algae have been successfully removed or harvested using coagulation processes that employ a variety of chemicals (e.g., metal salts, polymers, and bases). To understand algae removal mechanisms, many researchers have correlated parameters such as chemical dose, algae cell density, and zeta potential to algae removal efficiency.

Previous research has agreed that precipitation of magnesium hydroxide is the key element in algae removal processes that utilize pH adjustment (Vandamme et al., 2012; Wu et al., 2012). Also it has been suggested that charge neutralization and sweep flocculation mechanisms associated with  $\text{Mg(OH)}_{2(s)}$  are responsible for algae removal.

Currently, however, a detailed understanding of the role of the various algae removal mechanisms associated with dissolved ions and solid phases of calcium and magnesium is still limited. In particular, the algae removal mechanisms associated with dissolved ion or solid phases have not been isolated in previous experimental work. For example, few studies have investigated heterocoagulation between algae and precipitated solids (e.g.,  $\text{CaCO}_{3(s)}$ ,  $\text{Mg(OH)}_{2(s)}$ ). While the importance of  $\text{Mg(OH)}_{2(s)}$  to the removal of microalgae is evident in the literature, the specific role of calcium is not yet clearly understood. In addition, metal adsorption on algae has been viewed with respect to metal removal not from the algae removal perspective. Moreover, the influence of algae removal mechanisms on the overall algae biomass concentration process and subsequent downstream process has not been fully evaluated.

Understanding the removal mechanisms involved in algae harvesting is critical because the overall success of algae biomass production does not depend solely on the effectiveness of algae removal but also on the co-dependence of algae removal with up and downstream processes in an end to end growth to product recovery system. For instance, the pH of the effluent needs to be adjusted when the water is discharged or recycled back to the algae growth stage. The higher the pH in the algae harvesting stage, the more chemical will be required for subsequent neutralization of the effluent.

Moreover, it is important to minimize the mass of solid (non-algae) material produced during the harvesting step in order to reduce costs for downstream processing.

Therefore, the focus of this research is on developing a more complete understanding of algae removal mechanisms associated with dissolved ions and solid phases of calcium and magnesium in the pH-induced flocculation/ deflocculation process for algae harvesting. The results will provide guidance for effective design and operation of the overall process that includes algae growth, harvesting, concentration and product recovery. In addition, implications of each removal mechanism on overall algae biomass production are discussed from an engineering perspective.

## Chapter 3: Research Approach

### 3.1. INTRODUCTION

The primary goal of this research is to investigate the mechanisms associated with coagulation of algae by calcium and magnesium ions and precipitates using a pH-induced flocculation/deflocculation method. It has been suggested that charge neutralization and sweep flocculation mechanisms associated with  $\text{Mg}(\text{OH})_{2(\text{s})}$  are responsible for algae removal (Vandamme et al., 2012; Wu et al., 2012). However, a detailed understanding of the role of the various algae removal mechanisms associated with the dissolved  $\text{Mg}^{2+}$  ion and/or  $\text{Mg}(\text{OH})_{2(\text{s})}$  is still limited. Moreover, most algae suspensions contain both calcium and magnesium unless the growth medium is synthesized to specifically remove one or more of these ions. While the importance of  $\text{Mg}(\text{OH})_{2(\text{s})}$  in the removal of microalgae has been identified in the literature, the specific role of calcium is not yet clearly understood. Not only does this limit optimization of the flocculation process, but it may also interfere with deflocculation of the algae if and when that is necessary for downstream processing of the algae biomass. In order to achieve process optimization through a better understanding of the roles of magnesium and calcium during harvesting processes, a series of research tasks were divided into three phases as follows:

- Phase I: Investigate the role of magnesium in the pH induced flocculation/deflocculation process in the absence of calcium

- Phase II: Investigate the role of calcium in the pH induced flocculation/deflocculation process in the absence of magnesium
- Phase III: Evaluate potential strategies for optimizing algae harvesting via pH-induced flocculation for varying water chemistries.

The specific roles of calcium and magnesium were studied independently to isolate the different potential mechanisms associated with each of these cations. Phase I and II included a series of controlled batch reactor experiments (e.g., adsorption tests, jar tests, and deflocculation tests) as outlined in Table 3-1. Experiments were designed to quantify algae removal, characterize precipitate formation, assess deflocculation potential and identify the mechanisms of algae removal. In Phase III, the findings from previous phases were used to analyze the jar test results from a wide range of source waters. The waters were characterized and jar tests were performed to determine whether the mechanisms and key parameters identified in the controlled experiments in Phases I and II were consistent with the results with actual source waters. Evaluation of these results was conducted to identify strategies for optimizing the algae harvesting process.

The following section provides the rationale for the experimental approaches and the purpose of each of the experiments conducted in this research.

Table 3-1 Experimental approach

Test Type	Experiments	Independent variables	Dependent variables
Adsorption tests	Adsorption kinetics	Time	Me <sup>2+</sup> adsorbed
	Adsorption isotherm	Initial Me <sup>2+</sup> conc, ionic strength, pH	Me <sup>2+</sup> adsorbed
	Adsorption jar test	Initial Me <sup>2+</sup> conc, ionic strength, pH	% algae removal, Me <sup>2+</sup> adsorbed
Jar tests	Seeded test	Amount of seed, initial algae cell density	% algae removal, Me <sup>2+</sup> in solution, amount of seed particle
	Unseeded test	Initial Me <sup>2+</sup> conc, initial algae cell density	% algae removal, Me <sup>2+</sup> in solution
	Precipitation test	pH, initial Me <sup>2+</sup> conc, initial algae cell density, initial carbonate conc	% algae removal, Me <sup>2+</sup> in solution
Deflocculation	same as left	Initial Me <sup>2+</sup> conc, pH	Amount of solid dissolved

Note: Me<sup>2+</sup> refers to the specific divalent cation being tested (e.g., Ca<sup>2+</sup> or Mg<sup>2+</sup>)

### 3.2. EXPERIMENTAL APPROACH: THE PURPOSE OF THE DIFFERENT TYPES OF TESTS

The goal of this research was to elucidate the specific algae removal mechanisms associated with calcium and magnesium in the pH-induced flocculation/deflocculation algae harvesting technology. Many factors including the characteristics of the surrounding water (e.g., pH, temperature, ion concentrations, and ionic strength) and the surface properties of algae (e.g., surface charge, cell wall composition) determine the fate of calcium and magnesium ions. Three potential options for the fate of these ions are anticipated during algae harvesting: remaining as dissolved ions, adsorption to the algae

biomass, or mineralization (precipitation). With respect to the latter precipitation may precede either via homogeneous nucleation or heterogeneous nucleation that occurs on the surface of algae. Once precipitated, the solids can also coagulate with the free algae (Heterocoagulation) to form larger flocs or serve as a template for nucleation of additional precipitates. Finally, it has been suggested that the precipitated solids may form flocs that enmesh free algae. Thus, precipitation of the divalent cations can provide algae removal through a variety of mechanisms (heteronucleation or heterocoagulation). In this work, coagulation/flocculation of algae (and precipitate) via heteronucleation is referred to as precipitation-enhanced coagulation rather than the more traditional sweep flocculation term used in water treatment literature.

Adsorption of metal ions can also serve as a mechanism for algae destabilization. For instance, as the positively charged metal ions are adsorbed to the negatively charged algae surface, electrostatic repulsion can be reduced and destabilized particles can aggregate with each other (i.e., adsorption and charge neutralization). Moreover, as the ionic strength of a solution increases, the diffuse layer of the particle is compressed leading to reduction in the repulsive force and aggregation (i.e., compression of the diffuse layer). The possible algae destabilization mechanisms expected in this research are schematically described in Figure 3-1.

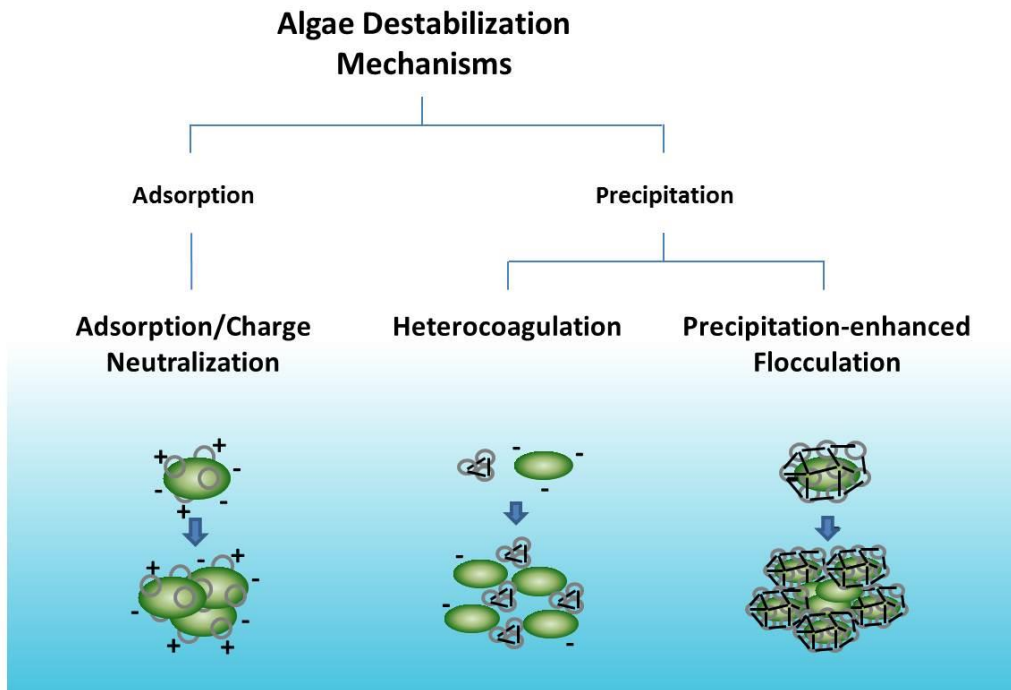


Figure 3-1 Schematic diagram of potential mechanisms of algae destabilization

In order to experimentally isolate and evaluate each of the potential mechanisms of algae destabilization, adsorption tests and jar tests listed in Table 3-1 were designed. For example, adsorption tests were designed to assess the role of calcium and magnesium ions that destabilize algae via a charge neutralization mechanism. Conducting the experiments in a CO<sub>2</sub>-free environment allows Ca adsorption to be evaluated in the absence of precipitation of CaCO<sub>3(s)</sub>. Adsorption kinetic tests, as shown in Figure 3-2, were conducted to determine the time required to reach an equilibrium state. Adsorption isotherms (i.e., adsorption of calcium or magnesium ions on the surface of algae at equilibrium and constant temperature) were conducted to characterize the adsorption

behavior during the algae harvesting processes. In addition, selected adsorption jar tests were conducted to quantify the algae removal associated with adsorption over a range of ionic strengths. These tests were conducted in the absence of CO<sub>2</sub>.

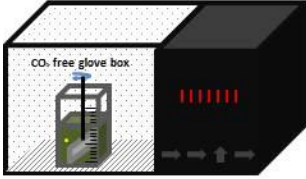
	<b>Adsorption Kinetics</b>	<b>Adsorption Isotherms</b>	<b>Adsorption Jar tests</b>
	Algae conc: 3 g/L pH: 9.7 and 10.6 Me <sup>2+</sup> conc: 3 mM	Algae conc: 3 g/L pH: 9.7 and 10.6 Me <sup>2+</sup> conc: varied up to 8 mM Ionic strength: 0.01, 0.1 M	Algae conc: 3g/L pH: 9.7 and 10.6 Me <sup>2+</sup> conc: 3 mM Ionic strength: 0.01, 0.1, 0.4 M

Figure 3-2 Schematic diagram of a series of batch reactor adsorption tests (e.g., adsorption kinetics, isotherms, and jar tests).

Jar tests were designed to elucidate the potential mechanisms in various water sample conditions (e.g., pH, ion concentration, type and concentration of algae, ionic strength). Jar tests as shown in Figure 3-3 included experiments conducted with pre-precipitated solids added (seeded tests), tests in which the algae and alkaline earth metal ions were added prior to pH adjustment (unseeded tests), and variable pH tests in which the pH of unseeded solutions was varied. The seeded tests were conducted to evaluate heterocoagulation via the addition of pre-precipitated solids (e.g., Mg(OH)<sub>2(S)</sub> or CaCO<sub>3(S)</sub>) to the algae sample solution. Unseeded tests were conducted to evaluate the effectiveness of the adsorption/charge neutralization and/or precipitation-enhanced coagulation mechanisms on algae removal via the addition of dissolved magnesium and

calcium ions prior to the jar tests. Variable pH tests were conducted to further elucidate the adsorption/charge neutralization and precipitation-enhanced coagulation mechanisms by monitoring the fraction of metal and algae removed from solution as a function of pH.

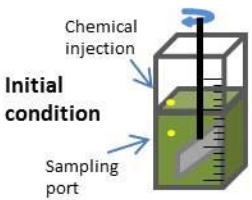
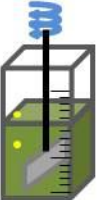
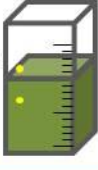
Jar test procedure	Seeded test	Unseeded test	Variable pH test
	Algae conc: varied 0.1 – 2.0 g/L pH: 10.6	Algae conc: varied 0.1 -2.0 g/L pH: 7.8 Me <sup>2+</sup> : varied up to 8 mM	Algae conc: 0.26 – 3.0 g/L pH: 7.8 Me <sup>2+</sup> : varied up to 8 mM Alkalinity: 1, 3, 10 meq/L Ionic strength: 0.01, 0.1, 0.4 M
<b>1 min rapid mixing</b> 		pH adjustment: fixed to 10.6	pH adjustment: varied up to 11.5
<b>20 min slow mixing</b> 	Addition of pre-precipitated solid: varied up to 1000 mg/L as Me <sup>2+</sup>		
<b>20min sedimentation</b> 			
	Sample collection	Sample collection	Sample collection
	Sample collection	Sample collection	Sample collection
	Sample collection	Sample collection	Sample collection

Figure 3-3 Schematic diagrams of a series of batch reactor jar test procedures (e.g., seeded test, unseeded test, and variable pH test). Typical jar test procedures were employed.

One of the challenges associated with algae harvesting using the pH-induced coagulation process is that the flocculated solids that are removed in the sedimentation process may need to be deflocculated or restabilized in order to generate an algae concentrate suitable for downstream processing. Thus, deflocculation tests were designed to examine the validity of the pH-induced flocculation/ deflocculation process as shown in Figure 3-4. One approach for the deflocculation step in the pH-induced flocculation/ deflocculation process is to mix CO<sub>2</sub> gas or an aqueous HCl solution through the algae/precipitate concentrate produced in the flocculation step. Either of these procedures lowers the pH of the concentrate and allows separation of the algae from the precipitated solids (e.g., CaCO<sub>3(s)</sub> or Mg(OH)<sub>2(s)</sub>) that are re-dissolved as the system becomes undersaturated with respect to the precipitated phases. Although both acids can lower the pH of the water, HCl is a stronger acid that has a greater impact on the conductivity and ionic strength of the deflocculated concentrate. This increase in conductivity and ionic strength is detrimental to certain lysing processes. As a result, CO<sub>2</sub> gas was the preferred acid for the deflocculation process.

Detailed materials and experimental methods utilized in this research are described in each of the following chapters.

### Deflocculation test procedure

---

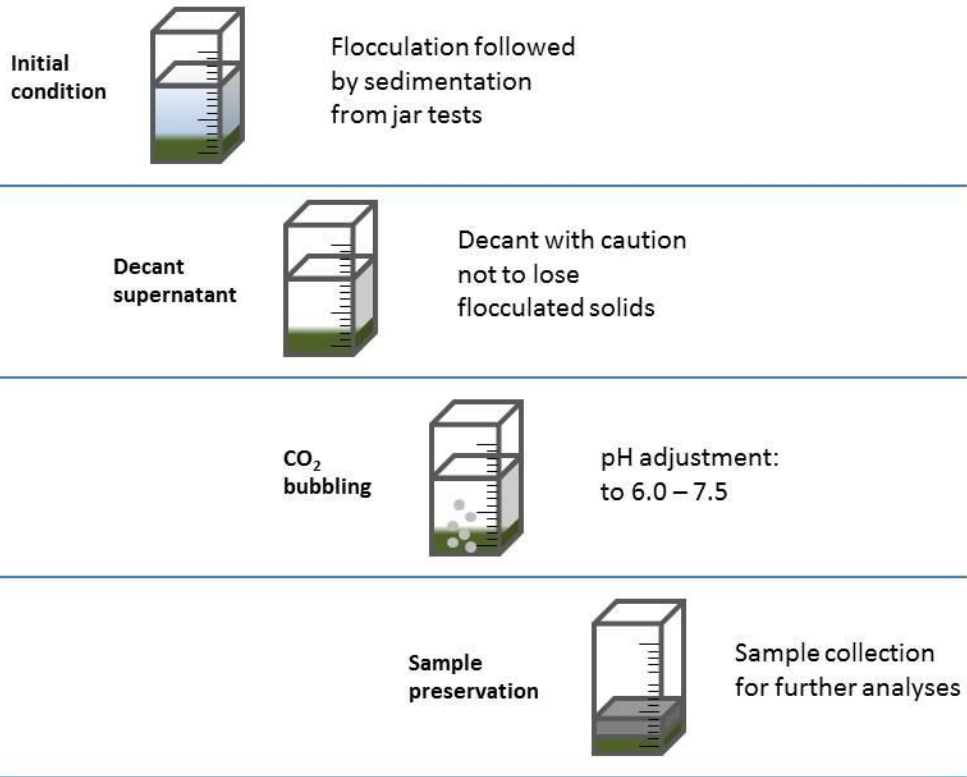


Figure 3-4 Schematic diagram of a series of batch reactor deflocculation tests. The variable pH test preceded the deflocculation test for the preparation of the sample solution.

## **Chapter 4: The role of magnesium on algae removal mechanisms and practical implications on algae harvesting process**

### **4.1. INTRODUCTION**

Microalgae have attracted public attention for their potential use as a source of biofuel and in a wide range of natural products. These applications require the development of a large-scale cultivation system for mass production (Del Campo et al, 2007; Li et al., 2011; Chiaramonti et al., 2013) that includes growth, harvesting, concentration, and product recovery. While challenges still remain with respect to many of the processes involved in mass production, one of the most technically and economically challenging steps is harvesting the algae from dilute growth cultures, especially in systems where the addition of chemical additives is of concern either within the algae concentrate or the effluent. For this reason, a pH-induced flocculation/deflocculation method using base (e.g., lime, caustic soda) to raise the pH is of particular interest for algae harvesting.

pH-induced flocculation is conceptually similar to the lime softening process which has been adopted in drinking water treatment plants and implemented at large scale. In this process, lime (and sometimes soda ash,  $\text{Na}_2\text{CO}_3$ ) is added to waters containing high concentrations of  $\text{Ca}^{2+}$  and/or  $\text{Mg}^{2+}$  in a rapid mix basin. The solution is then slowly mixed for a period of time to induce precipitation (of  $\text{Mg}(\text{OH})_{2(\text{s})}$  and  $\text{CaCO}_{3(\text{s})}$ ) and enmeshment of colloidal and suspended solids such as algae. The slurry is then transported to a sedimentation basin to facilitate solid/liquid separation.

Previous research focused on removal of algae has shown that increasing the pH between 10 and 12 using bases such as lime and NaOH was effective in algae removal and/or harvesting (Folkman and Wachs, 1973; Ayoub and Koopman, 1986; Elmaleh et al., 1996; Knuckey et al., 2006; Harith et al., 2009). Researchers have agreed that precipitation of  $\text{Mg}(\text{OH})_{2(\text{s})}$  is a key factor controlling the removal of algae from the suspension (Vandamme et al., 2012; Wu et al., 2012). It was postulated that the  $\text{Mg}(\text{OH})_{2(\text{s})}$  precipitate has a large adsorptive surface area and a positive surface charge, which attracts negatively charged colloidal particles, including  $\text{CaCO}_{3(\text{s})}$  flocs, thus inducing adsorption and agglomeration (Semerjian and Ayoub, 2003). They posited charge neutralization and sweep flocculation as the primary mechanisms of algae flocculation, which is consistent with the mechanisms proposed previously using other coagulation agents such as metal salts (Stumm and O'Melia, 1968; Tenney et al., 1969; Edzwald and Wingler, 1990; Bernhardt and Clasen, 1991). However, few studies have isolated the optimal operating conditions or assessed the removal potential of each of these mechanisms. Moreover, since many applications of algae require that the algal suspensions be free flowing (pumpable), deflocculation of the concentrated biomass is of concern. Few studies have examined the potential for deflocculation of the algae enmeshed with  $\text{Mg}(\text{OH})_{2(\text{s})}$ .

In this chapter, the specific algae removal mechanisms associated with removal of dissolved  $\text{Mg}^{2+}$  and algae during pH-induced flocculation was investigated using the microalgae, *Scenedesmus* sp. A series of batch reactor tests were conducted to evaluate

possible algae destabilization mechanisms that included; heterocoagulation with  $\text{Mg}(\text{OH})_{2(\text{s})}$ , adsorption and charge neutralization, and enmeshment/precipitation.

## **4.2. MATERIALS AND METHODS**

### **4.2.1. Preparation of the algae sample solution**

The algae culture (an AlgEternal proprietary polyculture consisting primarily of a *Scenedesmus* sp.) was obtained from the AlgEternal vertical reactor facility located at the Center for Electromechanics (CEM) at the University of Texas at Austin. *Scenedesmus* sp. (10  $\mu\text{m}$  in size) was selected for this research because *Scenedesmus* sp. are appropriate for biodiesel production due to their high lipid content (Mandal and Mallick, 2009; Jena et al., 2012). Cultures were collected in 5 gallon buckets and then stored at room temperature (20°C) for 30 min to allow time for possible debris from the reactor to settle. Algae was centrifuged at 5000 rpm for 15 min at 20°C and then resuspended in softened water (tap water treated via ion exchange) to achieve the target algae cell density required for each experiment. The concentrations of the major ions in the softened water are listed in Table 4-1.

The target magnesium ion concentrations were achieved by adding analytical grade hexahydrated magnesium chloride (i.e.,  $\text{MgCl}_2 \cdot 6\text{H}_2\text{O}$ ) to algae-resuspended solutions to achieve the desired levels for each experiment. Calcium was not supplemented to exclude the effects of calcium ion or precipitated  $\text{CaCO}_{3(\text{s})}$ . For the experiments where pre-precipitated  $\text{Mg}(\text{OH})_{2(\text{s})}$  (i.e., “seed”) was required, a known amount of salt ( $\text{MgCl}_2 \cdot 6\text{H}_2\text{O}$ ) was added to deionized water. The pH of each solution

was raised to induce precipitation and allowed to equilibrate for 24 hours and stabilize at pH 10.6. The resulting supernatant was gently decanted, and the solids that settled on the bottom were used as seed during the jar tests. Analytical grade sodium chloride (i.e., NaCl) was used if the ionic strength of the solutions needed to be adjusted.

Table 4-1 The concentrations of the major ions in the softened water

Major ions	Concentration (mg/L)
Ca	0.015
Mg	0.004
K	0.003
Na	0.079
Si	0.137
Cl	44.3
HCO <sub>3</sub>	0.98meq/L
SO <sub>4</sub>	Non-detect
NO <sub>3</sub>	Non-detect
PO <sub>4</sub>	1.194 (mg/L-P)

#### 4.2.2. Adsorption experiments

The adsorption isotherm experiments were conducted in a CO<sub>2</sub>-free nitrogen glove box to minimize the impact of CO<sub>2</sub> exchange on pH measurements. An algae pellet prepared by centrifugation was resuspended in deionized water and then centrifuged again. This washing procedure was repeated four times and a desired cell density of 3 g/L was achieved. The algae sample solution was degassed using N<sub>2</sub> gas for an hour and then

placed in the glove box. The “subsequent addition method” experimental procedure suggested by Pagnanelli et al (2000) was adopted as follows: after the first addition of a concentrated solution of CaCl<sub>2</sub> or MgCl<sub>2</sub> (250 mM), the pH of the algae solution in agitation was adjusted and the first 2 mL of sample was taken. After the established time for equilibrium (40 min) elapsed, 2 mL of sample was taken from the suspension. The collected samples were immediately filtered and analyzed to determine the dissolved metal ion concentration. A concentrated solution was added to (and mixed with) the algae solution for a second time and the previous procedure was repeated while maintaining the pH, if necessary. The experimental data points were fit to the Langmuir isotherm model as shown in Equation 4-1 below:

$$q = \frac{q_{max}k_aC_{eq}}{1 + k_aC_{eq}} \quad (4-1)$$

where  $q_{max}$  (mg of magnesium per gram of algae ) is the adsorption capacity,  $k_a$  (liter per mg of magnesium) is the equilibrium constant, and  $C_{eq}$  (mg of magnesium per liter) is the magnesium concentration at equilibrium.

#### **4.2.3. Jar tests**

A series of batch reactor jar tests were conducted to elucidate the potential mechanisms responsible for algae removal in the algae harvesting process. The typical jar test procedure adopted for this research included rapid mixing of sample solutions for 1

min using a magnetic stirrer, followed by slow mixing at 30 rpm for 20 min with a Phipps & Bird standard 6-paddle jar tester (Richmond, VA), followed by 20 min of quiescent conditions to allow time for settling. A sodium hydroxide solution (1M) was used as the primary base rather than lime to isolate the effects of pH from calcium ions. Depending on the focus of each experiment (e.g., seeded test, unseeded test, and variable pH test), base or pre-precipitated solids were added at the appropriate stage in the jar test procedure.

In the seeded tests, pre-precipitated  $\text{Mg}(\text{OH})_{2(\text{s})}$  was added to evaluate the heterocoagulation mechanism in which two dissimilar particles (e.g., algae and  $\text{Mg}(\text{OH})_{2(\text{s})}$ ) are attracted to each other. Pre-precipitated  $\text{Mg}(\text{OH})_{2(\text{s})}$  (i.e., seed solution) was added to the algae slurry that contained the same equilibrium ionic concentration as the seed solution (i.e., the dissolved  $\text{Mg}^{2+}$  concentration in the seed solution was the same as in the algae slurry in the beaker) at the beginning of the slow mixing stage. All tests were conducted at a fixed pH of 10.6. The pH of each solution was checked periodically ( $\text{pH } 10.6 \pm 0.01$ ) to confirm that no additional precipitation or dissolution occurred during the experiments. The concentrations of pre-precipitated  $\text{Mg}(\text{OH})_{2(\text{s})}$  were varied (up to 1000 mg/L as  $\text{Mg}^{2+}$ ) to achieve a target algae removal efficiency (e.g., 90% algae removal) for algae cell densities ranging from 0.1 to 1.5 g/L.

In the unseeded tests, dissolved magnesium ions were added prior to the jar tests to evaluate the effectiveness of the adsorption/charge neutralization and/or precipitation-enhanced coagulation mechanisms on algae removal. The initial  $\text{Mg}^{2+}$  concentration was varied from 1 to 8 mM for algae cell densities ranging from 0.2 to 1.5g/L to

determine the conditions at which 90% algae removal efficiency was achieved at pH 10.6.

In the variable pH tests, the concentration of magnesium and algae remaining in solution was monitored as a function of pH to further distinguish adsorption/charge neutralization from precipitation-enhanced coagulation mechanisms within the unseeded tests. The target pH of the sample solutions (from 9.5 to 11.5) was achieved during the rapid mixing stage for initial  $\text{Mg}^{2+}$  concentrations and algae cell densities ranging from 25 to 200 mg/L and 0.2 to 1.4 g/L, respectively.

#### **4.2.4. Deflocculation tests**

Deflocculation tests were conducted to examine the potential for deflocculation of the algae/ $\text{Mg}(\text{OH})_{2(\text{s})}$  flocs. The supernatant from the variable pH test was decanted to leave 10 % (by volume) of the original solution.  $\text{CO}_2$  was then bubbled through the remaining flocculated solids (e.g., concentrate containing algae/ $\text{Mg}(\text{OH})_{2(\text{s})}$  precipitate) until the target pH of 7.5 was reached. A sample of the acidified solution was collected for further analyses (e.g., microscopic analysis, ion concentration, and chemical composition of residual solids) to examine the extent of deflocculation of the algae and precipitated solids.

#### **4.2.5. Analytical methods**

Samples were collected at various stages in the experiments for further analyses. Prior to initiating an experiment, algae cells were filtered through a 0.2  $\mu\text{m}$  nitrocellulose membrane filter (Millipore, U.S.A) to measure the total suspended solid (TSS)

concentration and to determine the algae cell density (g/L). The alkalinity was determined in accordance with Standard Method 2320B except a 0.1 M nitric acid (HNO<sub>3</sub>) titrant was used instead of sulfuric acid (H<sub>2</sub>SO<sub>4</sub>). Five mL samples of the original algae sample solution and the supernatant of treated water were filtered through a 0.2 µm nitrocellulose membrane syringe filter (Millipore, U.S.A) and the metal ion concentrations were measured using inductively coupled plasma-optical emission spectrometer (ICP-OES, Varian 710-ES, U.S.A). A 0.05 mL sample was collected without filtration at the end of the slow mixing step of the jar tests for scanning electron microscopy (SEM) observation combined with energy dispersive X-ray (EDX) analysis using a FEI QUANTA 200 (Hillsboro, OR). For this analysis, a few drops of algae or algae-laden flocs were placed on black carbon tape attached on an aluminum alloy sample tray. Because the samples must be dried for this analysis, excess water droplets were removed by gently touching a “Kimwipe” to the surface of the droplets and using interfacial tension to remove excess water. This avoids a build-up of salts on the surface of the solids. The solids were then air-dried prior to the Au/Pd coating process. At the end of each jar test and adsorption test, the algae removal efficiency (%) was evaluated by comparing the optical density at 664 nm present in the original water to that present in the supernatant of the treated water as shown in Equation 4-2 below. The optical density was measured using an Agilent 8453E UV-visible Spectroscopy system with a 1-cm cuvette.

$$\text{Algae percent removal (\%)} = \left(1 - \frac{OD_S}{OD_O}\right) \times 100 \quad (4-2)$$

where  $OD_S$  is the optical density (664 nm) of supernatant after settling 20min and  $OD_O$  is the optical density of original algae sample solution prior to pH adjustment.

Based on the metal ion concentrations measured, magnesium removal (%) was evaluated using Equation 4-3 below:

$$\text{Percent magnesium removal (\%)} = \left(1 - \frac{\text{Conc. } S}{\text{Conc. } O}\right) \times 100 \quad (4-3)$$

where  $\text{Conc. } S$  is the concentration of dissolved magnesium ions in the filtered sample after the 20 min of quiescent settling and  $\text{Conc. } O$  is the concentration of dissolved magnesium ions in the filtered original sample prior to pH adjustment.

To verify the level of precipitation and compare the experimental data to equilibrium model predictions, an equilibrium model, Visual Minteq was used throughout the research.

### **4.3. RESULTS AND DISCUSSION**

#### **4.3.1. Adsorption isotherms**

Adsorption of cations onto the algae (as a potential biosorbent) has been investigated for a range of cations including toxic heavy metals, alkali, and alkaline-earth

metals (Crist et al., 1990; Schiewer and Volesky, 1997). The potential for adsorption of  $Mg^{2+}$  onto the microalgae found in this research is shown in Figure 4.1.

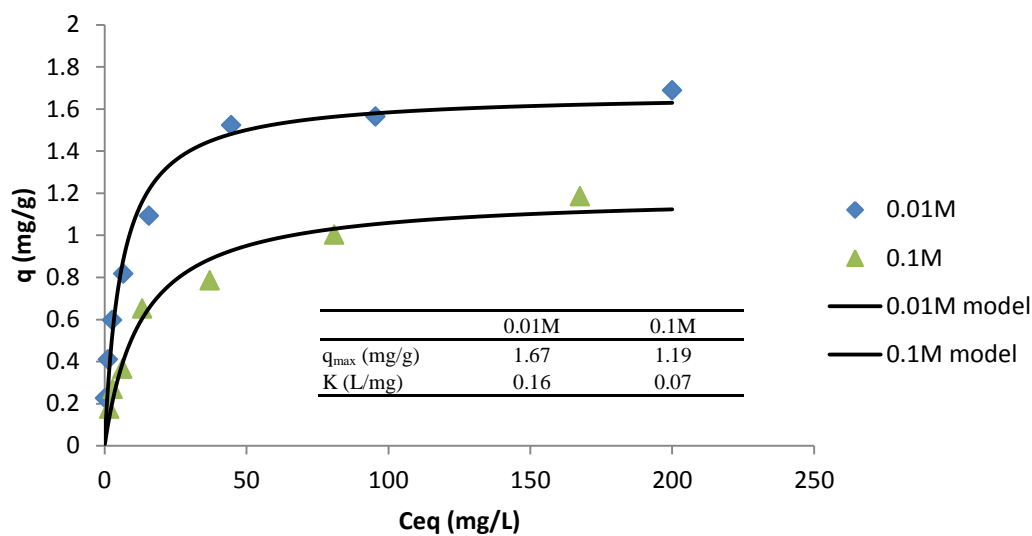


Figure 4-1 Adsorption isotherms and Langmuir model fits of  $Mg^{2+}$  sorption to *Scenedesmus* sp. at  $pH = 9.6 \pm 1$  at varying ionic strength (0.01 M and 0.1 M). Langmuir isotherm model fits (solid lines) were obtained using non-linear regression.

Langmuir model fits to data collected at  $pH 9.6 \pm 1$  yielded adsorption capacities,  $q_{max}$ , and equilibrium adsorption constants,  $k_a$  of 1.67 and 1.19 mg of magnesium per gram of algae and 0.16 and 0.07 liter per mg of magnesium, respectively for the ionic strengths of 0.01 and 0.1 M. Adsorption of magnesium was reduced at higher ionic strength. Magnesium ion is known as a weakly sorbing alkaline earth metal ion that is often noted to form outer sphere complexes, and sorption of this metal on mineral

surfaces typically decreases with increasing ionic strength of the solution (Chen et al., 2006). The adsorption of  $Mg^{2+}$  has the potential to reduce the negative surface charge of the algae which can lead to charge neutralization or compression of the electrical double layer. In addition, the accumulation of Mg on the surface of the algae can provide nucleation sites for  $Mg(OH)_{2(s)}$  precipitation as described in Chapter 2.

#### **4.3.2. Algae removal via heterocoagulation vs adsorption and/or precipitation**

Seeded and unseeded batch experiments were designed to isolate each algae destabilization mechanism as described in Figure 3-1 (heterocoagulation in the seeded tests and adsorption and/or precipitation-enhanced coagulation in the unseeded tests). These two types of tests were initially compared as shown in Figure 4-2. The amount of magnesium added as either dissolved  $Mg^{2+}$  or pre-precipitated  $Mg(OH)_{2(s)}$  that yields 90% algae removal is plotted as a function of algae cell density. The results show that addition of pre-precipitated  $Mg(OH)_{2(s)}$  (seeded test) is much less effective at algae removal compared to the simultaneous addition of algae,  $Mg^{2+}$ , and NaOH (unseeded tests). Nevertheless, heterocoagulation between algae and  $Mg(OH)_{2(s)}$  can achieve 90 percent removal of *Scenedesmus* sp.

$Mg(OH)_{2(s)}$  floc exhibits a gelatinous structure (Faust et al., 1998) and has a relatively high pH of point of zero charge. Parks (1967) reported a  $pH_{pzc}$  of approximately 12.4 and McLaughlin et al. (1993) reported an even higher value of 13.2. Moreover, precipitation of  $Mg(OH)_{2(s)}$  in the presence of excess  $Mg^{2+}$  produces coarse particles with better settleability than fine particles produced in the presence of excess

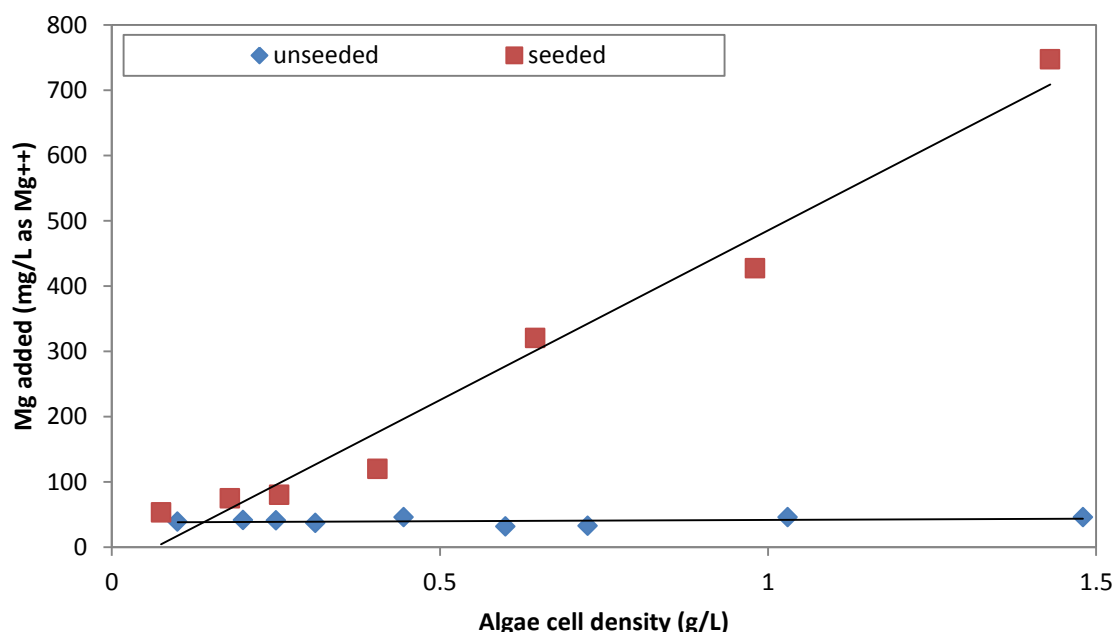


Figure 4-2 Magnesium addition required to achieve an algae removal efficiency of 90% as a function of algae cell density. Dissolved magnesium ions and pre-precipitated  $\text{Mg}(\text{OH})_{2(\text{s})}$  were added for unseeded and seeded tests, respectively. The pH of the sample solutions were maintained at 10.6 for all tests.

$\text{OH}^-$  (Turek and Gnot , 1995; Alamdari et al., 2008). For both seeded and unseeded tests, precipitation of  $\text{Mg}(\text{OH})_{2(\text{s})}$  was initiated at high activity ratio ( $\{\text{Mg}^{2+}\}/\{\text{OH}^-\}$ ). Thus, it is not surprising that high algae removal efficiencies (90% or higher) were achieved within the given retention time (20 min) regardless of whether pre-precipitated  $\text{Mg}(\text{OH})_{2(\text{s})}$  (seeded tests) was added to the algae slurry or  $\text{Mg}(\text{OH})_{2(\text{s})}$  was precipitated within the algae slurry (unseeded tests). However, with increasing algae cell density, adsorption to pre-precipitated solids in the seeded tests became increasingly less effective at algae removal compared to algae removal in the unseeded tests as indicated by the

steeper rise in required magnesium addition (to achieve 90 percent algae removal) with increasing cell density. These trends are supported by SEM observations as shown in Figure 4-3 which illustrate the degree of algae flocculation within the seeded and unseeded algae slurries.

The images in Figure 4-3 show that preformed  $\text{Mg}(\text{OH})_{2(s)}$  precipitated solids exhibit an amorphous structure (panel A). Algae are attached to the amorphous  $\text{Mg}(\text{OH})_{2(s)}$  precipitates in the seeded algae slurries (panels B and C), but the algae are sparsely distributed within the  $\text{Mg}(\text{OH})_{2(s)}$  floc under these heterocoagulation conditions. In contrast, algae are extensively flocculated in the unseeded algae slurry, and  $\text{Mg}(\text{OH})_{2(s)}$  precipitates are sparsely distributed within the algae floc (panel D).

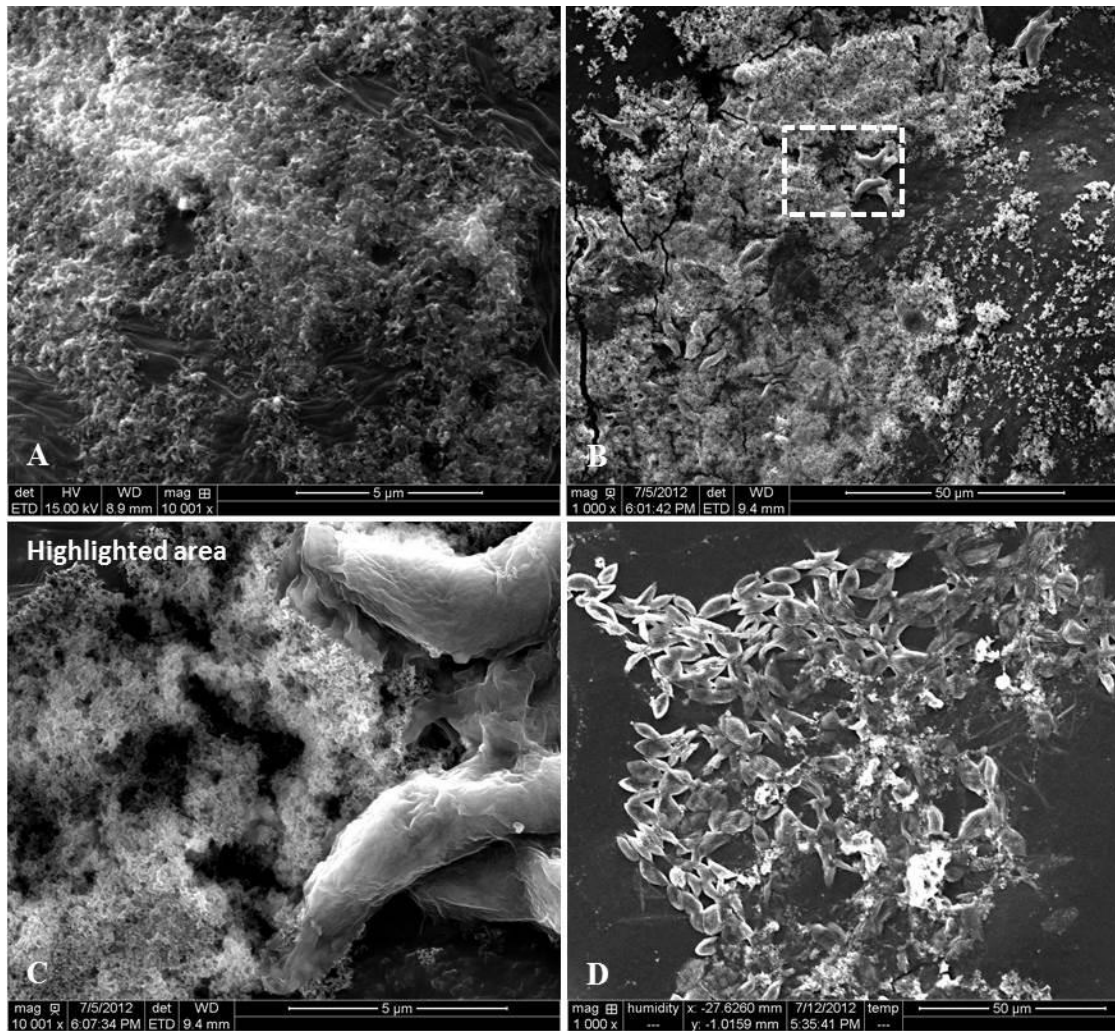


Figure 4-3 SEM images for preformed  $\text{Mg}(\text{OH})_{2(s)}$  precipitated solids (A), flocs in  $\text{Mg}(\text{OH})_{2(s)}$  seeded algae slurries (B, C), and  $\text{Mg}(\text{OH})_{2(s)}$  flocs formed within the algae slurry (unseeded tests) (D) for an algae cell density and pH of 0.26 g/L and 10.6, respectively. The quantity of  $\text{Mg}^{2+}$  added in the unseeded tests was 25 mg/L (D). The amorphous structure of preformed  $\text{Mg}(\text{OH})_{2(s)}$  precipitated solids is evident in panels A, B, and C.

### **4.3.3. Algae removal via adsorption/ charge neutralization vs precipitation-enhanced coagulation**

To further distinguish adsorption/charge neutralization from precipitation-enhanced coagulation mechanisms within the unseeded tests, a series of variable pH tests were performed over a range of pH values for different algae cell densities and initial  $Mg^{2+}$  concentrations. As shown in Figure 4-4, for all the algae cell densities and initial  $Mg^{2+}$  concentrations tested, algae removal efficiency increased with increasing pH of the solution. This result is expected given that both  $Mg^{2+}$  adsorption and  $Mg(OH)_{2(s)}$  precipitation increase with increasing pH, but confirms that algae removal is attributed, at least in part to  $Mg^{2+}$  removal by adsorption and/or precipitation (See Figure 4-6). In Figure 4-5, in which algae removals for two initial  $Mg^{2+}$  concentrations (25 and 100 mg/L) were replotted as a function of pH for three different algae cell densities, algae removal does not appear to be dependent on algae cell density for the higher initial  $Mg^{2+}$  concentration (i.e., 100 mg/L), but at lower pH, below 10.3, algae removal increases with decreasing algae cell density for the lower initial  $Mg^{2+}$  concentration (i.e., 25 mg/L). These results suggest that, at the low initial  $Mg^{2+}$  concentration, there is a limited amount of  $Mg^{2+}$  available for interaction with the algae, and the algae removal process is vulnerable to changes in algae cell density.

To further explore the relationship between  $Mg^{2+}$  and algae removal,  $Mg^{2+}$  removal for these experiments was also monitored as shown in Figure 4-6.

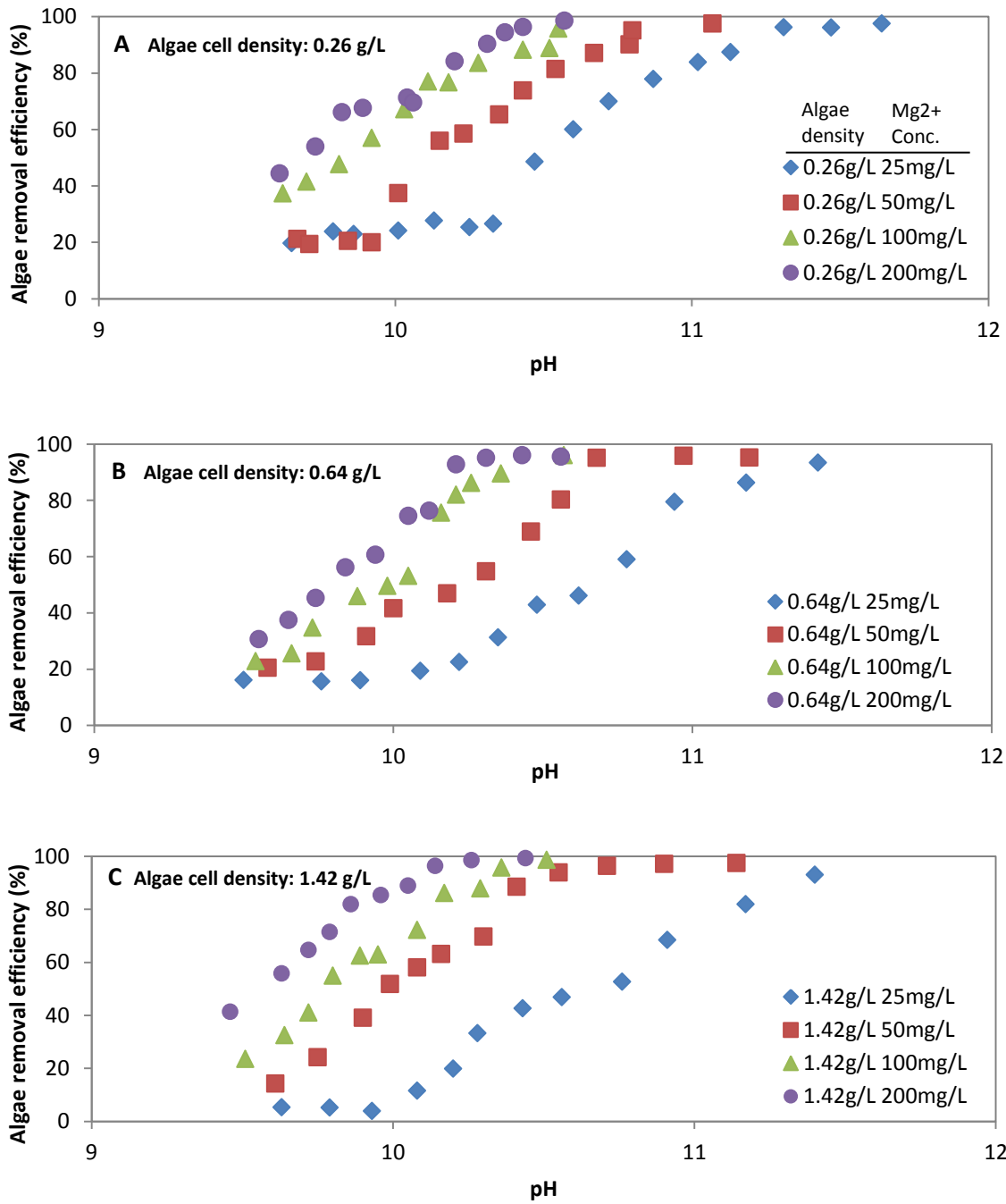


Figure 4-4 Algae removal as a function of pH for a range of initial Mg<sup>2+</sup> concentrations (25-200 mg/L as Mg<sup>2+</sup>) and algae cell densities (A: 0.26 g/L, B: 0.64 g/L, C: 1.42 g/L) in unseeded algae slurries.

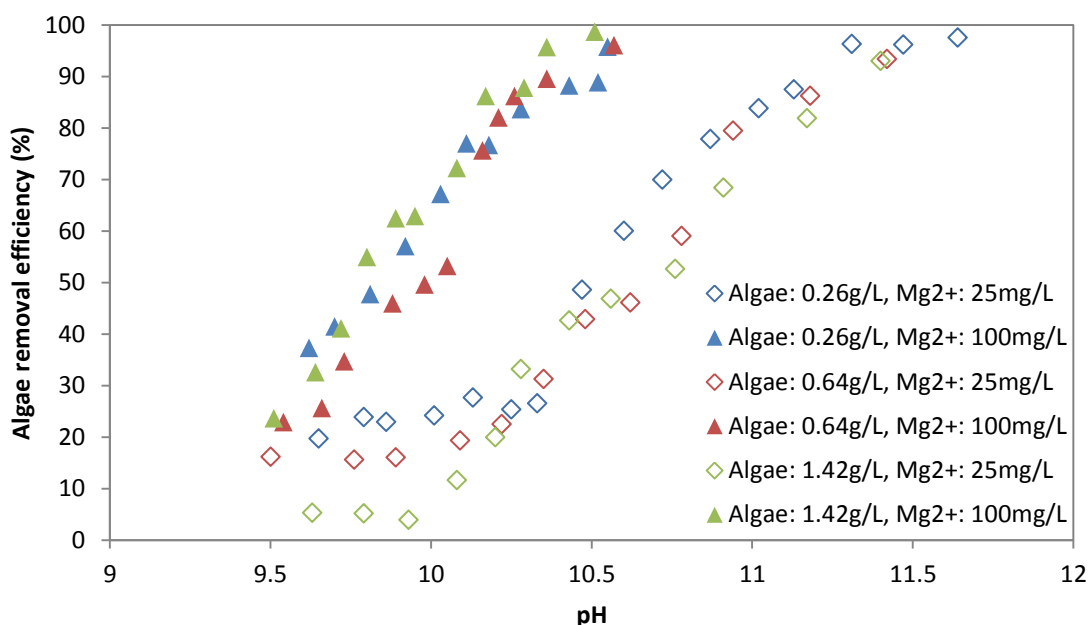


Figure 4-5 Algae removal as a function of pH for initial  $Mg^{2+}$  concentrations of 25 and 100 mg/L as  $Mg^{2+}$  and algae cell densities (A: 0.26 g/L, B: 0.64 g/L, C: 1.42 g/L) in unseeded algae slurries.

In Figure 4-6, two trends are apparent in the data. First, for lower  $Mg^{2+}$  doses,  $Mg^{2+}$  removal increases with increasing algae concentration (by comparing parts A, B, and C of the figure). Second,  $Mg^{2+}$  removal appears to increase with increasing Mg added, though more dramatically at lower algae cell densities. This latter trend is consistent with precipitation of  $Mg(OH)_{2(s)}$  as the increase in Mg increases the ion activity product for  $Mg(OH)_{2(s)}$  solubility. The increase in percent  $Mg^{2+}$  removal with increasing initial  $Mg^{2+}$  concentration is clearly observed in the model prediction for percent  $Mg^{2+}$  removal due to precipitation of  $Mg(OH)_{2(s)}$  as shown in Figure 4-6. However, as seen in Figure 4-6, the systems appear to be undersaturated with respect to amorphous  $Mg(OH)_{2(s)}$  (i.e., the model lines do not show a rise in  $Mg^{2+}$  removal until much higher pH values than was found experimentally).

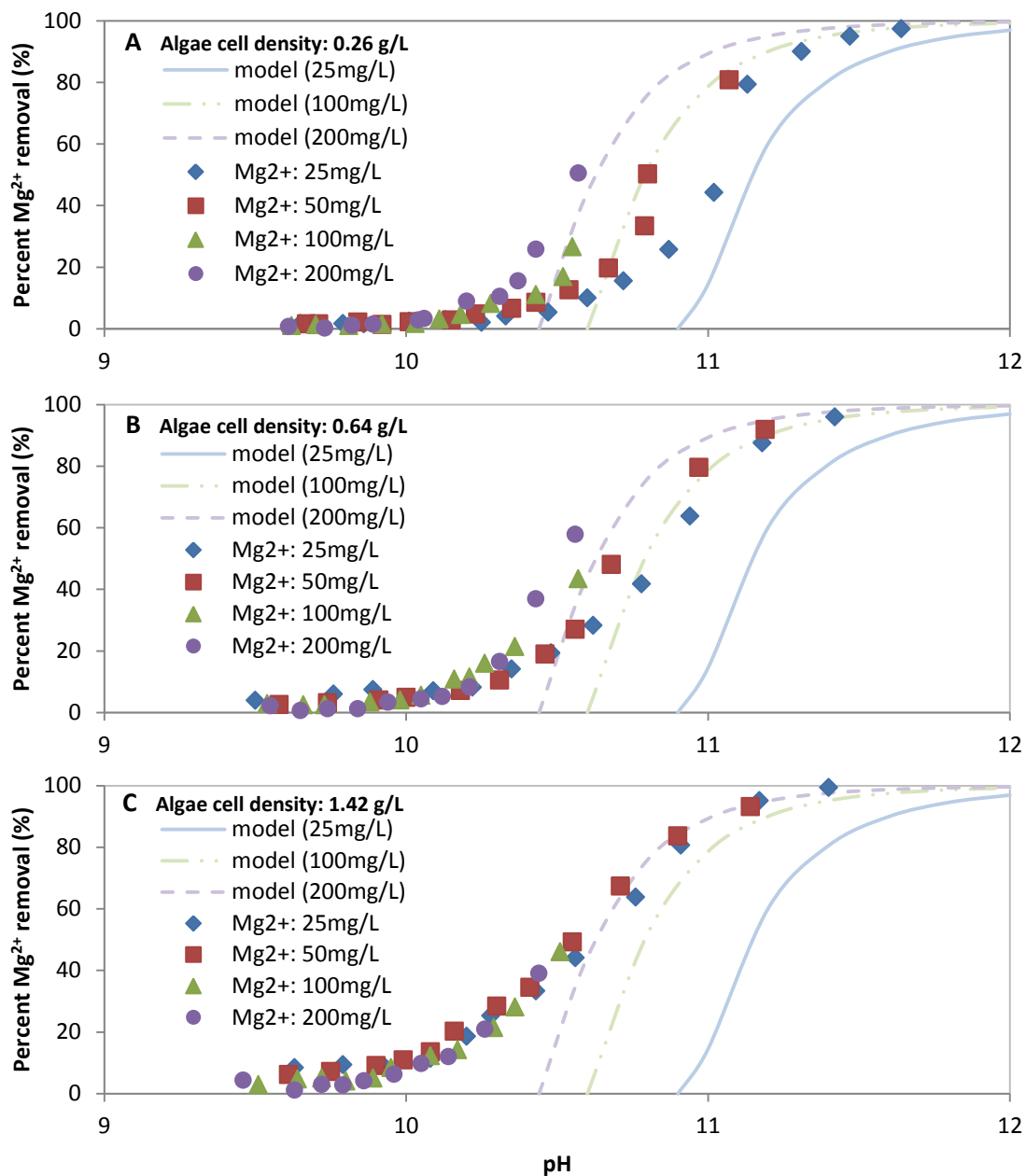
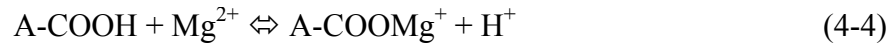


Figure 4-6 Mg<sup>2+</sup> removal (symbols) and Minteq model (lines) predicted removal (due to Mg(OH)<sub>2(active)</sub> precipitation) as a function of pH for a range of initial Mg<sup>2+</sup> concentrations and algae cell densities (A: 0.26 g/L, B: 0.64 g/L, C: 1.42 g/L).

Further examination of the data at lower pH (pH < 10) shows different trends in the data (Figure 4-7). At lower pH, the highest Mg<sup>2+</sup> concentration of 200 mg/L exhibited the lowest percent Mg<sup>2+</sup> removal for all algae cell densities. This trend is consistent with pH dependent adsorption to specific sites on the algae as shown in the following reactions in which A-COOH and A-POH represent surface sites on the algae (Brady et al., 2014).



Previous research has shown that alkaline earth metals interact with algae via relatively weak electrostatic bonding (Crist et al., 1988). As pH increases, functional groups on the surface of algae such as carboxyl (-COOH) and amino (-NH<sub>2</sub>) groups deprotonate and provide more sites for magnesium to be adsorbed. Since metal ion adsorption on algae is a site specific reaction, the amount of Mg<sup>2+</sup> ions that can be removed at a particular pH is dependent on the number of available sites, which is a function of algae cell density. Thus, the decrease in percent Mg<sup>2+</sup> removal with increasing initial Mg<sup>2+</sup> concentration and the pH dependent adsorption can be attributed to surface complexation reactions and surface site mass balance considerations.

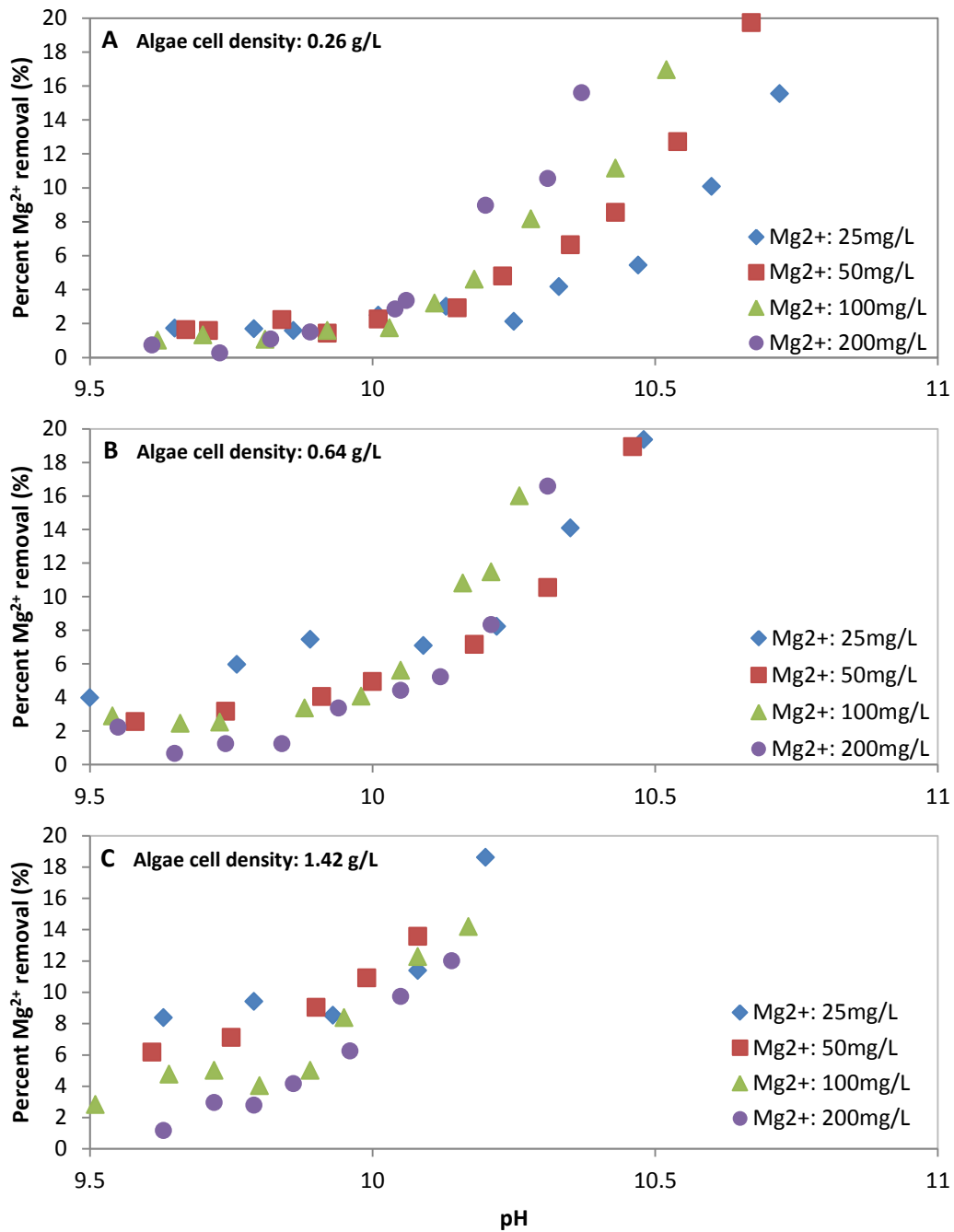


Figure 4-7  $Mg^{2+}$  removal as a function of pH for low Mg percent removal and varying algae cell densities: (A) 0.26 g/L; (B) 0.64 g/L; (C) 1.42 g/L respectively.

The data for Mg removal presented in Figures 4-6 showed a trend in adsorption consistent with precipitation; higher Mg concentrations lead to more precipitation. Certainly, it is also true that more Mg removal occurs with higher Mg concentration, though plotting percent removal may not reflect this visually. The reversal in the trends associated with  $Mg^{2+}$  addition at low and high pH apparent in Figure 4-7 suggests that the mechanism of adsorption changes over the pH range examined. Even though the solutions are undersaturated with respect to  $Mg(OH)_{2(s)}$ , the presence of the algae may be providing nucleation sites for clusters of  $Mg(OH)_2$  above pH 10 where the transition between the trends appears to occur. Thus, it appears that below pH 10, the mechanism for  $Mg^{2+}$  removal and hence algae removal is adsorption and charge neutralization. The SEM images of the floc formed below pH 10 in Figure 4-8 B (pH 9.97, 25 mg/L as  $Mg^{2+}$ ) appear to be well-flocculated but show no visible signs of precipitates. Moreover, the image shown in panel A in Figure 4-8 was formed under the same conditions as in Panel B except  $Mg^{2+}$  was replaced with an equivalent concentration of  $Na^+$ . Seemingly larger flocs are observed in Panel B possibly indicating that the surface charge of algae is more effectively neutralized in the presence of divalent cations. As pH and initial  $Mg^{2+}$  concentration increase (panel B: pH 9.97, 25 mg/L as  $Mg^{2+}$ , C: pH 10.6, 25 mg/L as  $Mg^{2+}$ , and D: pH 10.6, 200 mg/L as  $Mg^{2+}$ ), denser flocs are produced and clear evidence for  $Mg(OH)_{2(s)}$  is apparent. These observations not only support the previous results that showed that the algae removal efficiency increased with increasing pH and initial  $Mg^{2+}$  concentration, but also suggest that precipitation is occurring on the surface of the algae below  $Mg(OH)_{2(s)}$  solubility. Thus, it appears that adsorption/charge

neutralization is a key process for removal of algae under these conditions. The formation of a  $\text{Mg}(\text{OH})_{2(\text{s})}$  precipitate on the surface of the algae (i.e., surface precipitation or heteroprecipitation) provides enhanced removal as the precipitate and the algae form a denser mat.

To summarize the results, algae percent removal was plotted as a function of  $\text{Mg}^{2+}$  consumed per algae cell density as shown in Figure 4-9. Based on the trends observed in the adsorption data and the SEM images, the mechanism responsible for algae removal, adsorption (open symbols) and precipitation (close symbols) figures were sorted based on the change in the proposed mechanism that occurred near pH 10.

At high algae cell density (1.42 g/L represented as green symbols), magnesium was more efficiently consumed and achieved the highest algae removal levels. It is also apparent that relatively high algae removal efficiencies (85 to 88 %) could be achieved at a pH lower than 10 for the high algae cell density of 1.42 g/L and initial  $\text{Mg}^{2+}$  concentration of 200 mg/L. This result may indicate that an adsorption/charge neutralization mechanism can be solely employed to achieve high algae removal efficiency while minimizing precipitated solid concentrations. As the dominant mechanism shifts from adsorption/charge neutralization to precipitation-enhanced coagulation, algae removal efficiency reached a plateau for each algae cell density. The percent removal associated with the plateau increased with algae cell density indicating that precipitation-enhanced coagulation and possibly heterocoagulation can ensure high algae removal efficiencies during algae harvesting.

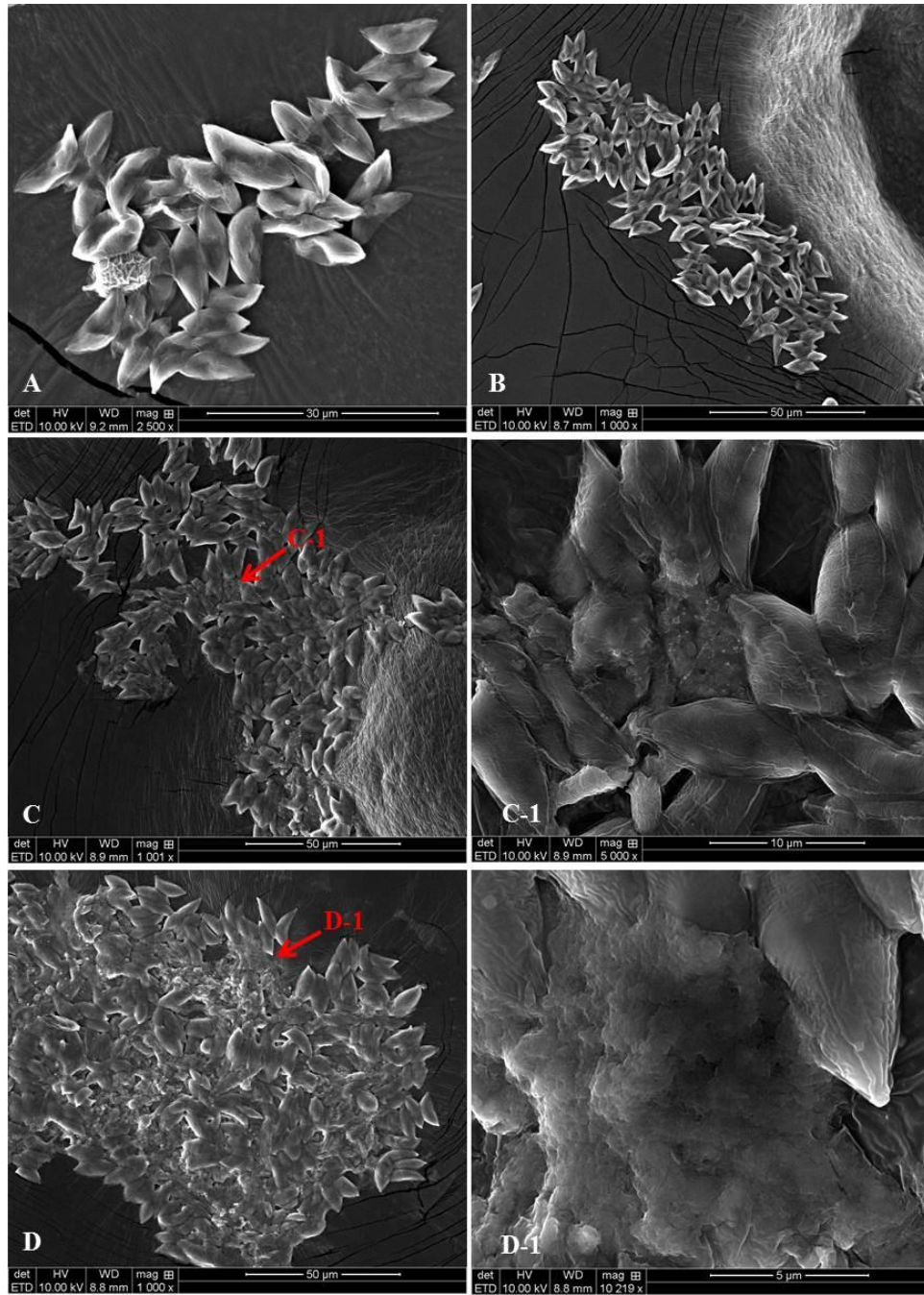


Figure 4-8 SEM images for flocs under adsorption/charge neutralization (A, B) and precipitation-enhanced coagulation (C, D) for an algae cell density of 0.26 g/L and varied pH and initial  $Mg^{2+}$  concentration: (A) pH 9.97, ionic strength adjusted with NaCl in the absence of  $Mg^{2+}$  (B) pH 9.97, 25 mg/L as  $Mg^{2+}$  (C) pH 10.6, 25 mg/L as  $Mg^{2+}$  (D) pH 10.6, 200 mg/L as  $Mg^{2+}$ . C-1 and D-1 are enlarged images of C and D, respectively.

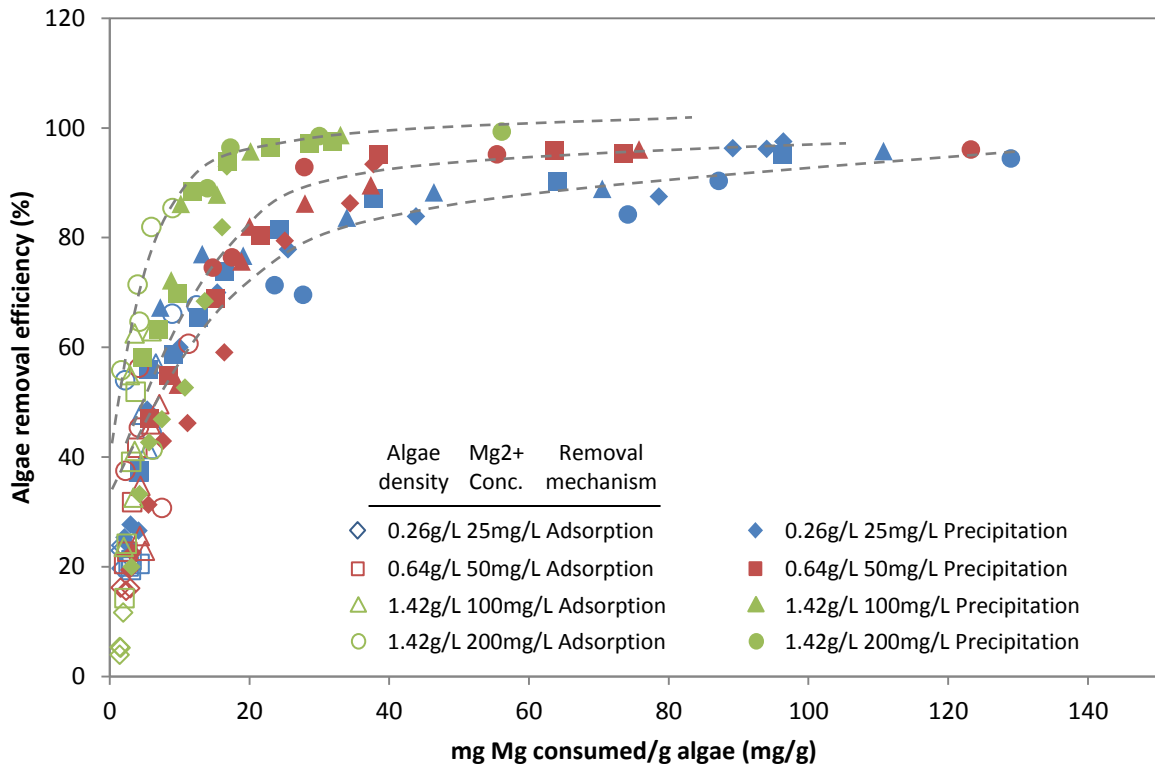


Figure 4-9 Algae removal efficiency as a function  $Mg^{2+}$  consumption normalized by algae cell density. A range of initial  $Mg^{2+}$  concentrations (25-200 mg/L) and algae cell density (0.26, 0.64, and 1.42 g/L) were tested. To indicate the removal mechanism responsible for algae removal, open (adsorption) and close (precipitation) figures were sorted based on the mechanism transition zone at pH near 10. The dotted lines are only a guide to the eye, not theoretical curves.

The results from the variable pH (Figure 4-9) tests showed that an increase in pH led to an increase in algae removal efficiency and magnesium consumption. As the dominant algae removal mechanism shifts from adsorption/charge neutralization to precipitation-enhanced coagulation with increasing pH, magnesium consumption

becomes proportional to the solids production (i.e., precipitates other than algae biomass). In other words, algae harvesting performance (i.e., algae removal efficiency, quality of effluent, and composition of algae slurry concentrate) can be characterized as a function of pH. In fact, pH is an important consideration with respect not only to harvesting but also to the success of overall algae biomass production. To explore the effect of operating pH on overall algae biomass production including the harvesting step as well as up and downstream processes, the target pH to achieve a certain algae removal efficiency was plotted as a function of initial  $Mg^{2+}$  concentration in the sample solutions as shown in Figure 4-10.

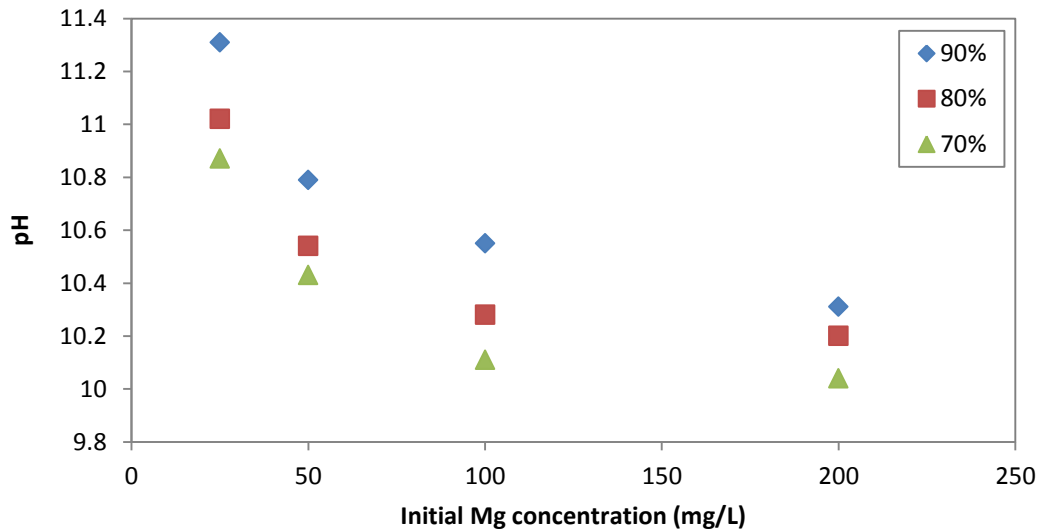


Figure 4-10 Operating pH necessary to achieve target algae percent removals as a function of initial  $Mg^{2+}$  concentration for an algae cell density of 0.26 g/L

It was observed that the operating pH required to achieve a particular algae removal efficiency decreases with increasing initial  $Mg^{2+}$  concentration in the water. If the initial  $Mg^{2+}$  concentration in the medium can be controlled by the addition of supplementary salts, an economical tradeoff between salt addition and dose of base can be determined for algae harvesting processes. In addition, high effluent pH may require acid addition (e.g.,  $CO_2$ ) to neutralize the water prior to discharge or recycle. Moreover, dense slurries containing large volumes of inorganic precipitated solids in the algae concentrate formed during high pH conditions may not be favorable for a process which uses acidification to deflocculate the algae slurry concentrate. It may also hinder downstream processes. In the case of algae-based biofuel production, the properties of the algae concentrate such as large floc size can impact the efficiency of subsequent oil extraction (Seibert, 2009). Therefore, pH can be a useful guideline for predicting and controlling the performance of the pH-induced flocculation/deflocculation process for algae harvesting as well as for examining economic efficiencies in the entire algae biomass production system.

#### **4.3.4. Deflocculation tests**

Flocculated solids generated from the variable pH tests for an algae cell density of 0.26 g/L, initial  $Mg^{2+}$  concentration of 200 mg/L as  $Mg^{2+}$ , and pH of 10.6 (as shown in panel D in Figure 4-8) were acidified to pH 7.5 by bubbling  $CO_2$  through flocculated solids. SEM observations of the flocculated solids after the deflocculation process are shown in Figure 4-11. It was observed that algae were distributed evenly and

Mg(OH)<sub>2(s)</sub> precipitates were not evident after the deflocculation process. Semi-quantitative EDX analysis (Table 4-2) on flocculated solids before and after the deflocculation test showed that the weight percent of magnesium decreased after acidification. These results indicate that simple pH adjustment using CO<sub>2</sub> effectively dissolved the Mg(OH)<sub>2(s)</sub> precipitates formed during flocculation producing a homogeneous deflocculated algae concentrate suitable for downstream processes.

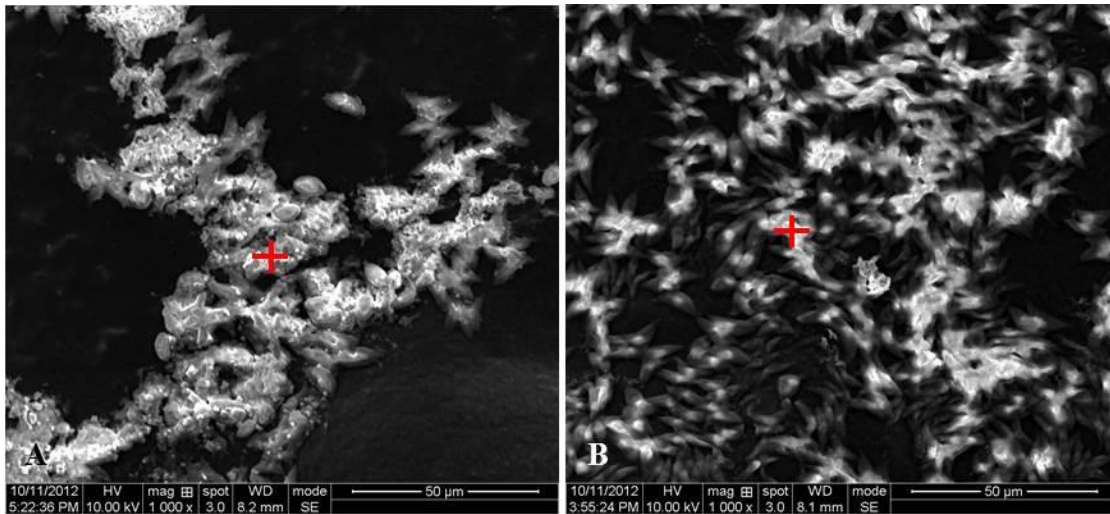


Figure 4-11 SEM images for flocs before deflocculation (panel A) and after flocculation (panel B) for the flocculated solids generated from a solution containing an algae cell density of 0.26 g/L and initial Mg<sup>2+</sup> concentration of 200 mg/L as Mg<sup>2+</sup>. The pH of the algae concentrates were acidified from 10.6 to 7.5 by bubbling the CO<sub>2</sub>. The cross marks indicate the spot on which EDX analyses were conducted.

Table 4-2 EDX analysis of the flocculated solids before and after the deflocculation test

Elements	Before (wt.%)	After (wt.%)
Carbon	40.87	71.22
Oxygen	34.75	26.77
Sodium	5.69	0.72
Magnesium	6.78	0.61
Chlorine	11.56	0.55
Calcium	0.34	0.14
	100	100

#### 4.4. CONCLUSIONS

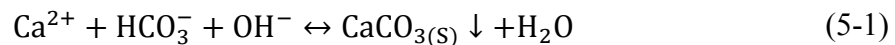
This chapter elucidated the specific algae removal mechanisms associated with the dissolved  $Mg^{2+}$  ion and  $Mg(OH)_{2(s)}$  during the algae harvesting process. A series of controlled bench-scale experiments were designed to isolate the possible mechanisms of algae destabilization and microscopic analyses were performed to characterize the flocculated algae/ $Mg(OH)_{2(s)}$  mixtures and deflocculated algae. *Heterocoagulation* was effective, but equivalent algae removal was achieved at lower magnesium concentrations via *adsorption* and/or *precipitation-enhanced coagulation*. The dominant algae removal mechanism shifts from *adsorption* to *precipitation-enhanced coagulation* with increasing pH. A “transition zone” between the two mechanisms was apparent at approximately pH 10. Moreover, dissolved  $Mg^{2+}$  *adsorption* to the algae surface led to effective algae coagulation (e.g., 85% removal efficiency), while minimizing the mass of precipitated  $Mg(OH)_{2(s)}$ . The overall process that includes deflocculation yielded a homogeneous and deflocculated algae concentrate suitable for downstream processing. These results

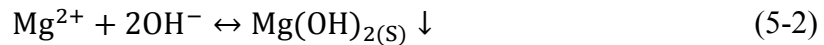
are supported by SEM observation coupled with EDX analyses. The results imply that algae harvesting via pH control can be achieved if the chemistry of Mg(II) is properly incorporated into the system design.

## Chapter 5: The role of calcium in harvesting algae in alkaline water

### 5.1. INTRODUCTION

Algae harvesting using chemical flocculation/sedimentation has been studied extensively in the past. Previous research has shown that effective algae removal can be achieved by encapsulating the algae in a calcium/magnesium precipitate formed simply by raising the pH of the algae source water (Folkman and Wachs, 1973; Ayoub and Koopman, 1986; Elmaleh et al., 1996; Knuckey et al., 2006; Harith et al., 2009). Autoflocculation is a term often used when CO<sub>2</sub> depletion during photosynthesis leads to increasing pH and the induction of flocculation (Golueke and Oswald, 1970; Shelef et al., 1984). However, this method may not be reliable because the pH increase caused by the photosynthetic activity of algae is not always sufficient (Spilling et al., 2011). pH adjustment (e.g., lime, NaOH addition) has been shown to effectively remove algae from suspensions for tertiary treatment applications (Folkman and Wachs, 1973; Friedman, 1977; Ayoub and Koopman, 1986; Elmaleh et al., 1996) as well as for harvesting algal biomass (McCaousland et al., 1999; D'Souza et al., 2002; Knuckey et al., 2006). Effective algae removal via pH-induced flocculation is often described by the following chemical precipitation reactions that occur as the pH of the solution increases:





Calcium carbonate typically begins to precipitate according to Equation 5-1 in a pH range between 9.1-9.5 for most natural water carbonate concentrations. Precipitation of calcium carbonate is often used in lime softening and in particle removal processes as it not only removes calcium from solution but acts as “sweep coagulation” and a “weighting” agent to remove suspended and colloidal particles from the suspension. (Leentvaar and Rebhun, 1982). However, the pH of the point of zero charge of calcium carbonate particles ranges between pH 8-9 (Park, 1967) and the negatively charged calcium carbonate particles are not very effective for algae flocculation (Folkman and Wachs, 1973). In addition, calcium carbonate precipitation did not induce flocculation of algae in the calcium range from 0 to 2.5 mM at a pH value higher than 10.5 (Vandamme et al., 2012). Thus, the use of Ca as the sole coagulant for algae removal is not expected to provide high efficiencies.

In contrast, the surface charge of  $\text{Mg}(\text{OH})_{2(\text{s})}$  is positive below pH 12 and negatively charged colloidal particles, including  $\text{CaCO}_{3(\text{s})}$  flocs are attracted to the positively charged  $\text{Mg}(\text{OH})_{2(\text{s})}$  flocs, inducing coagulation. Precipitation of magnesium hydroxide occurs at a pH value higher than 10.5 for typical Mg concentrations in natural waters. Above this pH, significant algae removal is achieved (Semerjian and Ayoub, 2003). However, the density of  $\text{Mg}(\text{OH})_{2(\text{s})}$  is relatively low compared to  $\text{CaCO}_{3(\text{s})}$  and the precipitate formed produces a gelatinous floc that can be difficult to concentrate.

Thus, the presence of both precipitates may be advantageous within the sedimentation phase of the coagulation/flocculation/ sedimentation process.

While the importance of  $\text{Mg}(\text{OH})_{2(\text{s})}$  for removal of algae has been demonstrated, the mechanistic understanding of the role of calcium which is easily precipitated out of a supersaturated solution in the form of  $\text{CaCO}_{3(\text{s})}$  is not clearly understood. The characteristics of  $\text{CaCO}_{3(\text{s})}$  including charge development, kinetics of the precipitation/dissolution processes, trace metal partitioning and biomineralization (i.e., calcification) have been investigated for decades.  $\text{CaCO}_{3(\text{s})}$  is of significant importance in geological, environmental, and industrial applications as it is a major component of the global carbon budget, and is important in metal remediation, water distribution systems and many consumer products (Stumm and Morgan, 1996; Alexandratos et al., 2007; Gebrehiwet et al., 2012; Dabrowski et al., 2010; Schlomach et al., 2006). Its potential for application to algae removal has been known for years; however, there is significant ambiguity regarding the mechanisms that are responsible for attachment of the algae to the precipitating  $\text{CaCO}_{3(\text{s})}$ . In many cases, the ambiguity results from the fact that most algae suspensions contain both calcium and magnesium unless the growth medium is synthesized to specifically exclude one or both of these ions. Separating the impact of Ca from Mg has not been a key focus of research in the past. For example, it is not clear whether the presence of the other ion is antagonistic or synergetic for effective algae harvesting (i.e., is algae removal reduced or enhanced when both Ca and Mg are present). Moreover, a lack of mechanistic understanding of the role of Ca hinders optimizing the algae removal process at field-scale.

In this chapter, the role of calcium in the harvesting algae process was elucidated via a series of bench-scale experiments with a *Scenedesmus* sp. Experimental conditions were designed to isolate potential algae destabilization mechanisms (heterocoagulation vs. adsorption and charge neutralization or enmeshment/precipitation). Experiments conducted in the presence and absence of carbonate and in the presence and absence of Mg provided an additional mechanistic understanding of the systems. Finally, a second algae species, *Chlorella* sp., was investigated to verify the extensibility of the findings to a different algal system.

## **5.2. MATERIALS AND METHODS**

### **5.2.1. Preparation of algae sample solutions**

The algae culture (an AlgEternal proprietary polyculture consisting primarily of a *Scenedesmus* sp.) was obtained from the Welch green house facility located at the University of Texas at Austin. *Scenedesmus* sp. (10  $\mu\text{m}$  in size) was selected for this research because *Scenedesmus* sp. have been suggested as a potential source for biodiesel production due to their high lipid content (Mandal and Mallick, 2009; Jena et al., 2012). *Chlorella* sp. was selected as a second algae species (obtained from the same facility) to verify the extensibility of the findings to a different algal system. Cultures were collected in 5 gallon buckets and then stored at room temperature (20°C) for 30 min to allow time for possible debris from the reactor to settle. Algae was centrifuged at 5000 rpm for 15 min at 20°C and then resuspended in deionized water to achieve the target algae cell density required for each experiment.

The target calcium ion concentrations were achieved by adding analytical grade anhydrous calcium chloride (i.e.,  $\text{CaCl}_2$ ) to algae-resuspended solutions to achieve the desired levels for each experiment. Analytical grade sodium bicarbonate (i.e.,  $\text{NaHCO}_3$ ) was used to control the initial total carbonate concentration in the solutions. Magnesium was excluded in most experiments to eliminate the effect of magnesium ion and precipitated  $\text{Mg}(\text{OH})_{2(\text{s})}$  on algae removal. For the experiments where pre-precipitated  $\text{CaCO}_{3(\text{s})}$  (i.e., “seed”) was required, a known amount of salts ( $\text{CaCl}_2$  and  $\text{NaHCO}_3$ ) was added to deionized water. The pH of the solutions was raised to induce precipitation and then allowed to equilibrate for 24 hours at pH 10.6. The resulting supernatant was gently decanted and solids settled on the bottom were used as seed during the jar tests. Analytical grade sodium chloride (i.e.,  $\text{NaCl}$ ) was used if the ionic strength of the solutions needed to be adjusted.

### **5.2.2. Adsorption experiments**

The adsorption isotherm experiments were conducted in a  $\text{CO}_2$ -free nitrogen glove box to prevent adsorption and precipitation of  $\text{CaCO}_{3(\text{s})}$ . The algae pellet prepared by centrifugation was resuspended in deionized water. This washing procedure was repeated four times and a desired cell density of 3 g/L was achieved. The algae sample solution was degassed using  $\text{N}_2$  gas for an hour and then placed in the glove box. The “subsequent addition method” experimental procedure suggested by Pagnanelli et al (2000) was adopted as follows: after the first addition of a concentrated solution of  $\text{CaCl}_2$  (250 mM), the pH of the algae solution in agitation was adjusted and the first 2 mL of the

sample was taken. After the established time for equilibrium (40 min) elapsed, 2 mL of sample was taken from the suspension. The collected samples were immediately filtered and analyzed to determine the dissolved metal ion concentration. A concentrated solution of Ca was added to the same algae solution and equilibrated for a second time. The previous procedure for sampling was repeated while maintaining the pH at the desired setpoint. The experimental data points were fit to the Langmuir isotherm model as shown in Equation 5-3:

$$q = \frac{q_{max}k_aC_{eq}}{1 + k_aC_{eq}} \quad (5-3)$$

where  $q_{max}$  (mg of calcium per gram of algae) is the adsorption capacity,  $k_a$  (liter per mg of calcium) is the equilibrium constant, and  $C_{eq}$  (mg of magnesium per liter) is the magnesium concentration at equilibrium.

Adsorption jar tests were also conducted in a CO<sub>2</sub>-free nitrogen glove box in the same beakers used for jar testing to investigate the effect of calcium adsorption on algae removal. The jar test procedure is described in the following section.

### **5.2.3. Jar tests**

A series of batch reactor jar tests were conducted to elucidate the potential mechanisms responsible for algae removal in the algae harvesting process. The typical jar test procedure adopted for this research includes rapid mixing of sample solutions for

1 min using a magnetic stirrer, followed by slow mixing at 30 rpm for 20 min with a Phipps & Bird standard 6-paddle jar tester (Richmond, VA), followed by 20 min of quiescent conditions to allow time for settling. A sodium hydroxide solution (1M) was used as the primary base rather than lime to control the calcium concentration. Depending on the focus of each experiment (e.g., seeded test, unseeded test, and variable pH tests defined as below) base or pre-precipitated solids were added at the appropriate stage in the jar test procedure.

In the seeded tests, pre-precipitated  $\text{CaCO}_{3(\text{S})}$  was added to evaluate the heterocoagulation mechanism in which two dissimilar particles (e.g., algae and  $\text{CaCO}_{3(\text{S})}$ ) are attracted to each other. Pre-precipitated  $\text{CaCO}_{3(\text{S})}$  (i.e., seed solution) was added to an algae slurry that contained the same concentration of  $\text{Ca}^{2+}$  and  $\text{CO}_3^{2-}$  as the seed solution at the beginning of the slow mixing phase. All tests were conducted at a fixed pH of 10.6. The pH of the solutions was checked periodically ( $\text{pH } 10.6 \pm 0.01$ ) to confirm that no additional precipitation or dissolution occurred during the experiments.

In the unseeded tests, the dissolved calcium concentration, algae cell density, and initial alkalinity (1.4 to 10 mM as bicarbonate) were adjusted prior to the jar tests to evaluate the effectiveness of the adsorption/charge neutralization and/or precipitation-enhanced coagulation mechanisms on algae removal as a function of these parameters. The dissolved  $\text{Ca}^{2+}$  ions were added directly to algae slurries followed by pH adjustment. The pH of the solution was then adjusted to 10.6 during the rapid mixing stage.

In the variable pH tests, calcium and algae concentrations in the solution were monitored in jar tests conducted over a range of pH values to further distinguish

adsorption/charge neutralization from precipitation-enhanced coagulation mechanisms within the unseeded tests. The target pH of the sample solutions (from 7.5 to 11.5) was achieved during the rapid mixing stage for initial  $\text{Ca}^{2+}$  concentrations and algae cell densities ranging from 120 to 320 mg/L and 0.25 to 3.0 g/L, respectively. In addition, the impact of pH on the removal mechanisms was examined for a different algae species (*Chlorella* sp.) and ionic strengths ranging from 0.01 to 0.4 M.

To confirm that atmospheric  $\text{CO}_2$  exchange during the retention time (i.e., 40 min) of the jar test experiments had a minimal impact on the results for the open jar systems used throughout this research, additional jar tests were conducted with floating covers (e.g., algae removal and  $\text{Ca}^{2+}$  removal) as shown in Table 5-1. The results indicate that minimal differences in algae removal efficiencies were apparent. The slight increase in removal in the open systems is likely the result of  $\text{CO}_2$  entrainment.

Table 5-1 Impact of atmospheric CO<sub>2</sub> exchange on algae removal and Ca<sup>2+</sup> removal for varying ion activity ratios ( $\{Ca^{2+}\}/\{CO_3^{2-}\}$ ). The floating cover prevented gas exchange during the retention time of 40 min. The algae cell density was 0.5 g/L.

Ca <sup>2+</sup> /CO <sub>3</sub> <sup>2-</sup>	Supersaturation (Ω)	Algae removal efficiency (%)		Percent Ca <sup>2+</sup> removal (%)	
		Open	Closed	Open	Closed
0.5	790	22.8±0.5	19.5±1.0	91.7±0.3	87.6±0.1
1.0	847	35.7±1.8	33.2±1.3	89.0±0.3	87.7±0.2
2.0	680	46.0±0.6	44.8±0.9	69.2±1.3	70.0±0.9

The standard deviation was calculated from each experiment (n = 3)

#### 5.2.4. Deflocculation tests

The deflocculation tests were conducted to examine the potential for deflocculation of the algae/CaCO<sub>3(S)</sub> flocs. The supernatant from the variable pH test was decanted to leave 10 % (by volume) of the original solution. CO<sub>2</sub> was then bubbled through the flocculated solids remaining (e.g., algae/precipitated solids concentrate) until the target pH of 6.0 was reached. A sample of the acidified solution was collected for further analyses (e.g., ion concentration) to examine the potential for deflocculation of the algae/CaCO<sub>3(S)</sub> flocs.

#### 5.2.5. Analytical methods

Samples were collected at various stages in the experiments for further analysis. Prior to initiating an experiment, algae cells were filtered through a 0.2 μm nitrocellulose

membrane filter (Millipore, U.S.A) to measure the total suspended solid (TSS) concentration and to determine the algae cell density (g/L). The alkalinity was determined in accordance with Standard Method 2320B except a 0.1 M nitric acid (HNO<sub>3</sub>) titrant was used instead of sulfuric acid (H<sub>2</sub>SO<sub>4</sub>). Five mL samples of the original algae sample solution and the supernatant of treated water were filtered through a 0.2 μm nitrocellulose membrane syringe filter (Millipore, U.S.A) and the metal ion concentrations were measured using inductively coupled plasma-optical emission spectrometer (ICP-OES, Varian 710-ES, U.S.A). A 0.05 mL sample was collected without filtration at the end of the slow mixing step of the jar tests for scanning electron microscopy (SEM) observation combined with energy dispersive X-ray (EDX) analysis using a FEI QUANTA 200 (Hillsboro, OR). For this analysis, a few drops of algae or algae-laden flocs were placed on black carbon tape attached on an aluminum alloy sample tray. Because the samples must be dried for this analysis, excess water droplets were removed by gently touching a “Kimwipe” to the surface of the droplets and using interfacial tension to remove excess water. This procedure avoids a build-up of salts on the surface of the solids. The solids were then air-dried prior to the Au/Pd coating process. At the end of each jar test and adsorption test, the algae removal efficiency (%) was evaluated by comparing the optical density at 664 nm present in the original water to that present in the supernatant of the treated water as shown in Equation 5-4 below. The optical density was measured using an Agilent 8453E UV-visible Spectroscopy system with a 1-cm cuvette.

$$\text{Algae percent removal (\%)} = \left(1 - \frac{OD_S}{OD_O}\right) \times 100 \quad (5-4)$$

where  $OD_S$  is the optical density (664 nm) of supernatant after settling 20min and  $OD_O$  is the optical density of original water prior to pH adjustment.

Based on the metal ion concentrations measured, calcium removal (%) was evaluated using Equation 5-5 below.

$$\text{Percent calcium removal (\%)} = \left(1 - \frac{\text{Conc. } S}{\text{Conc. } O}\right) \times 100 \quad (5-5)$$

where *Conc. S* is the concentration of dissolved calcium ions in the filtered sample after the 20 min of quiescent settling, and *Conc. O* is the concentration of dissolved calcium ions in the filtered original sample prior to pH adjustment.

### 5.3. RESULTS AND DISCUSSION

#### 5.3.1. Adsorption isotherm

An adsorption isotherm for  $\text{Ca}^{2+}$  adsorption to *Scenedesmus* sp. was initially conducted to characterize the extent of adsorption of  $\text{Ca}^{2+}$  onto algae. The experiments were conducted in a  $\text{CO}_2$  free glove-box to prevent adsorption and precipitation of  $\text{CaCO}_3(s)$ . In Figure 5-1, the adsorption of calcium is compared to magnesium adsorption data reported in Chapter 4. Data points collected at  $\text{pH } 9.6 \pm 1$  were fit to the Langmuir isotherm resulting in parameters ( $q_{max}$  and  $k_a$ ) for calcium and magnesium

adsorption listed in Table 5-2. Similar to magnesium, adsorption of calcium was reduced at high ionic strength; however the effect of ionic strength was significantly less for Ca adsorption. It was also demonstrated that adsorption of calcium onto the algae was lower than that of magnesium. This result is consistent with observed trends for adsorption of alkaline earth metals on mineral surfaces (e.g., gibbsite, goethite and silica) which suggest that adsorption increases inversely with the ionic radius of the alkaline earth cation (Sverjensky, 2006). This observation is also consistent with the results from a calcium adsorption jar test conducted in the absence of carbonate ion.

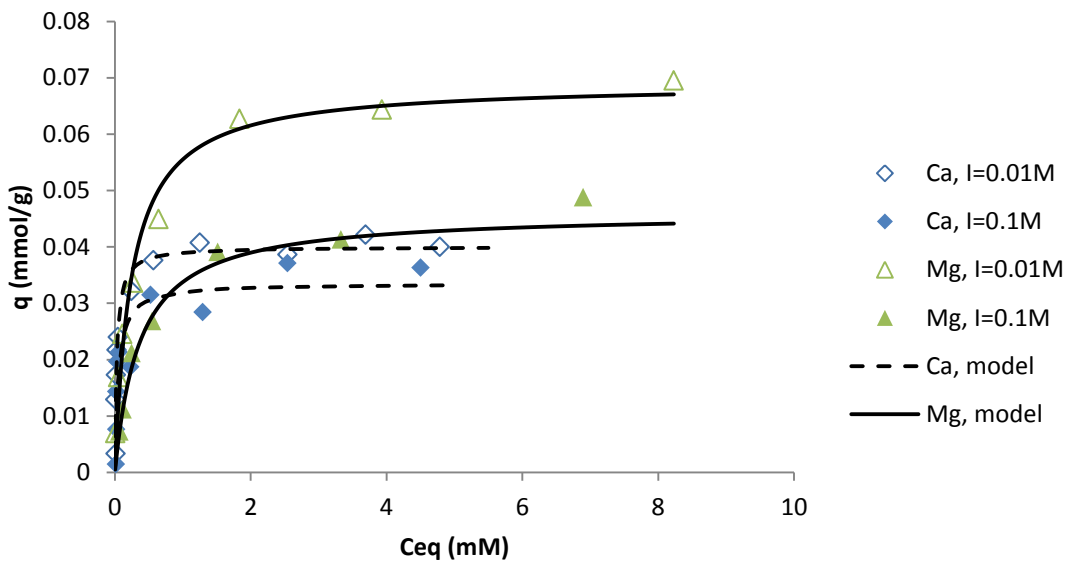


Figure 5-1 Adsorption isotherms for calcium and magnesium at fixed pH of  $9.6 \pm 1$ . The experimental data (symbols) were fit to the Langmuir isotherm using non-linear regression.

Algae removal associated with divalent calcium ions, shown in Figure 5-2, is slightly higher than that associated with monovalent sodium ions; however, it is slightly lower than the algae removal (22 – 34 % at algae cell density of 0.64 g/L and initial  $Mg^{2+}$  concentration ranging from 50 to 100 mg/L as  $Mg^{2+}$ ) associated with adsorption of  $Mg^{2+}$  described in Chapter 4. This result suggests that magnesium ion will be more effective at charge neutralization of algae due to the higher adsorption capacity.

Table 5-2 Langmuir parameters,  $q_{max}$  and  $k_a$ , obtained for two different ionic strength levels in solution

	Ca		Mg	
	0.01M	0.1M	0.01M	0.1M
$q_{max}$ (mg/g)	1.60	1.34	1.67	1.19
$k_a$ (L/mg)	0.88	0.50	0.16	0.07

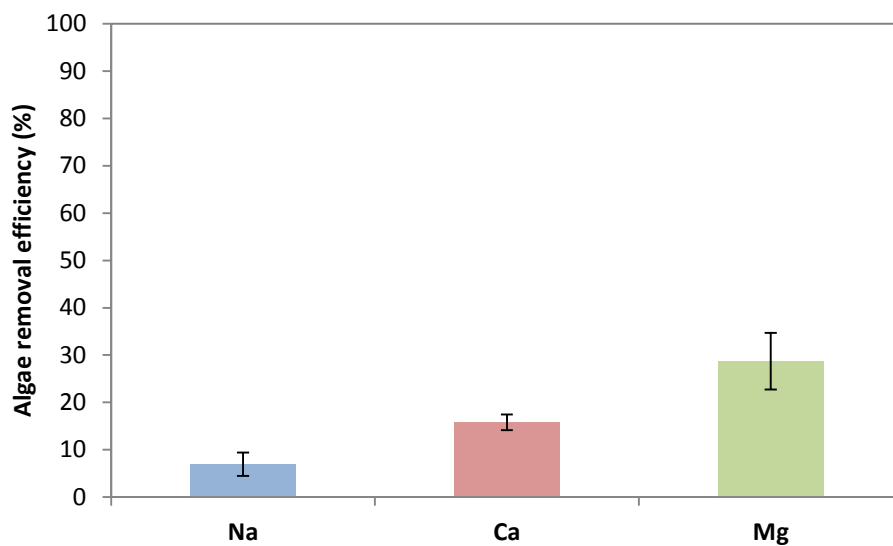


Figure 5-2 Comparison of algae removal at constant ionic strength (0.01 M) and fixed pH ( $9.6 \pm 1$ ) in the absence of carbonate. The target ionic strength for each jar test was achieved only by the addition of NaCl and CaCl<sub>2</sub> salts. 0.01 M CaCl<sub>2</sub> is equivalent to 120 mg Ca<sup>2+</sup>/L. The algae cell density was 0.5 g/L. For comparison, algae removal associated adsorption of Mg<sup>2+</sup> described in Chapter 4 is embedded (initial Mg<sup>2+</sup> concentration ranging from 50 to 100 mg/L as Mg<sup>2+</sup> at algae cell density of 0.64 g/L at pH 9.7).

Limited algae removal associated with adsorption or compression of the diffuse layer in the presence of ions was also evident in another jar test conducted at different ionic strengths with NaCl as the background electrolyte and in the absence of calcium and carbonate ions. Figure 5-3 shows that algae removal efficiency increases with increasing ionic strength but regardless of the ionic strength, overall algae removal never exceeded twenty percent.

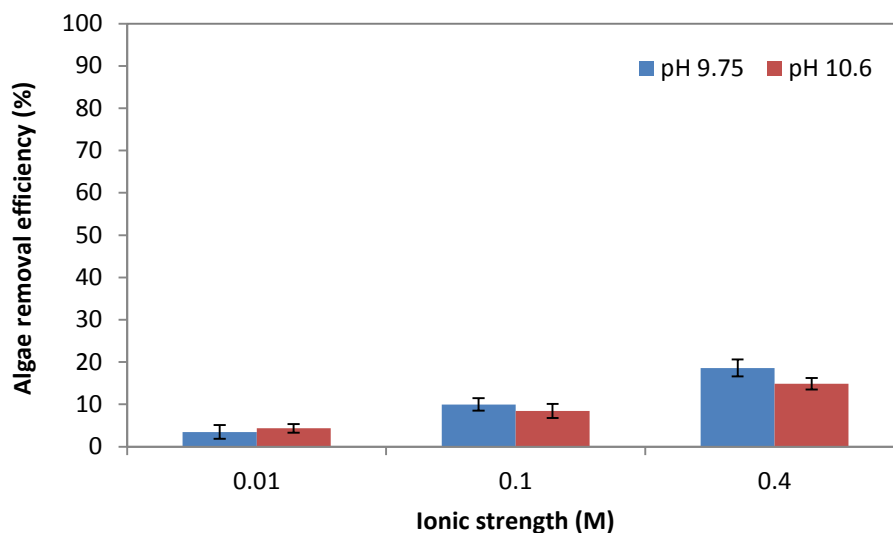


Figure 5-3 Effect of pH on algae removal efficiency for varying ionic strengths in solutions containing NaCl as the background electrolyte. Jar tests were conducted in a CO<sub>2</sub> free glove box in the absence of calcium. Only NaCl was added to deionized water to adjust the target electrolyte concentration. The algae cell density was 0.5 g/L.

### 5.3.2. Algae Removal in Heterocoagulation Experiments

To isolate the different potential mechanisms responsible for algae removal using Ca as a coagulant, experiments were conducted with pre-precipitated CaCO<sub>3(s)</sub> (seeded tests) added to an algae slurry, and the results were compared to experiments conducted with Ca ion added directly to algae slurries followed by pH adjustment (unseeded tests).

Figure 5-4 displays the algae removal efficiency as a function of calcium added as “seed” for different algae cell densities at pH 10.6. Since the ion concentrations of Ca<sup>2+</sup> and CO<sub>3</sub><sup>2-</sup> in both the seed solution and algae slurry were equivalent and at equilibrium with respect to CaCO<sub>3(s)</sub>, further precipitation or dissolution of CaCO<sub>3(s)</sub> was prevented

during this experiment. Thus, the operative mechanism responsible for algae removal in these systems was *heterocoagulation* in which the two dissimilar types of particles interact via electrostatic attraction and/or hydrophobic interactions.

Algae removal of up to 50% was achieved with the addition of seed  $\text{CaCO}_{3(s)}$  particles. However, the amount of calcium required for high removal far exceeds the calcium concentrations typically encountered in natural or engineered systems for algae growth. In addition, as evident in Figure 5-4 (Panel B, Jar 5), this process generates excessive solids that would hinder downstream recovery efforts.

Calcite, the most stable form of  $\text{CaCO}_{3(s)}$ , exhibits a highly-structured rhombohedral shape formed from six-fold coordination between the calcium cations and the oxygen atoms (Reeder, 1983). The pH of the point-of-zero-charge was measured at approximately pH 8–9 (Parks, 1967). Thus, it was not surprising that highly structured and negatively charged  $\text{CaCO}_{3(s)}$  did not effectively attract algae via heterocoagulation.

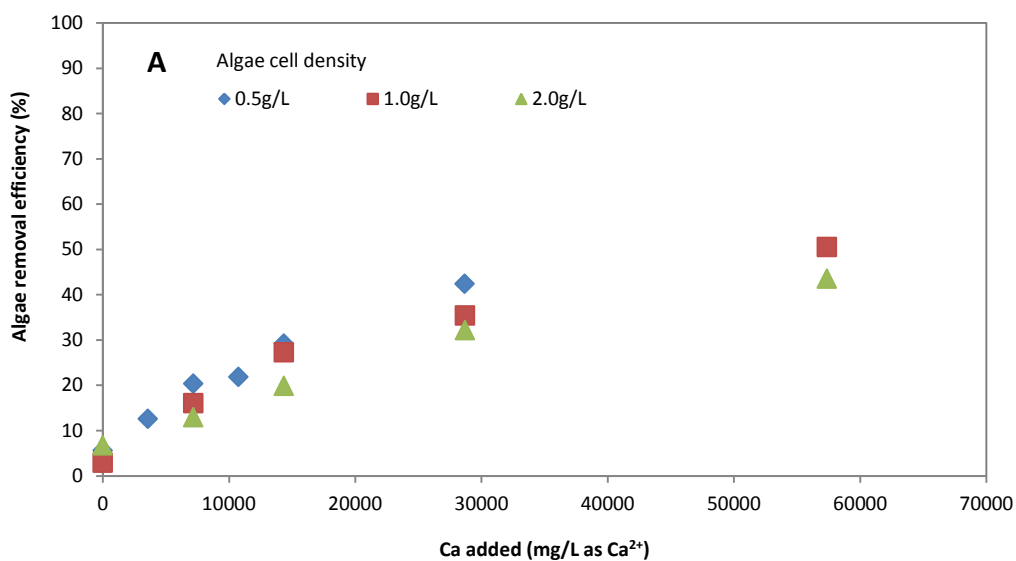


Figure 5-4 Effect of calcium carbonate dose (pre-precipitated  $\text{CaCO}_{3(s)}$ ) addition on algae removal efficiency for a range of algae cell densities (panel A). The pH of the solutions was maintained at 10.6. The image (panel B) represents the test results after sedimentation for an algae cell density of 2.0 g/L. “Raw” represents the untreated original solution and the numbers represent doses of 0, 7000, 14000, 28000, and 57000 mg  $\text{Ca}^{2+}$ /L, respectively from 1 to 5.

### 5.3.3. Algae Removal via Direct Addition of Calcium to Algae Slurries

The addition of dissolved  $\text{Ca}^{2+}$  to algae slurries was investigated over a range of algae cell densities and initial alkalinities (1.4 to 10 mM as bicarbonate). The results presented in Figure 5-5 demonstrate that equivalent algae removal efficiency could be achieved with much lower calcium addition in these unseeded experiments compared to the seeded experiments described above. All of the solutions were oversaturated (pH 10.6) and precipitation of  $\text{CaCO}_3(\text{s})$  was evident in all of the reactors. In general, lower initial alkalinity yielded higher removal which suggests that the initial ratio of  $\text{Ca}^{2+}/\text{CO}_3^{2-}$  may be an important factor for optimizing removal.

The data for the 1.0 g/L algae cell density in Figure 5-5B was re-plotted in Figure 5-5C by transforming the x-axis to calcium consumed (i.e., the difference between the initial and final  $\text{Ca}^{2+}$  concentration). Since all of the systems were supersaturated with respect to  $\text{CaCO}_3(\text{s})$ , the amount of calcium consumed is directly related to the amount of  $\text{CaCO}_3(\text{s})$  precipitated. The data show that algae removal initially increased with increasing precipitation of  $\text{CaCO}_3(\text{s})$  and then a plateau in algae removal efficiency was attained. While the initial results (low amounts of precipitation) are consistent with a “sweep coagulation” process (Leentvaar and Rebhun, 1982) in which the algae becomes enmeshed in the precipitating solid, the results at higher  $\text{CaCO}_3(\text{s})$  precipitation are less clear. Although other factors such as ionic strength and the ratio of calcium to carbonate ion concentration are subject to change with increasing initial  $\text{Ca}^{2+}$  concentration, the lack of increase in yield with increasing precipitation within this plateau region suggests that the mechanism is more complex.

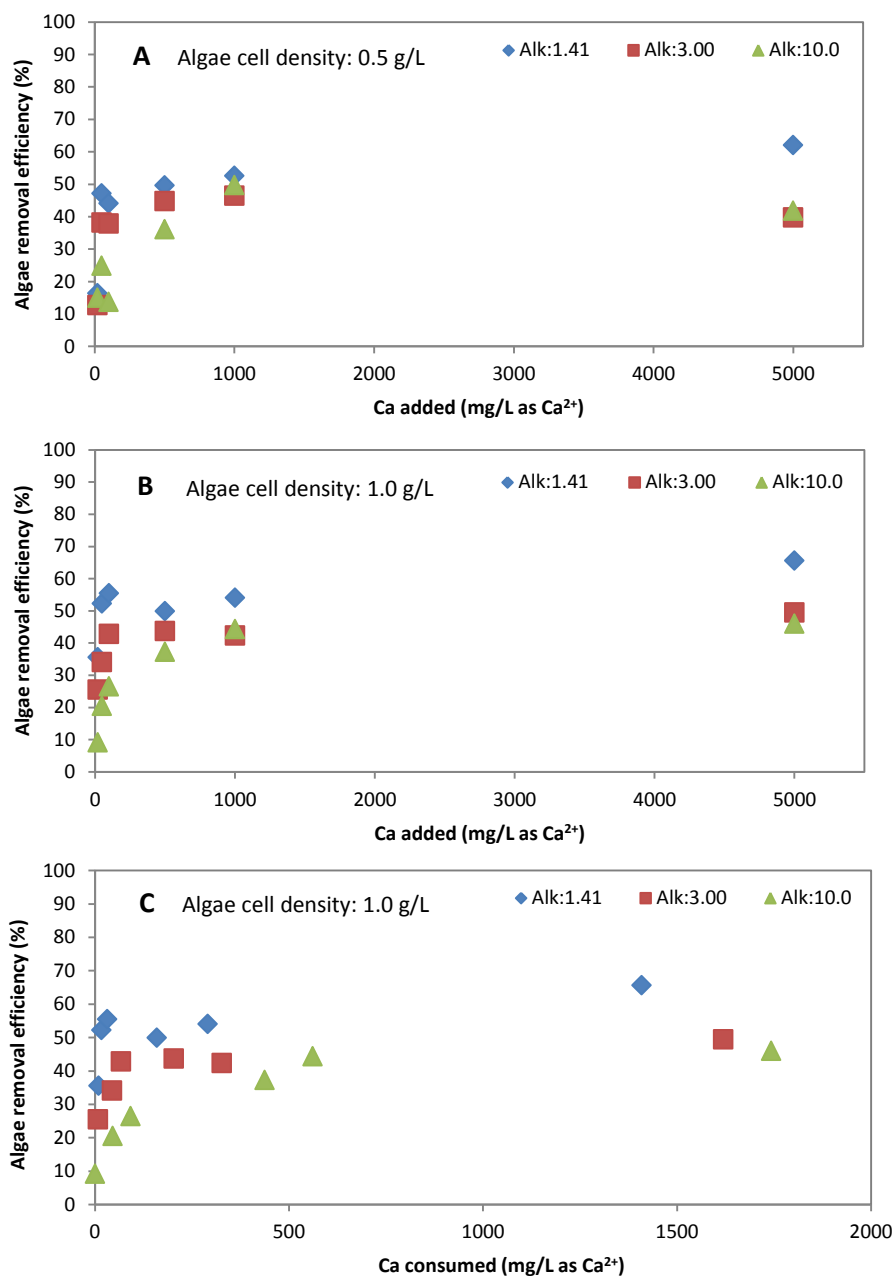


Figure 5-5 Effect of Ca addition (dissolved Ca<sup>2+</sup>) on algae removal for a range of initial alkalinity (1.41, 3.0, 10.0 meq/L) and for (A) 0.5 g/L and (B) 1.0 g/L algae cell density. (C) Algae removal for 1.0 g/L algae cell density is plotted as a function of calcium consumed. The pH of the solutions was adjusted to 10.6 thus, *in situ* precipitation of CaCO<sub>3(s)</sub> was allowed during the experiments.

To more fully understand the key parameters affecting algae removal during  $\text{CaCO}_3(\text{s})$  precipitation, additional unseeded experiments were conducted for different ion activity ratios ( $\{\text{Ca}^{2+}\}/\{\text{CO}_3^{2-}\} = 0.5, 1.0, \text{ and } 2.0$ ) as shown in Figure 5-6. The ionic strength of the solution was maintained at a constant level (0.05 M) and the pH of the solutions was adjusted to 10.6.

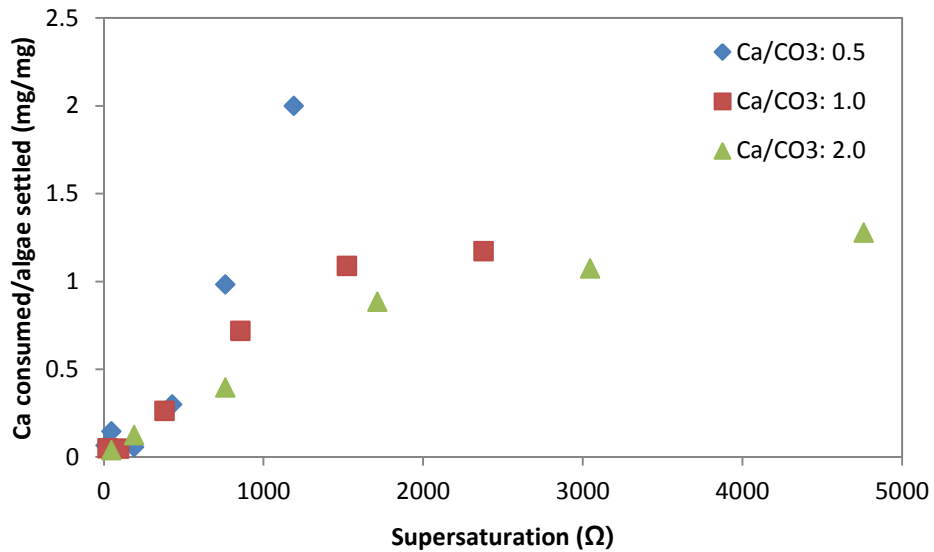


Figure 5-6 Calcium consumption normalized by the amount of algae that has removed (settled) in unseeded experiments for varying ion activity ratios ( $\{\text{Ca}^{2+}\}/\{\text{CO}_3^{2-}\}$ ). The algae cell density was 1.0 g/L.

In Figure 5-6, the plot of normalized calcium consumption (normalized by the amount of algae removed after settling) shows that the normalized calcium consumption increases with increasing supersaturation. These results suggest that the more oversaturated the system with respect to  $\text{CaCO}_3(\text{s})$ , the more precipitate is formed, but not all of the precipitate is associated with algae removal. Moreover, the trend was more

pronounced with decreasing ion activity ratio. Thus, not only is the degree of oversaturation a key parameter but the speciation, or more specifically, the ion activity ratio ( $\{Ca^{2+}\}/\{CO_3^{2-}\}$ ) is also important. Since Ca adsorbs to the algae surface and carbonate does not, this result suggests that initial Ca adsorption to the surface of the algae may be important. These observations can be attributed to (1) homogeneous nucleation under highly oversaturated conditions and (2) a higher likelihood of initial nucleation on the surface of algae at a high ion activity ratio (i.e., high  $Ca^{2+}$  concentrations and low alkalinity). In addition, the rate of precipitation under highly oversaturated conditions especially at a low ion activity ratio (i.e., high carbonate concentrations) is faster (Zeppenfeld, 2010).

In this experiment, dissolved calcium ions can be either precipitated as  $CaCO_{3(S)}$  on the surface of algae via heterogeneous nucleation or precipitated via homogeneous nucleation. If the former is the only case, algae can be enmeshed with precipitated  $CaCO_{3(S)}$  and the  $CaCO_{3(S)}$  also acts as a weighting agent to facilitate settling. If that were the only mechanism for removal, then the amount of precipitation of  $CaCO_{3(S)}$  would be proportional to the amount of algae removed, and the resulting graphs would exhibit linear trends. Thus, the results here suggest that homogeneous nucleation of  $CaCO_{3(S)}$  was also occurring within the system and did not contribute significantly to algae removal. This observation is in good agreement with the previous results that demonstrated that pre-precipitated  $CaCO_{3(S)}$  induced by homogeneous nucleation did not effectively attract algae via heterocoagulation.

To verify the occurrence of homogeneous nucleation in this system, the experiment was repeated in the absence of algae. The percent difference in the amount of calcium precipitated in the presence and absence of algae was plotted as a function of the degree of oversaturation. The oversaturation or supersaturation ( $\Omega$ ) was calculated as:

$$\Omega = \text{IAP}/K_{sp} = \{Ca^{2+}\}\{CO_3^{2-}\}/K_{sp} \quad (5-6)$$

where IAP is the ion activity product,  $K_{sp}$  is the calcite thermodynamic solubility product of calcite ( $K_{sp}= 8.42$  at 25 °C (Stumm and Morgan, 1996)) and  $\{ \}$  denotes the activity of constituent ions of  $\text{CaCO}_{3(s)}$  solid. It should be noted that activities of the ions were calculated with the activity coefficients ( $\gamma_z$ ) determined by the Davies ion activity coefficient equation (Stumm and Morgan 1996) as:

$$-\log \gamma_z = 0.5z^2 [I^{0.5}/(I + I^{0.5}) - 0.3I] \quad (5-7)$$

where  $I$  is the ionic strength and  $z$  the charge of the corresponding ion.

$\Omega$  is used rather than the saturation ratio ( $S$ ) for the degree of oversaturation in order for our values to be comparable to the values calculated by many others (Nielsen, 1984; Nancollas and Reddy, 1971; Stabel, 1986; Zeppenfeld, 2010; many others). However, it should be noted that the trends observed are similar regardless of whether  $S$  or  $\Omega$  is used.

The results plotted in Figure 5-7 show that the presence of algae leads to greater enhancement in calcium removal when the degree of oversaturation is lower. At high values of  $\Omega$  (greater than 1,000) virtually no enhancement is observed.

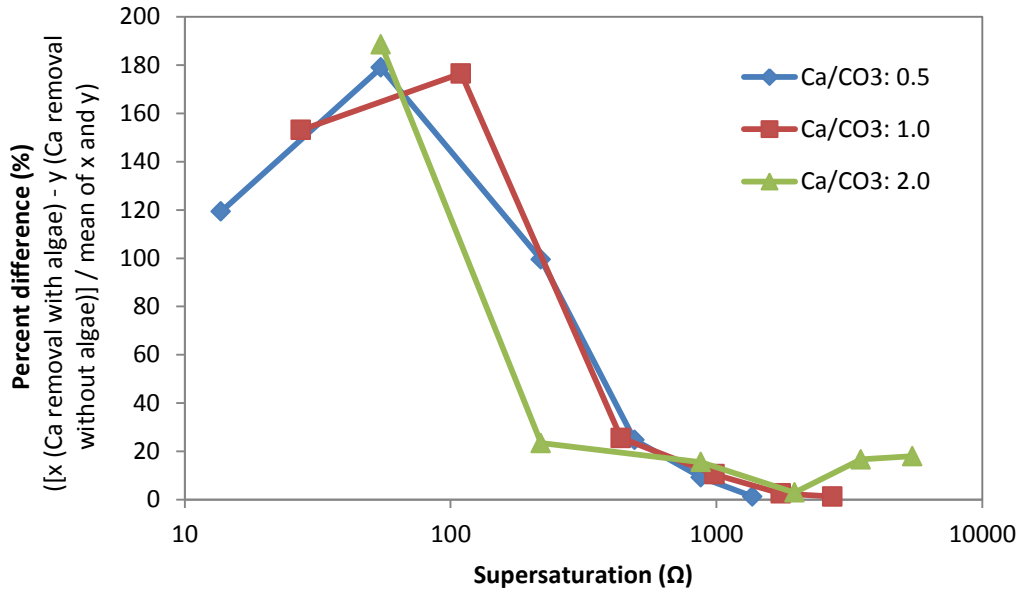


Figure 5-7 Impact of the degree of supersaturation on enhanced calcium removal in the presence of algae (algae cell density of 1.0 g/L). The percent difference plotted on the y-axis is the difference in removal of Ca in the presence and absence of algae. The supersaturation ratio with respect to  $\text{CaCO}_{3(s)}$  was calculated based on the initial calcium concentration and carbonate concentration at target pH 10.6.

Homogeneous nucleation for the formation of  $\text{CaCO}_{3(s)}$  nuclei often requires higher energy (i.e., higher IAP) than that required for heterogeneous nucleation. But at high supersaturation (i.e.,  $\Omega = \text{IAP}/K_{sp} > 100$ ), homogeneous nucleation is almost instantaneous (Stabel, 1986). Thus, the results can be interpreted in terms of the different nucleation mechanisms; the occurrence of homogeneous nucleation does not

contribute significantly to algae removal at high supersaturation. Heterogeneous nucleation, by definition, can occur on the surface of algae in this system. The proportion of these two modes of nucleation is governed not only by the surface properties of algae but also by the composition of water in which algae are grown.

Evidence for nucleation of calcite on biological surfaces is present in the literature. Biomineralization (often termed as calcification) occurs on microbial cell surfaces (e.g., bacteria, algae), and extracellular polymeric substances (EPS) provide sites responsible for  $\text{CaCO}_{3(s)}$  nucleation due to their capacity for binding  $\text{Ca}^{2+}$  ions (Lowenstam, 1981; Arp et al., 1999; Kawaguchi and Decho, 2002; van Lith et al., 2003; Gilbert et al., 2005; Obst et al., 2009). It has been suggested that surface functional groups of cyanobacteria, such as carboxylic and phosphate groups, are responsible for  $\text{Ca}^{2+}$  adsorption (Dittrich and Sibling, 2006). According to a mechanistic model suggested by Thompson and Ferris (1990), nucleation can be initiated by adsorption of  $\text{Ca}^{2+}$  ions binding to the cell surface. Subsequently, diffusion of hydroxyl ions through the cell membrane induces local supersaturation due to the uptake of bicarbonate ions via photosynthesis. In our system, elevated pH was shown to enhance Ca adsorption which was likely the initial step for the heterogeneous nucleation. In addition, the higher the concentration of  $\text{Ca}^{2+}$  ions in solution with the algae (i.e., high ion activity ratio ( $\{\text{Ca}^{2+}\}/\{\text{CO}_3^{2-}\}$ ), the greater the likelihood of nucleation on the surface of algae. Therefore, the experimental observation that the amount of precipitation of  $\text{CaCO}_{3(s)}$  required for the removal of an equivalent mass of algae increases with decreasing ion activity ratio ( $\{\text{Ca}^{2+}\}/\{\text{CO}_3^{2-}\}$ ) can be attributed to decreased available  $\text{Ca}^{2+}$  in the

solution for adsorption. The lower availability of  $\text{Ca}^{2+}$  in turn yields less heterogeneous nucleation on the surface of algae.

Moreover, it is also possible that enhanced kinetics of precipitation with increasing  $\text{Ca}^{2+}$  added is responsible for the increase in the normalized calcium consumption with increasing  $\text{Ca}^{2+}$  added at a high ion activity ratio. This trend was more pronounced with decreasing ion activity ratio. Previous research has shown an increased rate of crystal growth due to the increased number of carbonate active sites (i.e.,  $\equiv \text{CaCO}_3^-$ ) at the surface of  $\text{CaCO}_{3(\text{s})}$  (Nisson and Sternbeck, 1999; Zeppenfeld, 2010). In addition to the surface species, the change in the solute species with decreasing ion activity ratio can increase precipitation rates. Hydrated calcium ions in the solution can replace their water molecules with carbonate ligands, forming partially dehydrated  $\text{CaCO}_3^0$  species. Since cation dehydration is required for crystal growth prior to incorporation into the crystal lattice, this ligand exchange promotes the rate of crystal growth because the water exchange rate of  $\text{CaCO}_3^0$  is higher than that of hydrated calcium ions (Nillson and Sternbeck, 1999; Zeppenfeld, 2010; Ruiz-Agudo et al., 2011).

### **5.3.4. Impacts of Homonucleation vs. Heterocoagulation**

#### **5.3.4.1. Effect of the mode of nucleation on algae removal**

The previous data examining the impact of the degree of supersaturation highlighted the importance of the mode of nucleation of  $\text{CaCO}_{3(\text{s})}$  precipitation. To verify this conclusion, further testing was conducted. Algae removal and calcium

removal were monitored as a function of pH at fixed Ca and algae biomass addition. In addition, the extensibility of the findings to a different algal system was investigated.

Algae removal and calcium removal were monitored over a wide range of pH values (7.5 – 11.5) as shown in Figure 5-8. Removal of both Ca and algae initially increased with increasing pH; however, the removal of algae peaked, declined and then plateaued for both total Ca concentrations tested. In both cases, the initial rise in algae removal occurs at a pH just below (0.2-0.3 pH units) the onset of observable Ca removal. In contrast to the trend in algae removal with pH, the percent calcium removal continued to increase with increasing pH throughout the range of pH values tested.

The driving force for precipitation of  $\text{CaCO}_{3(s)}$  (the degree of supersaturation) gradually increased with increasing pH of the solution. In the presence of algae particles, heterogeneous nucleation should precede homogeneous nucleation due to the lower energy required for the formation of nuclei of  $\text{CaCO}_{3(s)}$  on the surface of algae. With further pH increases, homogenous nucleation is favorable and eventually dominates in highly supersaturated conditions. Therefore, it can be hypothesized that algae removal associated with calcium (e.g., the sharp increase and decrease in algae removal after the peak) is highly dependent on the nucleation process for  $\text{CaCO}_{3(s)}$  (i.e., hetero and homogeneous nucleation).

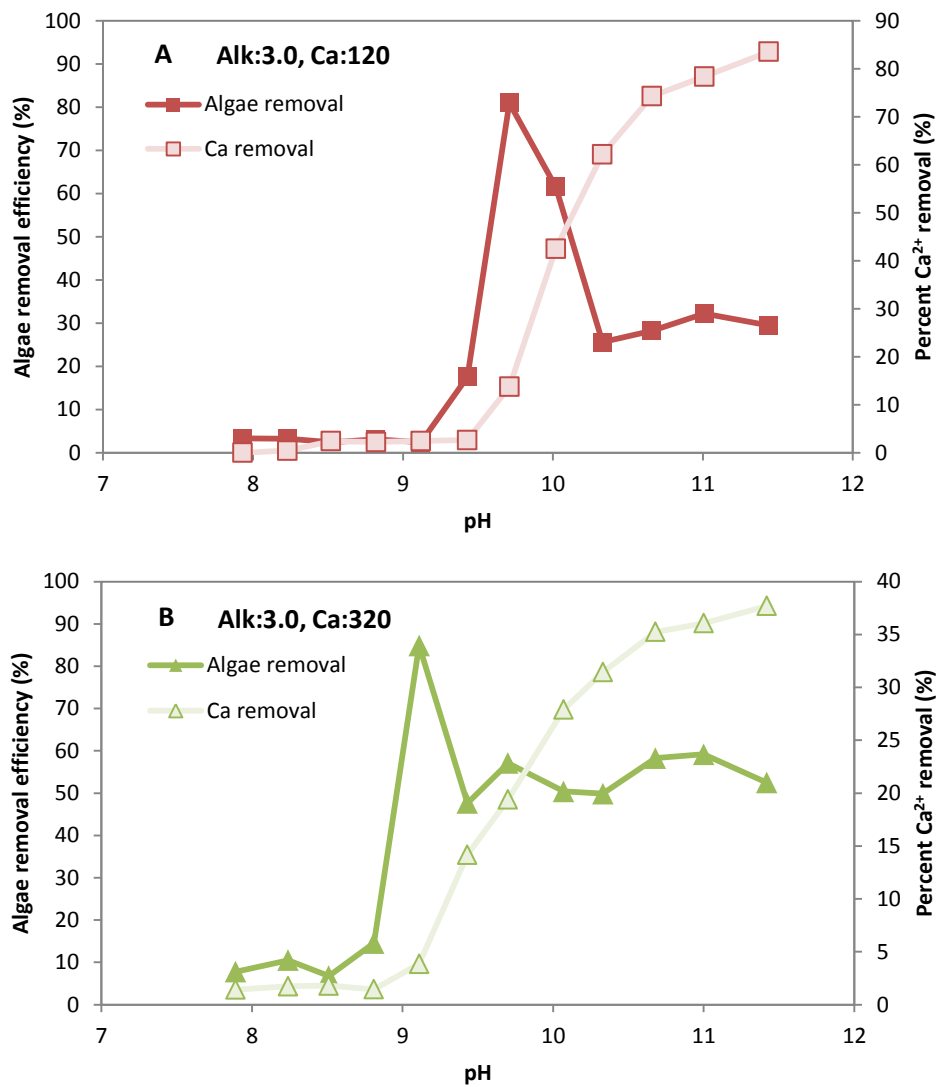


Figure 5-8 Effect of pH on algae removal and  $\text{Ca}^{2+}$  removal for two different initial calcium ion concentrations, 120 mg/L as  $\text{Ca}^{2+}$  (A) and 320 mg/L as  $\text{Ca}^{2+}$  (B), respectively. Initial alkalinity was 3.0 meq/L for both tests. The algae cell density was 0.5 g/L.

Further testing was conducted in the absence and presence of magnesium ions as shown in Figure 5-9, because magnesium has been known to exhibit an inhibitory effect

on the kinetics of  $\text{CaCO}_3(\text{s})$  precipitation, retarding nucleation (Bischoff, 1968; Reddy, 1995) and crystal growth (Reddy and Nancollas, 1976; Gutjarh et al., 1996).

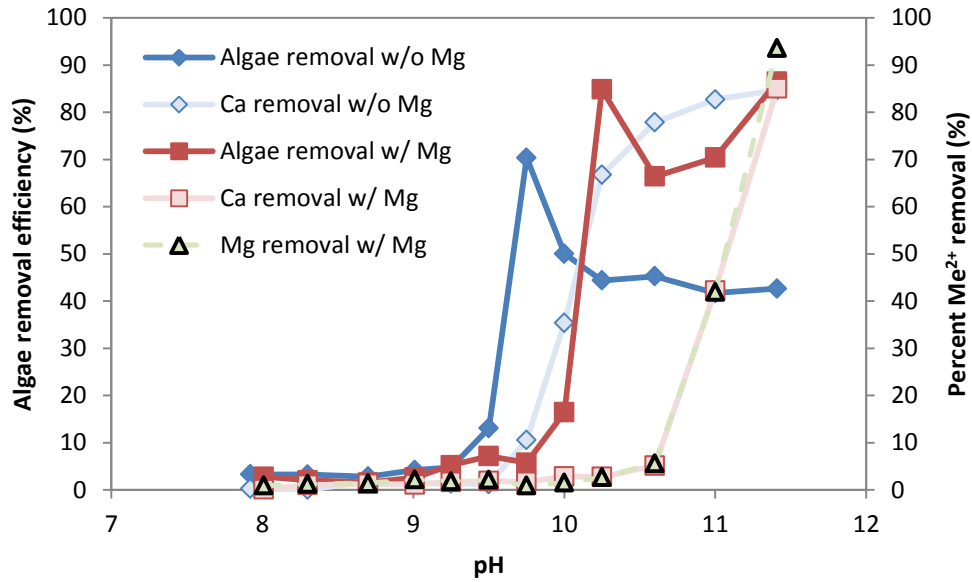


Figure 5-9 Comparison of algae removal in the presence and absence of magnesium. Percent algae removal on the left axis and  $\text{Me}^{2+}$  ( $\text{Ca}^{2+}$  or  $\text{Mg}^{2+}$ ) removal on the right axis were plotted as a function of pH. Initial concentrations of calcium, magnesium, algae and alkalinity were 120, 100 mg/L (when present) and 3.0 meq/L, respectively. The algae cell density was 0.5 g/L.

In the presence of magnesium, both the peak in algae removal and the location of the calcium removal edge shifted to the right. For example, algae removal at pH 9.75 decreased from approximately 70% to 6% in the presence of an initial  $\text{Mg}^{2+}$  concentration of 100 mg/L. In addition, both the Mg and Ca removal edges are coincident and located at significantly higher pH than the edge or onset of algae removal.

However, the peak in algae removal still occurs at the apparent onset of Ca and Mg removal.

These experimental results can be interpreted in the context of heterogeneous nucleation of  $\text{CaCO}_{3(\text{S})}$  at moderate supersaturation that is affected by the presence of Mg. The peak in algae removal in the absence of magnesium was at pH 9.75. In the presence of magnesium, there is a shift in the algae removal peak to a higher pH value of 10.25 consistent with Mg inhibition that retards heterogeneous nucleation of  $\text{CaCO}_{3(\text{S})}$ . The resulting algae removal of 84 % (i.e., algae removal at peak) in the presence of Mg is higher than that in the absence of Mg (e.g., 70 %) likely due to the more positive charge provided by Mg incorporation into the precipitating  $\text{CaCO}_{3(\text{S})}$  phase or adsorption of  $\text{Mg}^{2+}$  directly to the algae surface. Neutralization of the negative surface charge of algae was shown to be more effective with  $\text{Mg}^{2+}$  as it exhibits higher adsorption capacity than  $\text{Ca}^{2+}$  (see Figure 5-1).

The resulting algae removal of 84 % in the presence of Mg is in good agreement with the observed algae removal associated with magnesium in Chapter 4 (e.g., 86 % algae removal at pH 10.26 in Figure 4-4 B). However, in this case, Ca is most certainly partially involved in algae removal or there would not be a decrease in algae removal at higher pH. Thus, the mechanisms responsible for these similar algae removal in two different systems (i.e., in the presence of both Ca and Mg vs the system in which only Mg is present) may not be the same. As indicated in Figure 5-10, Mg removal is also retarded with respect to pH in the presence of Ca. This is possibly due to competition between Ca and Mg for adsorption sites on the algae and interaction between Mg and the

precipitating calcium (i.e., Mg inhibition) which reduces the amount of Mg available for charge neutralization of the algae. The results of this phase of research imply that Ca and Mg are interacting with each other and that the interaction not only affects the extent of removal but also the pH at which optimum removal occurs. Moreover, the mechanism for algae removal appears to be pH dependent. Further evidence for the change in mechanisms of removal as a function of pH in the Ca/Mg system is reflected in the increase in algae removal above pH 10.6 where the system is oversaturated with respect to  $\text{Mg(OH)}_{2(s)}$ .

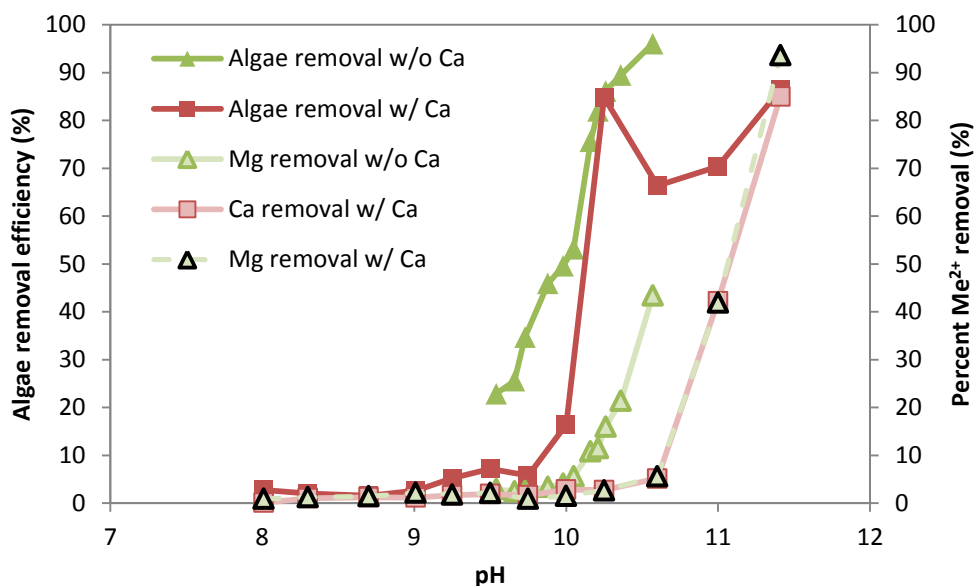


Figure 5-10 Effect of calcium on algae and magnesium removal. Percent algae removal on the left axis and  $Me^{2+}$  ( $Ca^{2+}$  or  $Mg^{2+}$ ) removal on the right axis were plotted as a function of pH. In the absence of calcium, initial concentrations of magnesium, alkalinity, and algae cell density were 100 mg/L, 0.98 meq/L, and 0.64 g/L, respectively. In the presence of calcium, initial concentrations of magnesium ion, calcium ion, initial alkalinity, and algae cell density were 100 mg/L, 120 mg/L, 3.0 meq/L, and 0.5 g/L, respectively.

Justification for the impact of magnesium on the surface charge and morphology of  $CaCO_{3(S)}$  is available in the literature. Russell et al (2009) observed a more positive surface charge (more favorable for attracting algae) with increasing  $Mg^{2+}$  concentration, which they attributed to incorporation of  $Mg^{2+}$  into the calcite crystal lattice. They also observed a change in morphology from highly structural to a rounded and elongated shape which is consistent with the classical study by Folk (1974) that showed that incorporation of magnesium ions into the crystal lattice impedes sideward growth and results in an elongated crystal structure. If that were the case, the algae removal would

have continued to increase. However, experimental results (algae removal slightly decreased after the peak in the presence of magnesium) suggest that the positive effect of magnesium on the characteristics of  $\text{CaCO}_{3(s)}$  exhibit the minimal impact on algae removal compared to the negative effect of homogeneous nucleation of  $\text{CaCO}_{3(s)}$ .

It was obvious from the previous tests that the pH values of 9.7 and 10.6 are representatives of the two modes of nucleation that affect algae removal mechanisms. Therefore, scanning electron microscopy (SEM) analysis was performed to characterize the flocculated solids that formed at the pH values of 9.7 (panel A-D) and 10.6 (panel E-H) as shown in Figure 5-11.

SEM images provided additional information as to how the nucleation processes for  $\text{CaCO}_{3(s)}$  affect the floc formation. At pH 9.7, it appears that nucleation occurred at the edge of the cells. As the crystals grow, they bridge cells leading to aggregation and larger flocs. It should be noted that the shape of the crystal formed on the surface of the algae could be species-dependent. Dittrich and Obst (2004) observed that *Chlorella* was embedded in calcite crystals. However, Obst et al. (2009) did not observe embedment, but rather precipitates were located at the edges of their cyanobacteria cells.

At pH 10.6, more precipitation is evident on the algae surfaces. Crystals induced by homogeneous nucleation were also observed. The larger number of structural and negatively charged  $\text{CaCO}_{3(s)}$  crystals could prevent algae from aggregating within the given retention time.

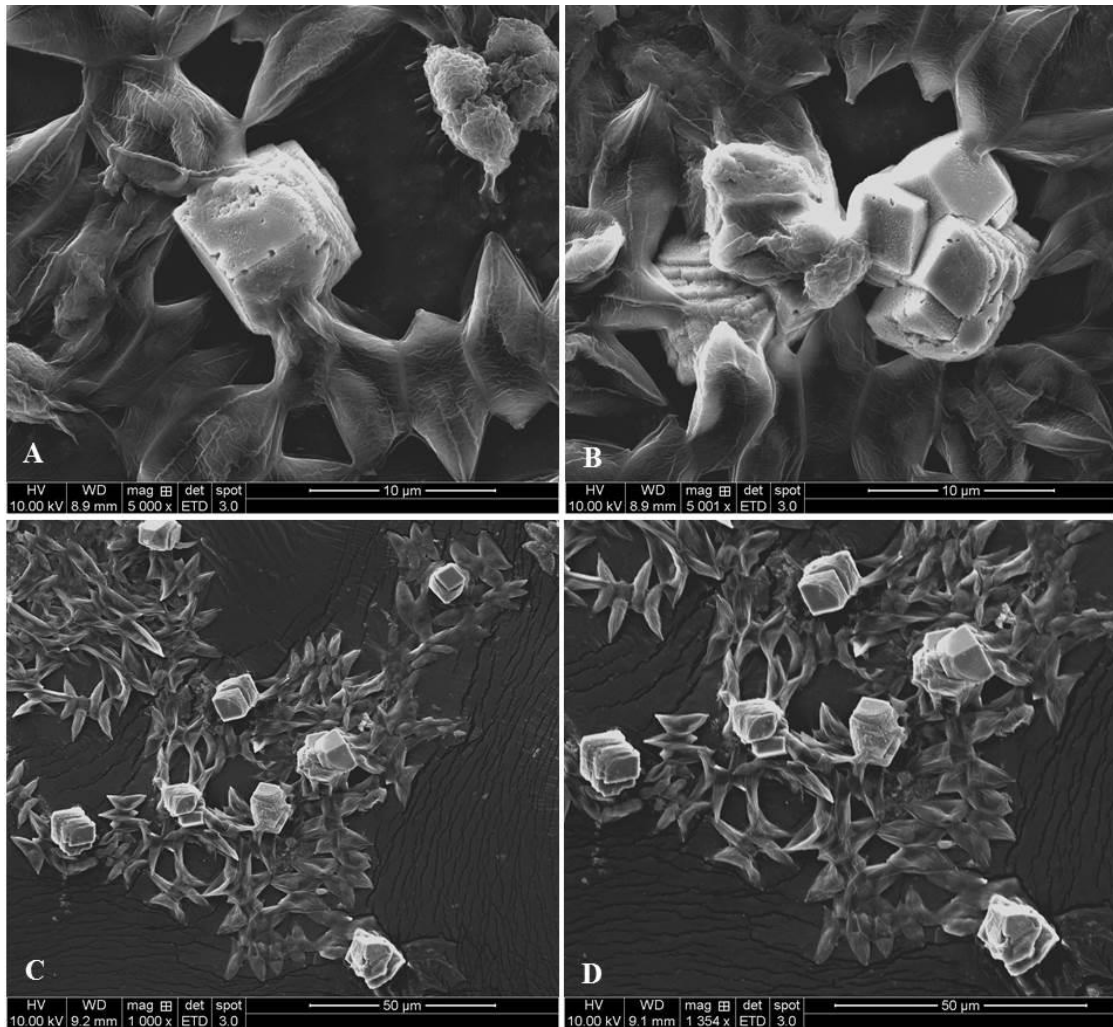


Figure 5-11

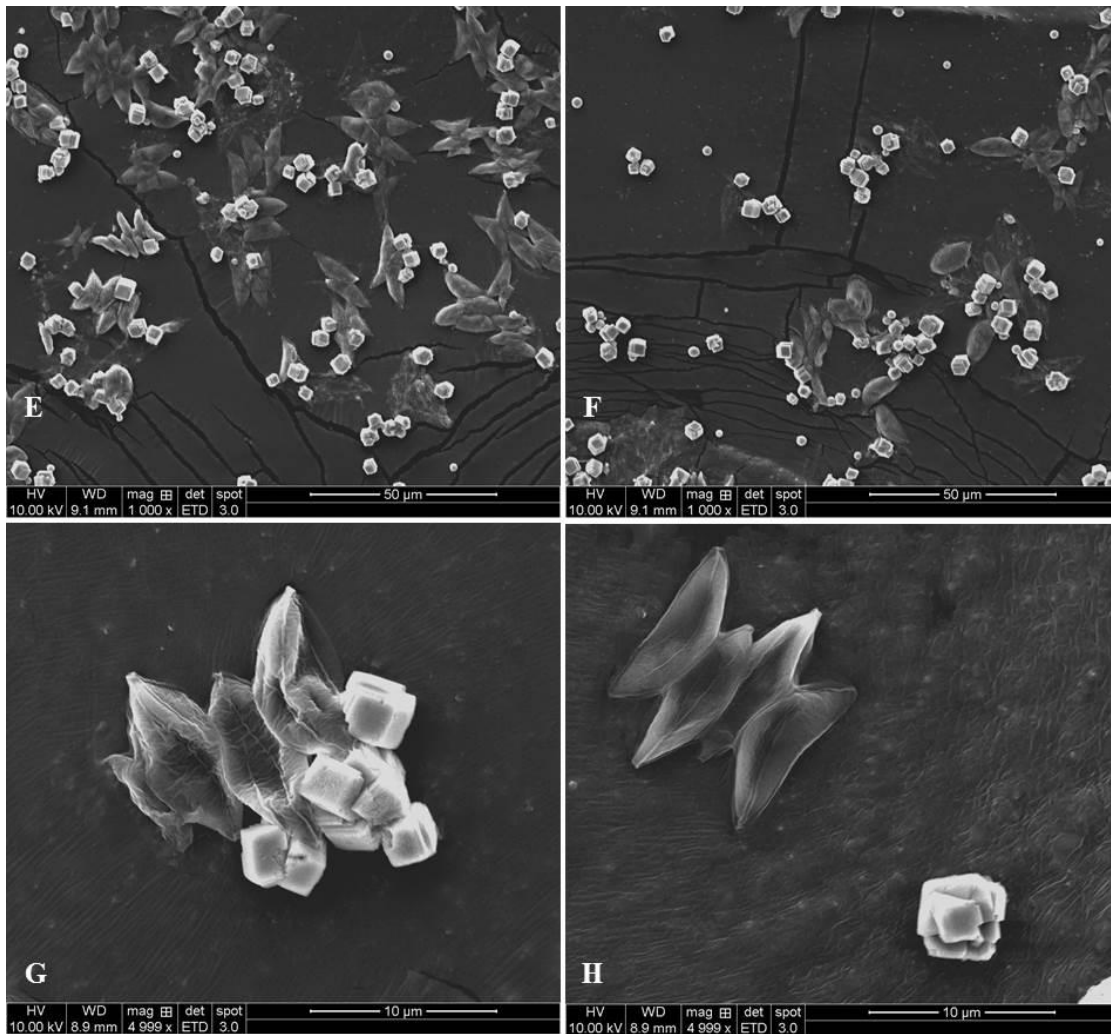


Figure 5-11 Scanning electron microscopic (SEM) images of flocculated solids formed at the pH 9.7 (panel A-D) and 10.6 (panel E-H) during the variable pH tests. Initial concentration of calcium and initial alkalinity were 120 mg/L and 3.0 meq/L, respectively.

It was experimentally and microscopically shown that, in systems containing only Ca as the divalent cation, high pH yields lower algae removal. These findings were also evident in the variable pH tests conducted for different ionic strengths of the

solutions, as shown in Figure 5-12 in which the removals are plotted versus the degree of oversaturation. The experimental conditions employed in the previous variable pH tests (e.g., initial  $\text{Ca}^{2+}$  concentration of 120 mg/L as  $\text{Ca}^{2+}$  and 3.0 meq/L of alkalinity) were repeated for the three different levels of ionic strength (0.01, 0.1, and 0.4 M) shown in the figure. It was observed that, regardless of the ionic strength of the solution, algae removal efficiency (panel A) and percent  $\text{Ca}^{2+}$  removal (panel B) started to increase at the same level of supersaturation. This consistency is in good agreement with the previous variable pH tests that showed that the pH of the algae removal peak matches the pH at which the percent  $\text{Ca}^{2+}$  removal starts to increase. However, an apparent peak was not observed for the higher ionic strength of 0.1 and 0.4 M. Moreover, algae removal decreased with increasing ionic strength in highly supersaturated regions. In other words, the negative impact of homogeneous nucleation becomes more pronounced with increasing ionic strength of the solution. This result is counterintuitive to the fact that more compression of the diffuse layer occurs at higher ionic strength which should lead to increased algae coagulation, as seen in the jar test in the absence of carbonate (see Figure 5-3). Because repulsive forces are reduced by the compression of the diffuse layer, particles are aggregated via van der Waals attraction. However, the experimental results at high supersaturation may indicate that homogeneous nucleation is favored in a solution with a higher ionic strength due to reduced adsorption of  $\text{Ca}^{2+}$  on the algae surface with increasing ionic strength.

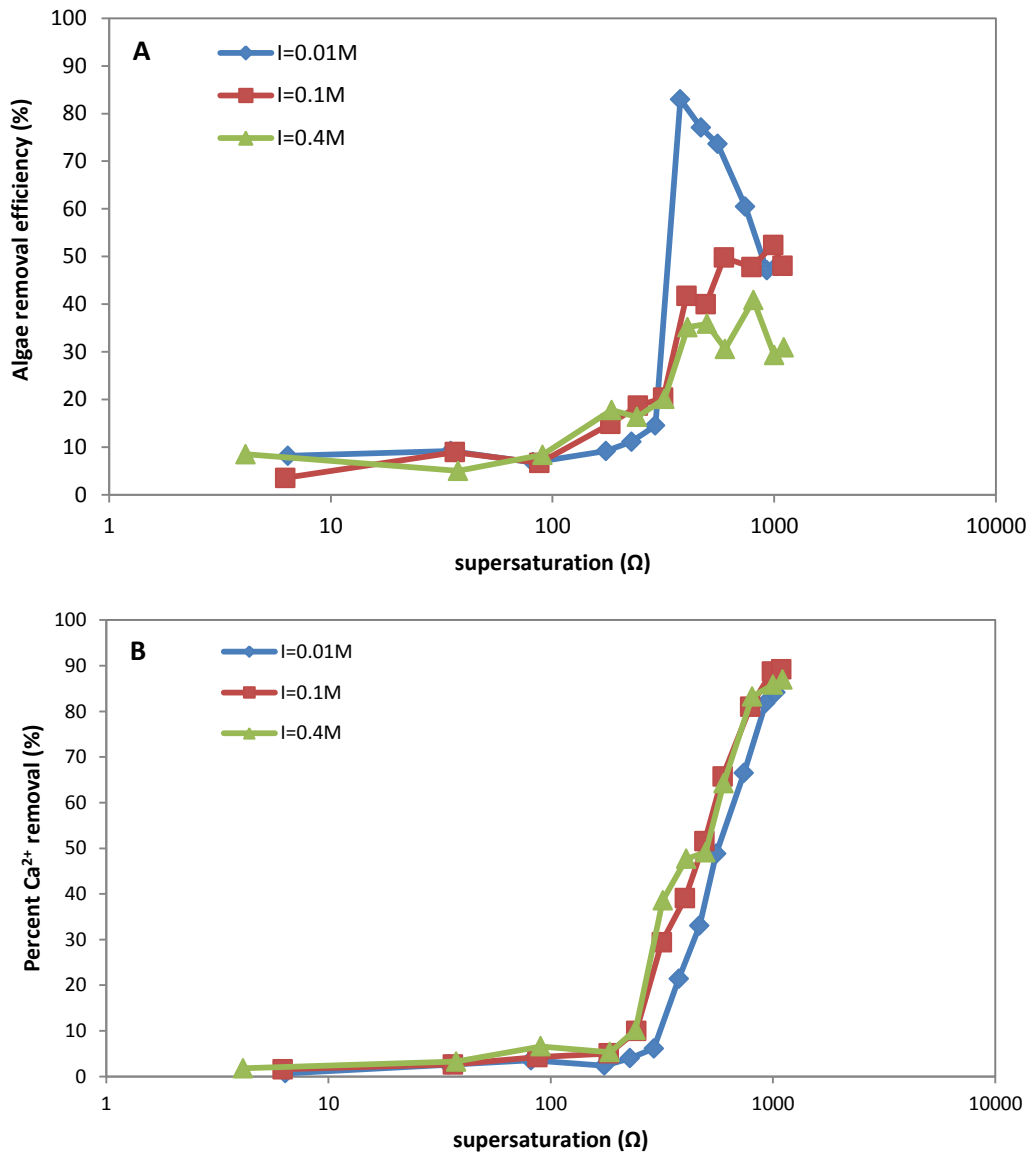


Figure 5-12 Effect of ionic strength on algae removal efficiency and percent  $\text{Ca}^{2+}$  removal. Algae removal efficiency (A) and percent calcium removal (B) at three levels of ionic strength were plotted as a function of supersaturation ratio. The experimental condition in the previous variable pH test (e.g., initial  $\text{Ca}^{2+}$  concentration of 120 mg/L as  $\text{Ca}^{2+}$  and 3.0 meq/L of alkalinity) was carried out in three levels of ionic strength of the solution. Initial activities of calcium and bicarbonate ions for all the cases of ionic strength were set equal.

#### 5.3.4.2. Effect of algae cell density on algae removal

The extent of algae removal is likely affected by the concentration of algae present since algae provide the sites for the reactions associated with calcium including adsorption and precipitation of  $\text{CaCO}_{3(s)}$ . Therefore, the variable pH tests were conducted to investigate the effect of algae cell density on algae removal associated with calcium. One of the experimental conditions (i.e., initial  $\text{Ca}^{2+}$  concentration of 120 mg/L as  $\text{Ca}^{2+}$  and initial alkalinity of 3.0 meq/L) was carried out for different algae cell densities ranging from 0.25 to 3.0 g/L as shown in Figure 5-13.

At low pH below 9.7, algae removal generally increased with increasing algae cell density possibly due to the higher frequency of collisions between the cells. At moderate pH, however, the trend in algae removal was reversed. As indicated in panel B, calcium removal was no longer dependent on algae cell density as the pH is increased above 9.7. In other words, the amount of  $\text{CaCO}_{3(s)}$  precipitated via heteronucleation might be fixed regardless of algae cell density. This result suggests that the amount of algae that can be aggregated via heteronucleation is fixed, leaving a higher number of algae not effectively aggregated with increasing algae cell density. This limited effectiveness of heteronucleation could result in diminished algae removal efficiency with increasing algae cell density at pH values higher than 9.7, even though the collision efficiency is higher with higher algae cell density.

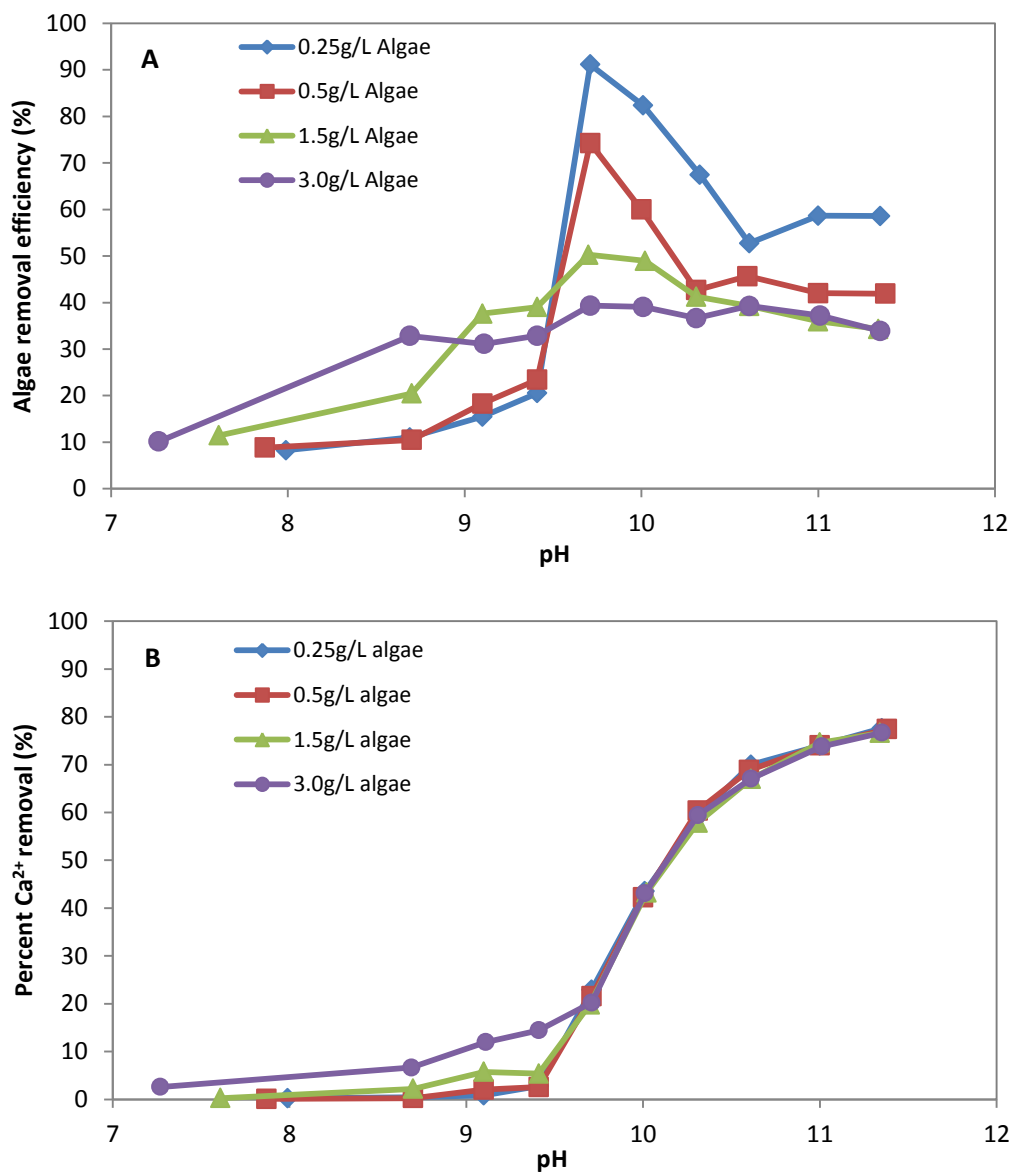


Figure 5-13 Effect of algae cell density on algae removal. Percent  $\text{Ca}^{2+}$  removal (A) and algae removal efficiency (B) were plotted as a function of pH. The experimental condition in the previous variable pH test (e.g., initial  $\text{Ca}^{2+}$  concentration of 120 mg/L as  $\text{Ca}^{2+}$  and 3.0 meq/L of alkalinity) was carried out algae cell densities of 0.25, 0.5, 1.0, and 3.0 g/L.

#### **5.3.4.3. Extensibility to a different algal species**

Currently, a large number of algal species are being studied and cultivated for a variety of applications. In addition to the characteristics of the surrounding water (e.g., pH, types and concentration of ion, organic matter, alkalinity, temperature, and ionic strength) and the interactions between algae and background water species (e.g., metal adsorption and surface precipitation), the characteristics of the algae (e.g., size, density, surface charge, morphology, EPS) are also major factors affecting the algae harvesting process. To investigate the extensibility of the findings to a different algal system, a second algae species, *Chlorella* sp. was used and compared to *Scenedesmus* sp. as shown in Figure 5-14. Comparison of the characteristics of the two algae species are shown in Table 5-3.

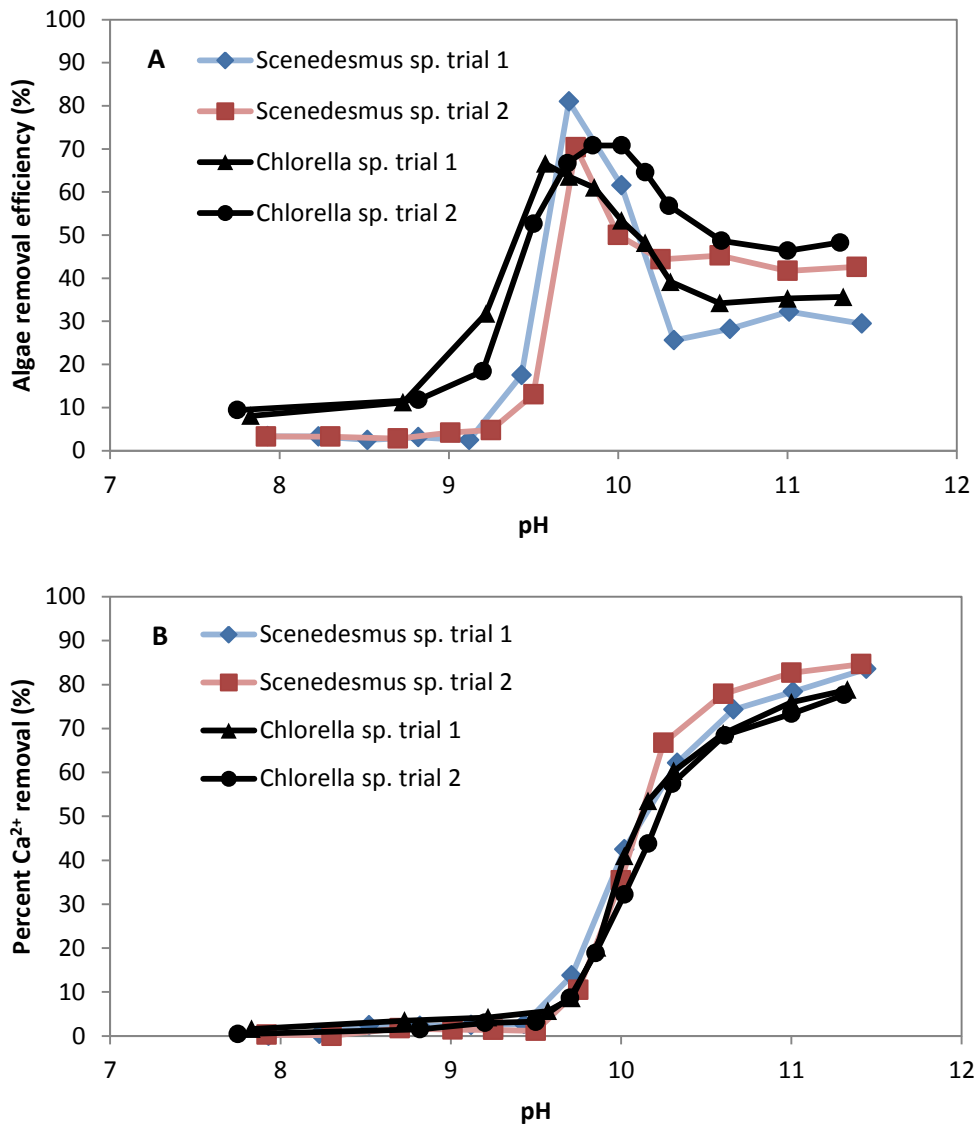


Figure 5-14 Effect of the modes of nucleation for  $\text{CaCO}_3(\text{s})$  on algae removal for the two common algae species, *Scenedesmus* sp. and *Chlorella* sp. Algae removal efficiency (A) and percent calcium removal (B) for two different algae species were plotted as a function of pH. Initial calcium ion concentration and initial alkalinity were 120 mg/L and 3.0 meq/L, respectively. Algae cell density was 0.5 g/L for two algae species. Colored and black lines are assigned to *Scenedesmus* sp. and *Chlorella* sp., respectively.

Table 5-3 Characteristics of two algal species studied in this research (*Chlorella* sp. and *Scenedesmus* sp.).

	<b>Chlorella vulgaris</b>	<b>Chlorella sp.</b>	<b>Scenedesmus quadricauda</b>	<b>Scenedesmus obliquus</b>
Size (µm)	5.3	3.5	13.1	3-9(d); 6-17(l)
Colonial	Single cell	Single cell	Row(s) of 4-16 cells with spinal appendages	Row(s) of 4-16 cells with spinal appendages
Shape	Sphere	Sphere	Ellipsoidal	Ellipsoidal
Density (kg m <sup>-3</sup> )	1070	1070	-	-
Zeta potential (mV)	-10.0	-10	-25 to -35	-11.2
Test condition (pH, test water)	7, distilled water	4-8, distilled water	7-10, distilled water	7
Reference	Ives (1959)	Liu et al. (1999)	Phoochinda and white (2003)	Bernhardt and Clasen (1991)

It was observed in Figure 5-14 that the algae removal efficiency of *Chlorella* sp. started to increase at lower pH compared to *Scenedesmus* sp. Although further work was not conducted, differences in the surface characteristics of the algae are likely responsible for this experimental result. For example, the surface charge of *Chlorella* sp. might have been more effectively neutralized due to the lower value of zeta potential indicated in Table 5-3. Previous research (Ometto et al., 2014) has suggested that *S. obliquus* with lower charge density ( $1 \pm 0.06 \text{ peq } \mu\text{m}^{-2}$ ) require less coagulant than *C. vulgaris*

( $4.6 \pm 0.22$  peq  $\mu\text{m}^{-2}$ ) based on their charge density measurements. But the larger surface area and the higher protein content (responsible for complexation with cations) justifies the higher coagulant dosage observed in *S. obliquus* compared to *C. vulgaris* despite the lower charge density (Pivokonsky et al., 2006; Henderson et al., 2010). It is also possible that the collision efficiency for *Chlorella* sp. is higher since the mass-based algae cell density of 0.5 g/L yields a higher number of cells of *Chlorella* sp. (with the assumption that the densities of two algae species are similar). Even though deviations in algae removal efficiency between the two species can be attributable to the different surface properties or to other parameters, the overall trends in algae removal efficiency (e.g., the existence of removal peak and decrease in removal after the peak) and percent  $\text{Ca}^{2+}$  removal for the two common algae species are similar suggesting that the modes of nucleation for  $\text{CaCO}_{3(s)}$  play an important role in algae removal process regardless of algal species of interest.

### **5.3.5. Potential for acid deflocculation of algae flocculated with Ca**

Flocculated solids prepared over a range of initial  $\text{Ca}^{2+}$  concentrations at pH 10.6 were acidified to pH 6.0 by bubbling  $\text{CO}_2$  through the flocculated solids. By measuring the  $\text{Ca}^{2+}$  concentration before and after acidification, the percent Ca dissolved (i.e., amount of  $\text{CaCO}_{3(s)}$  redissolved via acidification) was calculated as shown in Figure 5-15. To determine whether the system was supersaturated with  $\text{CaCO}_{3(s)}$  at pH 6.0, the Langelier Index (L.I.) was used. L.I. can be calculated as (Langelier, 1939):

$$L.I. = pH_a - pH_s \quad (5-8)$$

$$pH_s = pK_{a,2} - pK_{so} + p[Ca^{2+}] + p[HCO_3^-] - \log\gamma_{Ca^{2+}} - \log\gamma_{HCO_3^-} \quad (5-9)$$

where  $pH_a$  is the actual pH of water,  $pH_s$  is the pH of water if it were in equilibrium with  $CaCO_{3(s)}$  at the existing solution concentrations of  $Ca^{2+}$  and  $HCO_3^-$ ,  $K_{a,2}$  is the second dissociation constant of carbonic acid,  $K_{so}$  is the solubility constant of  $CaCO_{3(s)}$ , and  $\gamma_i$  is the activity coefficient of each ion.

The results suggested that complete dissolution was not achieved. For example, the L.I. for the 320 mg/L as  $Ca^{2+}$  and 3 meq/L initial alkalinity is -0.83 indicating that the acidified algae concentrate is theoretically undersaturated with respect to  $CaCO_{3(s)}$  at pH 6.0. However, the experimental results demonstrated that precipitated  $CaCO_{3(s)}$  solids were not rapidly redissolved. Less solids were redissolved with increasing initial  $Ca^{2+}$  concentration and initial alkalinity indicating that the effectiveness of the deflocculation process can be a function of the initial water composition. During the experiments, the target pH of 6.0 was reached within a minute, but substantially more time would be required to achieve complete dissolution. Nonetheless, at low Ca concentration, over 70 percent of the solids could be redissolved.

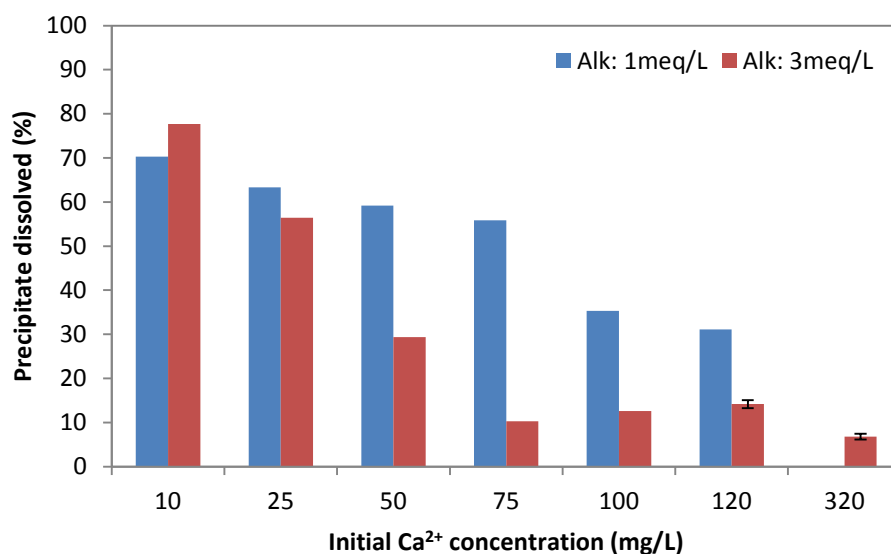


Figure 5-15 Effect of the initial water composition on the deflocculation process. Flocculated solids for a range of initial Ca<sup>2+</sup> concentrations and pH of 10.6 were acidified to pH 6.0 by bubbling the CO<sub>2</sub>. The error bars indicate the standard deviation calculated from each experiment (n=3).

#### 5.4. CONCLUSIONS

In this chapter, the role of calcium in the algae harvesting process was elucidated in the absence of multivalent cations other than calcium via bench-scale experiments with *Scenedesmus* sp. The results indicate that algae removal in this system is dependent on the nucleation process for CaCO<sub>3(s)</sub>. In other words, the modes of CaCO<sub>3(s)</sub> nucleation (heterogeneous and homogeneous nucleation) control algae removal efficiency. Effective algae coagulation (e.g., up to 82% algae removal efficiency) can be achieved via heterogeneous nucleation for CaCO<sub>3(s)</sub> at low supersaturation and ionic strength. Algae removal can be attributed to adsorption of Ca<sup>2+</sup> onto the algae cell surface which

provides nucleation sites for  $\text{CaCO}_3(\text{s})$  precipitation. Bridging of calcite particles between the cells leads to more rapid aggregation and formation of larger flocs in the presence of algae. In the same vein, the process is favored in solutions containing a higher ratio of  $\text{Ca}^{2+}/\text{CO}_3^{-2}$ . At high supersaturation, algae removal is diminished due to the occurrence of homogeneous nucleation even for high algae cell densities in which better collision efficiency can be expected. Thus, the results indicate that water chemistry, pH, ionic strength, alkalinity and  $\text{Ca}^{2+}$  concentration can be optimized for algae harvesting operations. Algae-laden flocculated solids can be acidified by  $\text{CO}_2$  injection for deflocculation and the effectiveness of the deflocculation process is a function of initial water composition.

## **Chapter 6: Evaluation of pH Induced Flocculation for a Range of Source Waters**

### **6.1. INTRODUCTION**

Algae removal from water is required for a number of applications including water treatment, biofuel production, and nutraceutical production. The costs of harvesting a microalgal biomass can be significant, accounting for up to 20-30% of the total cost of producing biomass (Grima et al., 2003). The high cost of dewatering has been a major bottleneck to microalgae bioprocess engineering for algae biodiesel production (Uduman et al., 2010). Thus, it is not surprising that cost effective harvesting of microalgae is considered to be the most problematic area of algal biofuel production (Greenwell et al., 2010).

The goals for harvesting algae from water are dependent on the specific application but often include production of a metal free biomass (i.e., no aluminum or heavy metals), effluent water suitable for discharge or reuse, and a deflocculated, concentrated algae slurry. For the entire process of algae growth to product recovery to work efficiently, the output of the algae harvesting step must be suitable for the subsequent processing steps that may involve cell lysing and lipid extraction. In addition to the complexities associated with meeting these criteria for algae harvesting, a significant amount of water is required for algae cultivation and harvesting for mass production. Freshwater is increasingly scarce and thus, a wide range of source waters should be considered for algae-based applications. Fortunately, algae can grow in a

wide range of waters including fresh water, saline or brackish water and even in treated wastewater effluents (Yun et al., 1997). Since most natural waters contain both calcium and magnesium, the pH-induced flocculation/deflocculation method discussed in this research has potential as an effective algae harvesting method.

To evaluate the suitability of the pH-induced flocculation/ deflocculation method for a wide range of algae source waters, field testing is required with a variety of source waters. In this research, a number of waters were evaluated in baseline jar tests prior to pilot scale testing to identify the operating conditions (e.g., target pH, chemical dose) for the pilot-scale testing. However, most of this work was conducted prior to the fundamental research described in Chapters 4 and 5. Nevertheless, it is worthwhile to reexamine the baseline jar test results in light of the findings from the previous chapters to assess whether the results with field waters are consistent with the mechanisms identified for the particular water and conditions employed. In this chapter, the results from baseline jar tests and pilot scale tests with a range of field waters are presented and reexamined to assess whether the removals observed for a range of source water chemistries support the mechanisms identified previously in Chapters 4 and 5. In some cases, options for improving the performance of the pH-induced flocculation/deflocculation process for a particular water chemistry are discussed.

## **6.2. MATERIALS AND METHODS**

### **6.2.1. Algae source waters**

The algae source waters investigated were collected from a variety of sites for use in the pilot scale testing of an algae-to-algal oil process developed at the University of Texas at Austin. In this process, the algae-laden waters from a variety of sources were processed through the pH-induced flocculation/deflocculation system; the deflocculated algae concentrate recovered from this system was then sent to a downstream electromechanical lysing process followed by an oil separation and recovery process that requires deflocculated algae cells to avoid membrane clogging. In support of this pilot-scale effort, a series of baseline jar tests were conducted to assess the conditions necessary to achieve algae removal via pH-induced flocculation.

The algae species and site descriptions for the algal-laden waters tested in this research are summarized in Table 6-1. The sample solutions were kept in an ice chest until they were delivered to the lab at the University of Texas at Austin for analysis of water composition and jar testing. Large quantities of algae solution were also delivered to the Center for Electromechanics (CEM) at the University of Texas at Austin for use in the pilot-scale evaluations of the algae-to-algae oil system.

Table 6-1 Algae species and site descriptions for the range of algae source water tested in this research.

<b>Source Water Designation</b> (Supplier Name)	<b>Algae species</b>	<b>Description</b>
A (AlgaEternal)	<i>Scenedusmus</i> sp.	Pilot-scale photobioreactor utilizing nutrient-enhanced softened water
B (BlueSundial)	<i>Nannochloropsis</i> sp.	Pilot-scale pond utilizing nutrient rich wastewater from a WWTP
C (Conoco)	Multispecies	Lake water with naturally grown algae
D (Hornsby Bend)	Multispecies	Stabilization pond receiving anaerobic digestion effluent
E (South Texas)	Spherical green algae (size of 2 - 3 $\mu\text{m}$ in diameter)	Aquaculture pond water containing brackish water
F (Synthetic)	<i>Nannochloropsis</i> sp.	Pilot-scale pond water utilizing synthetic salt water
G (CEM)	<i>Chlorella</i> sp.	Pilot-scale pond water utilizing synthetic salt water

### 6.2.2. Jar tests

Jar tests were conducted to determine the operating conditions (e.g., pH, addition of supplementary salt, base composition) necessary to harvest algae from each of the source waters. The typical jar test procedure adopted for this research included rapid mixing of sample solutions for 1 min using a magnetic stirrer, followed by slow mixing at 30rpm for 20 min with a Phipps & Bird standard 6-paddle jar tester (Richmond, VA), followed by 20 min of quiescent conditions to allow time for settling. Hydrated lime

solution (10 g/L of  $\text{Ca}(\text{OH})_2$ ) and/or sodium hydroxide solution (1M) were used as the bases to raise the pH of the solution. Depending on the source water characteristics and jar test results, the initial metal ion concentration (e.g.,  $\text{Ca}^{2+}$ ,  $\text{Mg}^{2+}$ ) of the solution was adjusted to the desired levels via the addition of salts. Analytical grade anhydrous calcium chloride and hexahydrated magnesium chloride (i.e.,  $\text{CaCl}_2$  and  $\text{MgCl}_2 \cdot 6\text{H}_2\text{O}$ ) were dissolved in deionized water and added to the algae sample solutions.

### **6.2.3. Pilot-scale tests**

The pilot-scale performance of a pH-induced flocculation/deflocculation process for harvesting algae was evaluated using pilot-scale units capable of treating water with feed flow rates ranging from 1 gph to 5 gpm. Performance of the pilot scale process was evaluated in terms of algae removal efficiency and concentration factors achieved in processing the raw water into the algae concentrate. Based on the target operating conditions (e.g., operating pH, chemical dosage) determined in the lab-scale jar tests, chemicals (e.g., lime, NaOH, supplementary salt ( $\text{MgCl}_2$ )) were blended in a liquid form at a constant flow rate with the source water feed. A schematic of the pilot-scale system and pilot-scale units utilized in this research are provided in Figure 6-1 and 6-2, respectively. Samples for analysis were collected from various points in the pilot scale system (e.g., incoming water, effluent, flocculated solids, acidified algae concentrate) to evaluate the performance of the pilot-scale process.

### “pH-Induced Flocculation/Deflocculation Process”

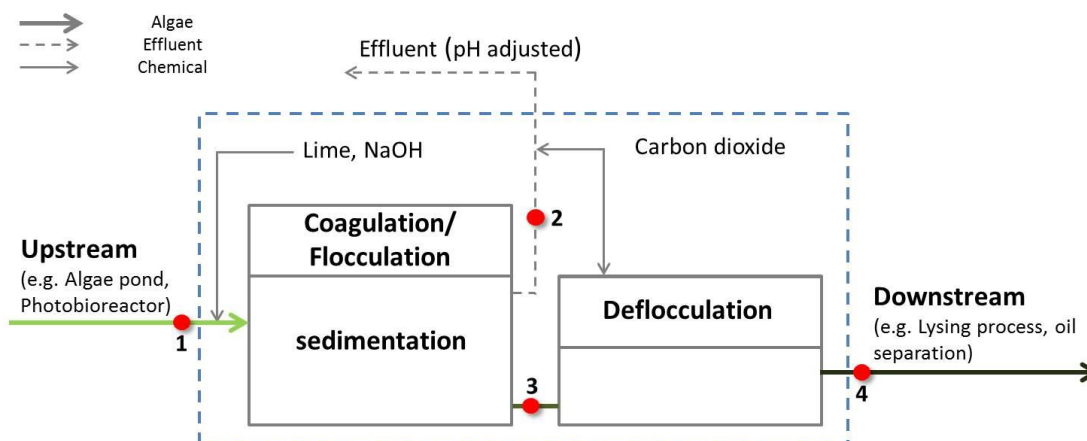


Figure 6-1 Schematic of the pilot-scale system for the algae harvesting process utilized in this research. Samples were collected from the incoming water (1), effluent (2), flocculated solids (3), and acidified algae concentrate (4) for analysis.

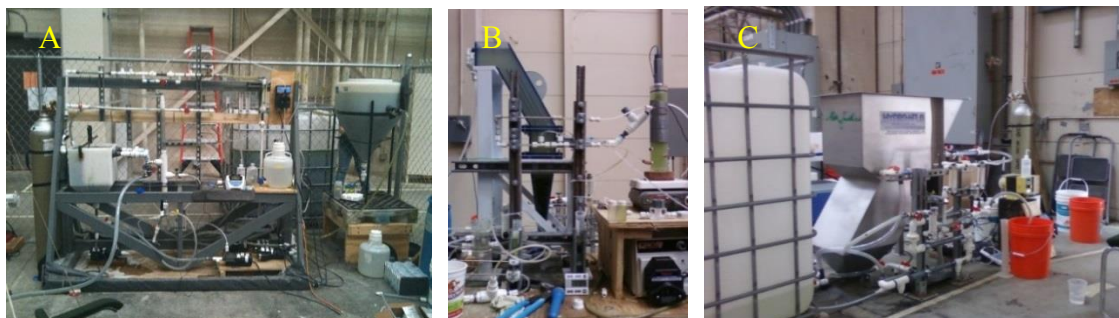


Figure 6-2 Pilot-scale units for harvesting algae from source water. Plate settlers (60° inclined) were used for effective solid/liquid separation. The range of operating feed flow rates were 0.2 – 1.0 gpm (A), 1.0 – 10 gph (B), and 1.0 – 5.0 gpm (C).

#### 6.2.4. Analytical methods

Samples were collected at various stages in the jar tests for further analyses. Prior to initiating an experiment, algae cells were filtered through a 0.2 µm nitrocellulose membrane filter (Millipore, U.S.A) to measure the total suspended solid (TSS) concentration and to determine the algae cell density (g/L). The alkalinity was determined in accordance with Standard Method 2320B except a 0.1 M nitric acid (HNO<sub>3</sub>) titrant was used instead of sulfuric acid (H<sub>2</sub>SO<sub>4</sub>). 5 mL samples of the original algae sample solution and the supernatant of treated water were filtered through a 0.2 µm nitrocellulose membrane syringe filter (Millipore, U.S.A) metal ion concentrations of the filtrates were then measured using inductively coupled plasma-optical emission spectrometer (ICP-OES, Varian 710-ES, U.S.A). Based on the metal ion concentrations measured, the percent of metal ion removal (%) was evaluated using Equation 6-1 below.

$$\text{Percent metal ion removal (\%)} = \left(1 - \frac{\text{Conc. } S}{\text{Conc. } O}\right) \times 100 \quad (6-1)$$

where *Conc. S* is the concentration of dissolved calcium ions in the filtered sample after the 20 min of quiescent settling and *Conc. O* is the concentration of dissolved calcium ions in the filtered original sample prior to pH adjustment.

The algae removal efficiency (%) was evaluated by comparing the optical density at 664 nm present in the original water to that present in the supernatant of the treated water as

shown in Equation 6-2 below. The optical density was measured using an Agilent 8453E UV-visible Spectroscopy system with a 1-cm cuvette.

$$\text{Algae removal efficiency (\%)} = \left(1 - \frac{OD_S}{OD_O}\right) \times 100 \quad (6-2)$$

where  $OD_S$  is the optical density (664 nm) of the supernatant after settling 20 min and  $OD_O$  is the optical density of the original algae sample solution prior to pH adjustment.

The concentration factor was calculated using Equation 6-3 below:

$$\text{Concentration factor} = \left(\frac{OD_a}{OD_O}\right) \quad (6-3)$$

where  $OD_a$  is the optical density (664 nm) of the acidified algae concentrate after the deflocculation process and  $OD_O$  is the optical density of the original algae sample solution prior to pH adjustment.

In some cases, samples from the flocculated and deflocculated solids were collected for X-ray powder diffraction (XRD) analysis to verify the chemical composition and crystal structure of the solid samples. Prior to XRD, samples were freeze-dried under low pressure and temperature (e.g., 60m Torr and -60°C) and ground with a mortar and pestle. XRD spectra were collected for varying  $2\theta$  ranges using a  $0.02^\circ$  step and a 1 second dwell time.

## 6.3. RESULTS AND DISCUSSION

### 6.3.1. Examination of jar test results and strategies for process optimization

Jar tests were conducted to determine the target operating conditions for the evaluation of the pilot-scale pH-induced flocculation/ deflocculation process for each of the source waters. The composition of each source water was characterized with respect to calcium and magnesium concentrations as well as alkalinity as shown in Table 6-2 below.

Table 6-2 Characteristics of algae source waters from various sites

	Type of water	pH	Alkalinity (meq/L)	Ca <sup>2+</sup> (mg/L)	Mg <sup>2+</sup> (mg/L)	Algae dry cell density (g/L)
A (AlgaEternal)	Fresh	7.9	0.96	2.11	3.72	n/a
B (BlueSundial)	Fresh	7.4	2.2	40.4	30.0	0.12
C (Conoco)	Fresh	7.5	4.0	18.8	3.05	n/a
D (Hornsby)	Fresh	7.7	8.04	98.3	43.7	n/a
E (South Texas)	Brackish	7.7	3.7	283	318	0.1 – 0.3 mg/L as Chl-a <sup>(a)</sup>
F (Synthetic)	Brackish	8.4	2.4	154	327	0.26
G (CEM)	Salt	8.7	2.6	478	831	0.1 – 0.3

<sup>(a)</sup> Chlorophyll-a measurements were conducted in accordance with Standard Method 10200H

Baseline jar tests were conducted for each source water to determine the operating pH necessary to achieve algae removals in excess of 85%. The typical jar test procedure described in the Materials and Methods Section was utilized; the pH was adjusted in the

solutions via the addition of lime or NaOH. For selected source waters (A, D), additional jar tests were conducted to investigate potential methods for improving algae removal based on the results of the baseline jar tests. Baseline jar test results for each algae source water are summarized in Figure 6-3. The algae removal efficiency is plotted as a function of pH.

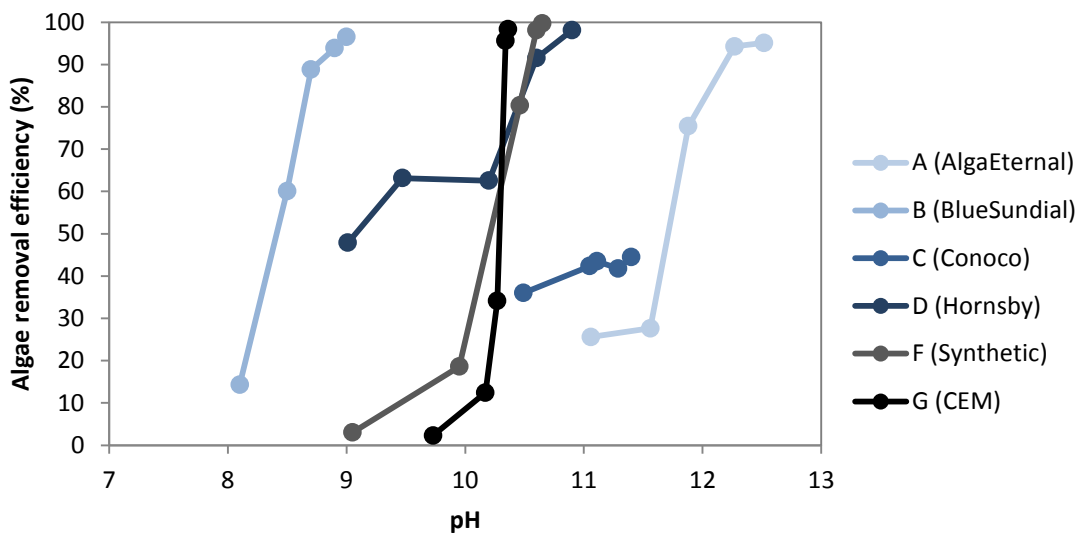


Figure 6-3 Jar test results for a range of algae source waters. The pH was adjusted by the addition of lime or NaOH.

Source water A (AlgaEternal) was collected from a pilot scale photobioreactor. The algae growth medium was prepared by using a tap water source ( $\text{Ca}^{2+}$ : 15 mg/L and  $\text{Mg}^{2+}$ : 19 mg/L) that had been pre-treated via ion exchange to remove Ca and Mg. The resulting algae solution exhibited relatively low calcium and magnesium levels as shown in Table 6-2. The jar test results for source water A in Figure 6-3 demonstrated that

algae removal increases with increasing pH adjusted via NaOH addition. However, high removal efficiency (> 90 %) was only achieved at high pH conditions (> pH 12) which could have a negative impact on the process since the effluent neutralization was required prior to discharge and cell damage is known to occur at high pH levels (Lee et al. 2009). One approach to resolve these issues would be to supplement the solution with magnesium ions through salt addition consistent with the results presented in Chapter 4 (see Figure 4-10 showing excellent removal at lower pH with Mg addition). Moreover, previous research has suggested that precipitation of magnesium hydroxide is the principle factor needed for algae removal (Folkman and Wachs, 1973; Friedman, 1977; Ayoub and Koopman, 1986; Elmaleh et al., 1996, Knucky et al., 2006, Vandamme et al., 2012; Wu et al., 2012). Thus, the initial  $Mg^{2+}$  concentration of source water A was raised from 3.72 to 200 mg/L as  $Mg^{2+}$  in an additional jar test.

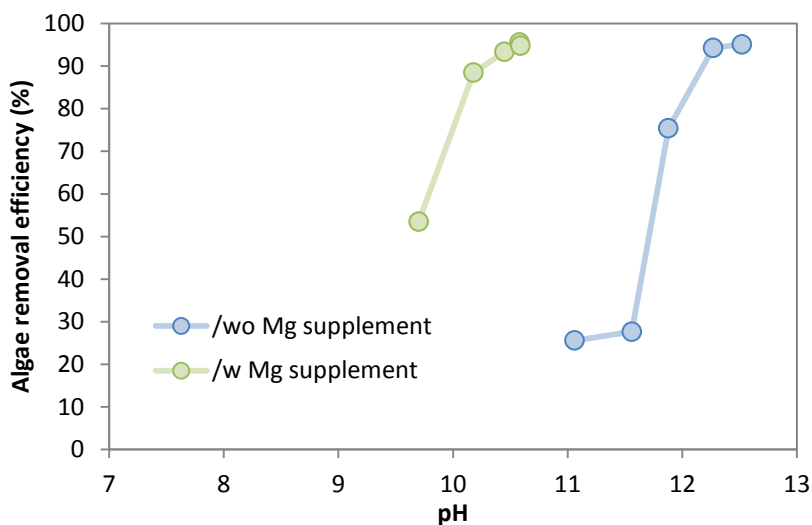


Figure 6-4 Effect of Mg salt on the optimum pH for algae recovery for source water A (AlgaEternal). The Mg ion concentration was increased to 200 mg/L as  $Mg^{2+}$  with supplementary salt addition prior to the Mg supplement jar test.

The results (Figure 6-4) demonstrate that an algae removal efficiency of 88 % was achievable at a lower pH value of 10.2 when the initial  $Mg^{2+}$  concentration was raised to 200 mg/L. The pH required to achieve this level of removal (10.2) is consistent with the onset of precipitation observed in our previous experiments with synthetic water described in Chapter 4 (see Figure 4-4). For example, an algae removal efficiency of 84 – 92 % was achieved at pH 10.2 for algae cell densities of 0.26 and 0.64 g/L in the previous experiments presented in Chapter 4. This result supports the experimental findings described in Figure 6-4 that high algae removal can be achieved at lower pH for higher  $Mg^{2+}$  concentrations. Removal of algae via precipitation-enhanced coagulation is expected for a  $Mg^{2+}$  dose of 200 mg/L and pH of 10.2 based on the results presented in Chapter 4.

The advantages of using a lower pH for algae removal are several fold. The lower level of pH adjustment is desirable because less base is required and there are downstream costs associated with deflocculation (e.g., sludge handling) and discharge regulations (e.g., acid requirement). For example, data from Chapter 4 show that Mg consumption (and hence production of inorganic solids (i.e., precipitates other than algae biomass) increased with increasing pH of the solution as shown in Figure 6-5. In addition to increased solids production, the higher effluent pH required for significant algae removal without Mg addition is too high for either effluent recycling to the algae growth ponds or discharge to sanitary sewers.

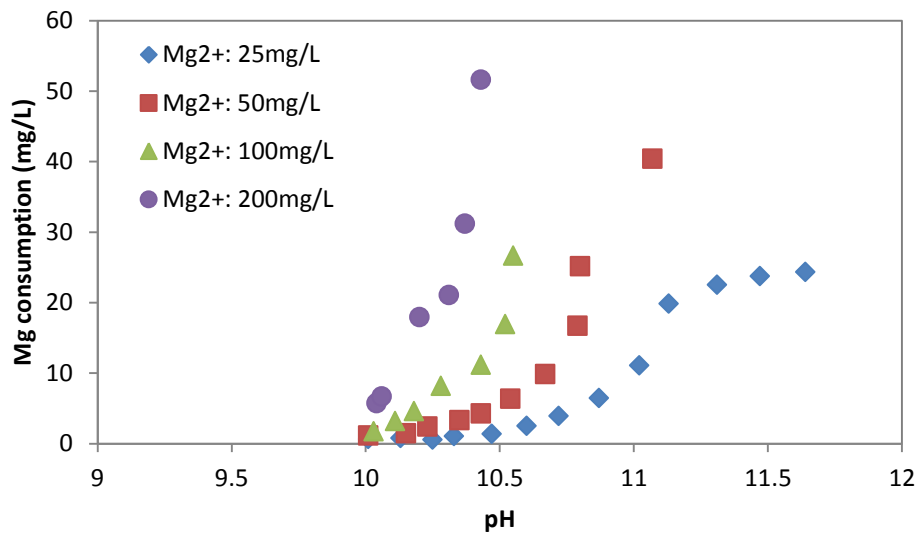


Figure 6-5 Effect of pH on solid production in a synthetic water for an algae cell density of 0.26 g/L (from experiments presented in Chapter 4). Mg consumption was directly related to mass precipitated above pH 10.

Although Mg addition enhanced algae removal for source water A, an alternative approach to consider would have been lime addition since this source water had a low initial alkalinity level. Although it was not experimentally tested in the source water tests, the results from Chapter 5 (see Figure 5-6) suggest that lime addition could be optimized to induce heterogeneous nucleation of  $\text{CaCO}_{3(s)}$  which is more favorable when the ion activity ratio ( $\{\text{Ca}^{2+}\}/\{\text{CO}_3^{2-}\}$ ) is high. Indeed, the jar tests results for source water B (Figure 6-3) appear to support this hypothesis.

Source water B (BlueSundial) was collected from a pilot-scale pond that contained nutrient-rich wastewater. The jar test results for source water B indicate that algae removal efficiency increases with increasing pH (adjusted via lime addition) and a high removal efficiency of > 90 % was achieved at approximately pH 9. This is below the pH value at which precipitation of  $\text{Mg}(\text{OH})_{2(s)}$  would be expected based on a  $\text{Mg}^{2+}$  concentration of 30 mg/L. The addition of lime for pH adjustment may have provided a favorable condition (e.g., a high activity ratio of  $\text{Ca}^{2+}$  to  $\text{CO}_3^{2-}$ ) for heterogeneous nucleation of  $\text{CaCO}_{3(s)}$ . The lime addition necessary to adjust the pH by one unit (i.e., pH from 8 to 9) should increase the ion activity ratio ( $\{\text{Ca}^{2+}\}/\{\text{CO}_3^{2-}\}$ ) by approximately two fold (i.e., 9.6 to 20). As discussed previously in Chapter 5 (see Figure 5-6), a higher likelihood of initial nucleation of  $\text{CaCO}_{3(s)}$  on the surface of algae can be induced at a high ion activity ratio (i.e., high  $\text{Ca}^{2+}$  concentrations and low alkalinity). In addition to the high ionic activity ratio induced by the lime addition, the relatively low initial  $\text{Mg}^{2+}$  concentration prevents significant Mg inhibition that retards heterogeneous nucleation of  $\text{CaCO}_{3(s)}$  as shown previously in Chapter 5 (See Figure 5-9). This leads to effective

coagulation via heterogeneous nucleation of  $\text{CaCO}_{3(s)}$  at a lower pH region. Another factor to consider when evaluating the Source Water B results is that a high removal efficiency was achieved at a low algae cell density of 0.12 g/L. High algae removal efficiency achieved at relatively low algae cell density is consistent with the previous experiments that showed that the highest algae removal via heterogeneous nucleation for  $\text{CaCO}_{3(s)}$  can be achieved at the lowest algae cell density (see Figure 5-13 A). These results suggest that the use of lime can be effective for algae removal while maintaining the operating pH at a lower level.

Source water C (Conoco) was delivered from Lake Charles located in Lake Charles, Louisiana. This water had a relatively high alkalinity and a low magnesium concentration. Low algae removal efficiency (< 50 %) was observed for pH values ranging from 10.4 to 11.4 (Figure 6-3). The high initial alkalinity (4.0 meq/L) and moderate Ca concentration (40.4 mg/L) yielded an ion activity ratio of only 0.69. As the pH increased with lime addition, the ion activity ratio (i.e.,  $\{\text{Ca}^{2+}\}/\{\text{CO}_3^{2-}\}$ ) decreased to 0.62 with increasing pH from 10.49 to 11.4. Under these conditions and a high supersaturation, homonucleation is favored (as observed in Chapter 5), and low algae removals are expected. Indeed, as seen in SEM images presented in Chapter 5 (see Figure 5-10), the large number of structural and negatively charged  $\text{CaCO}_{3(s)}$  crystals induced by homogeneous nucleation could prevent algae from aggregating within the given retention time. The low magnesium concentration present in the water was insufficient to induce precipitation of  $\text{Mg}(\text{OH})_{2(s)}$  which would have improved the algae removal efficiency.

The negative impact of a high initial alkalinity condition on algae removal was also observed in the jar test results for source water D as shown in Figure 6-6 below. Source water D (Hornsby) was collected from the stabilization pond located at Hornsby Bend in Austin, Texas. The water quality analysis indicated that source water D contained a high concentration of calcium (98.3 mg/L) and a high alkalinity (8 meq/L).

The jar test results presented in Figure 6-6 demonstrated that 90% calcium removal was achieved at pH 9.5, but only 63% algae removal was attained. In addition, a significant amount of precipitate was observed at this pH. Although Ca removal increased with increasing pH, algae removal did not increase, rather it diminished slightly from pH 9.5 to pH 10.2. Since source water D had a high initial alkalinity, this observation can be attributed to homogeneous nucleation of  $\text{CaCO}_{3(s)}$  induced by a high supersaturation and a low ion activity ratio. As demonstrated in Chapter 5 (Figures 5-6 and 5-7), the value of supersaturation (i.e.,  $\Omega = 2166$ ) for water D is favorable for homogeneous nucleation of  $\text{CaCO}_{3(s)}$  which leads to low to moderate algae removal. In fact, the plateau observed in Figure 6-5 was also observed in the synthetic water system with Ca concentrations of 120 and 320 mg/L and an alkalinity of 3.0 meq/L shown previously in Figure 5-8.

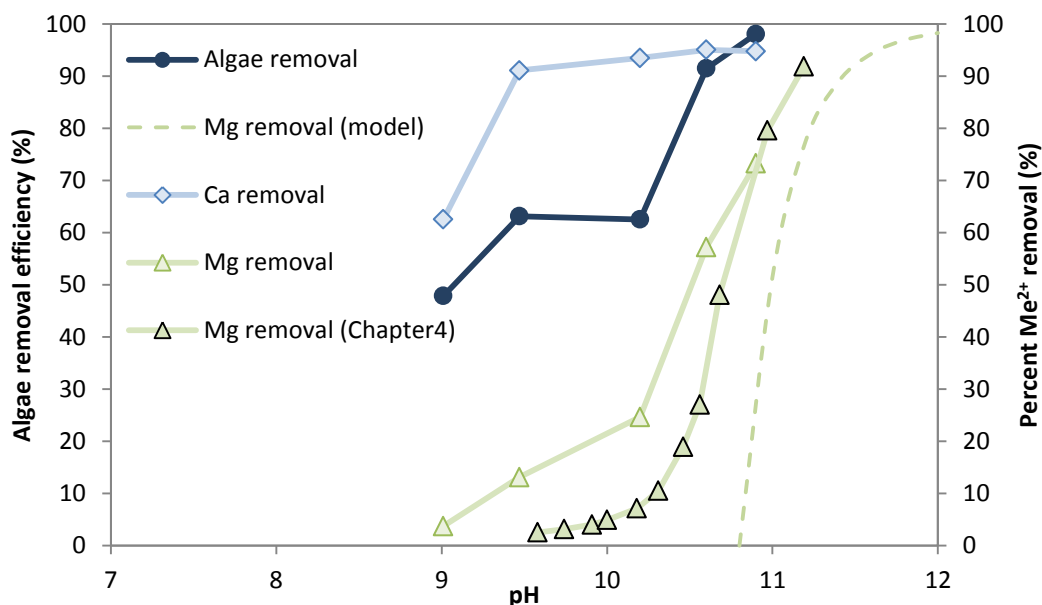


Figure 6-6 Effect of pH on algae removal efficiency and percent metal ion removal for source water D (Hornsby). The increase in initial  $\text{Ca}^{2+}$  concentration via the addition of lime was taken into account for the calculation of percent metal ion removal with the assumption of complete dissolution of lime. Mg removal tested in synthetic waters with similar water quality as water source D (initial  $\text{Mg}^{2+}$  concentration: 50 mg/L, algae cell density: 0.64 g/L in Figure 4-4) is shown for comparison. The dotted line represents the model prediction for percent  $\text{Mg}^{2+}$  removal due to precipitation as  $\text{Mg}(\text{OH})_{2(\text{s})}$  active in Minteq for an initial  $\text{Mg}^{2+}$  concentration of 43.7 mg/L.

The negative impact of homogeneous nucleation of  $\text{CaCO}_{3(\text{s})}$  on algae removal was evident not only in the system with only Ca (see Figures 5-8 and 5-12) but also in the system with both Ca and Mg (see Figure 5-9). However, in the Ca and Mg system examined in Chapter 5, algae removal decreased slightly after the algae removal peak but then started to increase again due to the onset of Mg removal in the presence of both Ca

and Mg. While no peak was present for source water D, due to a higher ionic strength (0.06 M), a similar increase in algae removal was observed above pH 10.8.

In contrast to the shift in Mg removal (toward higher pH in the presence of both Ca and Mg in Figure 5-10), Mg removal in source water D shifts toward lower pH when it is compared to that observed for similar conditions in Chapter 4 (i.e., initial  $\text{Mg}^{2+}$  concentration of 50 mg/L and algae cell density of 0.64 g/L). Thompson and Ferris (1990) suggested that algae cells diffuse hydroxyl ions through the cell membrane inducing local supersaturation due to the uptake of bicarbonate ions via photosynthesis. Thus, the initial high alkalinity condition (i.e., abundant bicarbonate ions) may promote Mg precipitation, which shifted Mg removal toward lower pH.

Although a high algae removal efficiency of 90 % was achievable with increasing Mg removal via precipitation of  $\text{Mg}(\text{OH})_{2(\text{s})}$ , the large amount of  $\text{CaCO}_{3(\text{s})}$  precipitated via homogeneous nucleation made deflocculation difficult. As shown previously in Chapter 5 (see Figure 5-14), the deflocculation process using  $\text{CO}_2$  cannot completely redissolve precipitated  $\text{CaCO}_{3(\text{s})}$  solids rapidly and thus excess  $\text{CaCO}_{3(\text{s})}$  precipitate would hinder algae recovery from the concentrate. These results indicate that the use of lime is of limited utility for source waters with high initial alkalinity due to the higher likelihood of homogeneous nucleation of  $\text{CaCO}_{3(\text{s})}$  as well as excessive  $\text{CaCO}_{3(\text{s})}$  production.

In order to minimize unnecessary solids production, additional jar tests were conducted with Source Water D using NaOH solution as a means to increase the pH of the solution. The algae removal efficiency was not evaluated as this test was conducted at

the pilot plant site during operation, but visually clear supernatant was achievable at a lower pH value of 10.51 when the base was switched from lime to NaOH, and the initial  $Mg^{2+}$  concentration was increased to 200 mg/L via magnesium salt addition. These results support the hypothesis that magnesium salt addition is useful for enhancing algae removal at lower operating pH values.

The results from Source Waters C and D indicate that high initial alkalinity conditions can negatively impact algae removal and process efficiency. Indeed, high alkalinity water (greater than 150 mg/L as  $CaCO_3$ , equivalent to 3 meq/L) has been shown to cause scaling in water/wastewater treatment processes and this would also be of concern in algae harvesting system as well. In addition, in the algae harvesting process, source waters with high initial alkalinity may require excessive base addition to achieve algae removal but this would negatively affect the subsequent algae deflocculation step. One potential option to address this problem in waters with high alkalinity is to employ a dealkalization pretreatment process. Generally, dealkalization can be achieved using a range of processes including nanofiltration,  $Cl^-$  anion exchange, or acid addition. In pilot testing conducted by OpenAlgae with a high alkalinity source water, the addition of HCl acid prior to the pH induced-deflocculation process yielded excellent results for a three month pilot-plant study (Hoyt, 2014).

Source Waters E (South Texas), F (Synthetic), and G (CEM) had both high calcium and high magnesium levels. Source Waters F and G were synthesized via the addition of sea salts (Instant Ocean<sup>®</sup>) whereas Source Water E was collected from aquaculture pond water containing brackish water. The jar test results for source waters

F and G shown in Figure 6-3 indicate that high algae removal efficiencies of > 90 % were achieved at pH values of 10.3 and 10.6, respectively without further modifications other than pH adjustment via the addition of lime. For source water E, large floc formation was initiated at pH 10.5 and visually clear supernatant was obtained after 20 min of sedimentation. These results are within our expectation that high algae removal can be achieved due to the presence of an abundant level of magnesium, much greater than Ca in the source water. In order to correlate algae removal with metal ion removal in these types of source waters, the removals of algae and metal ions for source water G were monitored as a function pH as shown in Figure 6-7.

These jar test results for source water G showed that the percent  $\text{Ca}^{2+}$  removal increased with increasing pH and then fluctuated with further increase in pH. The increase in the amount of Ca in the system (due to lime addition) leads to a reduction in percent Ca removal (not actual Ca removal). However, the dip in percent Ca removal suggests that there is insufficient carbonate to remove this additional Ca. Minteq calculations suggest that 99 percent of the carbonate, but only 21 percent of the Ca, is expected to be removed at pH 9.7. In addition, the fluctuation in Mg removal tracks the Ca removal. Figure 6-7 also shows that Ca and Mg removal are linked perhaps due to a mixed  $\text{CaMgCO}_3$  precipitate. Indeed, Minteq calculations suggest that the system is oversaturated with respect to dolomite ( $\text{CaMg}(\text{CO}_3)_2(\text{s})$ ) which may occur more rapidly than calcite precipitation.

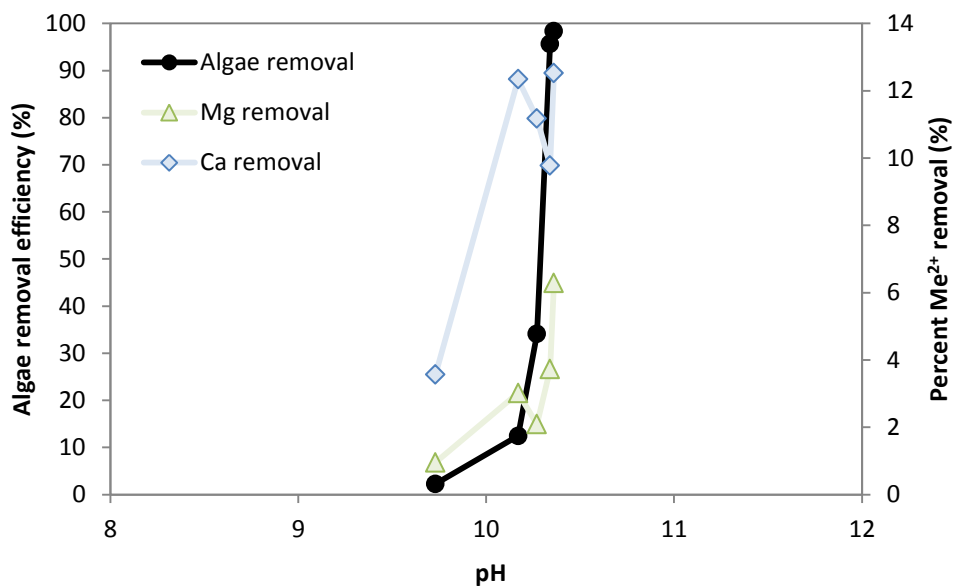


Figure 6-7 Effect of pH on algae removal efficiency and percent metal ion removal for source water G (CEM). The increase in initial  $\text{Ca}^{2+}$  concentration via the addition of lime was taken into account for the calculation of percent metal ion removal with the assumption of complete dissolution of lime.

One other significant difference between water G and other waters is the high ionic strength in source water G. While the use of synthetic salt water led to a high ionic strength (0.7 M), it also yielded high ion activity ratio ranging from 23 to 10.5 ( $\{\text{Ca}^{2+}\}/\{\text{CO}_3^{2-}\}$ ) which decreased with increasing pH due to the increase in carbonate ion concentration. Thus, although the ion activity ratio and borderline degree of supersaturation (see Table 6-3), is favorable for heterogeneous nucleation of  $\text{CaCO}_{3(s)}$ , algae removal under the initial water pH of pH 9.7 led to lower algae removal compared to the synthetic algae sample water tested in Chapter 5 (i.e., synthetic algae water with  $\text{Ca}^{2+}$  concentrations of 120 mg/L and 320 mg/L, initial alkalinity of 3.0 meq/L, and algae

cell density of 0.5 g/L). This result is not surprising as results in Chapter 5 demonstrated a significant reduction in removal at higher ionic strengths. Two factors likely contribute to this reduction. First, adsorption of Ca, a prerequisite for heterogenous nucleation, is reduced at higher ionic strength. Second, in seawater, aqueous complexation of Mg and Ca with sulfate will also reduce adsorption of each of these species.

High algae removal efficiency was achievable at pH values from 10.17 to 10.36 with the onset of observable  $Mg^{2+}$  removal. Under the conditions of this experiments, the system begins to be oversaturated with respect  $Mg(OH)_{2(s)}$ . At this pH, removal via enhanced precipitation of  $Mg(OH)_{2(s)}$  is consistent with previous results.

Table 6-3 Water parameters at pH 9.7 for two different synthetic waters tested in Chapter 5 and source water G.

	Synthetic water (Figure 5-8 A)	Synthetic water (Figure 5-8 B)	Source water (G) (Figure 6-7)
pH	9.71	9.7	9.73
Ion activity ratio ( $\{Ca^{2+}\}/\{CO_3^{2-}\}$ )	4.8	13.6	23
Supersaturation ( $\Omega$ )	228	424	172
Ca consumed (mg/L)	16.4	61.5	19.5
Algae removal (%)	80.9	57.1	2.2
Ionic strength (M)	0.01	0.02	$\cong 0.7^{(a)}$

<sup>(a)</sup> Ionic strength of typical sea water ( $I = 0.7$ ) is considered for source water G.

### **6.3.2. Examination of pilot-scale results and strategies for process optimization**

A series of pilot-scale tests for the pH-induced flocculation/deflocculation process were conducted with the continuous flow reactors shown in Figure 6-2 (panel A, B, and C) for source waters D - G to evaluate how the process performs as it is scaled up. The successful transition from laboratory to pilot-scale algae harvesting processes requires an integrated testing effort to evaluate the performance of the algae removal process and to resolve issues associated with scaling (e.g., retention time for the flocculation basin, mixing properties, discrepancy in pH measurement, maintaining steady feed flow rates and lime feeding system, CO<sub>2</sub> injection system, system automation, etc.). As shown in Table 6-4, excellent algae removals were achieved in all of the pilot tests. Moreover, the algae removals were consistent with removal in the jar tests at similar pH values. In most cases, the systems were not operated long enough to accumulate sufficient solids to optimize concentration. Thus, concentration factors in the pilot studies never exceeded 25.

Table 6-4 Operating conditions and performance of pilot-scale tests for source waters D-G

	<b>Source water D</b>	<b>Source water E</b>	<b>Source water F</b>	<b>Source water G</b>
<b>Pilot unit</b>	B / not shown	not shown	B	A / C
<b>Feed flow rate</b>	1.0 gph / 5 – 10 gpm	10 gpm	4.5 – 5.5 gph	0.25 gpm / 1.0 – 1.5 gpm
<b>Operating pH</b>	11.0 / 10.75	10.5	10.5	10.4 / 10.37
<b>Base</b>	NaOH / Lime	NaOH	Lime	NaOH / NaOH
<b>Algae removal efficiency</b>	92.7 – 95.7 / > 85 %	92.8 %	98.6 %	96.4 % / > 96 %
<b>Concentration factor</b>	14.1 / n/a	20.9	n/a	19.3 / 24.0

The pilot scale test for source water G was designed specifically to examine the deflocculation and composition of the solids formed during continuous flow operation. Source water G was collected from the pilot-scale pond located at the Center for Electromechanics (CEM) at the University of Texas at Austin. The operating pH of the pilot test of 10.37 was based on the baseline jar test results showing excellent removal at this pH. The samples of incoming water and effluent samples were collected after 40 minutes of operation which is the minimum time required to fill up the reactor with treated water. Algae removal efficiencies of > 96 % collected from approximately 3 to 8 residence times during the pilot-scale test are shown in Figure 6-8.

It was demonstrated that high algae removal efficiency was achieved throughout the test in which precipitation (of  $Mg(OH)_{2(s)}$ ) enhanced coagulation was expected to be the dominant mechanism. It is also possible that precipitation of  $CaCO_{3(s)}$  acted as weighting agent that aided in the compression of sludge and helped to prevent sludge overflow which would reduce algae removal efficiency. Ultimately, an algae biomass concentration factor of 24 x (Equation 6-3) was calculated based on comparison of the influent algae concentration with the concentration of algae in the material collected in the bottom of the sedimentation compartment of the system. Longer run times could yield greater compression of the biomass layer.

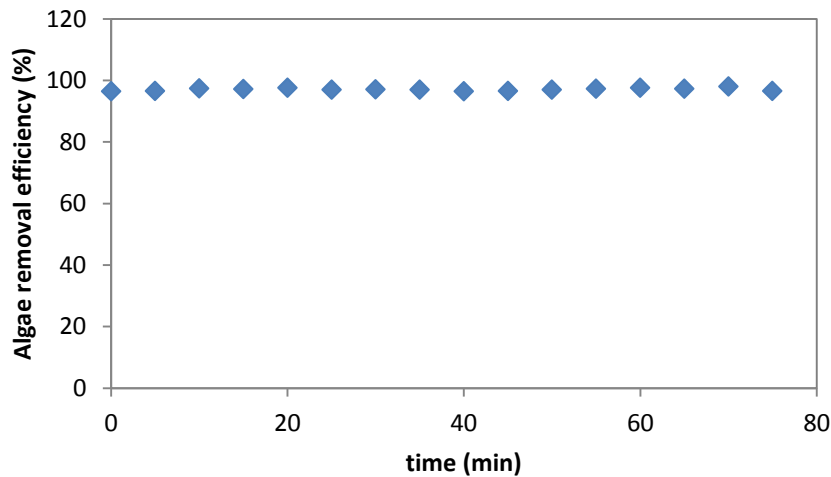


Figure 6-8 Algae removal efficiency during the pilot-scale test. Time zero represents the time at which the first samples of influent and effluent were collected right after the reactor was filled up with treated water.

In order to compare the chemical composition of the flocculated solids before and after the deflocculation process (i.e., algae-laden flocculated solids vs inorganic solid residue), samples were collected before and after the deflocculation stage: the samples of the flocculated solids at the bottom of the cone-bottomed tank were collected before being transferred to the deflocculation stage where pure CO<sub>2</sub> gas was bubbled through the flocculated solids until the target pH (6.0 – 6.5) was reached. The samples of inorganic solid residue were collected from the deflocculated solids that had undergone solid/liquid separation (i.e., algae concentrate/inorganic solid residue). X-ray diffraction analysis results for samples of the flocculated solids and the solids residue after the deflocculation process are as shown in Figure 6-9. Crystals of sodium chloride were observed due to the freeze drying process for sample preparation. However, it is evident that magnesium hydroxide and calcium carbonate were the dominant precipitates in the flocculated solids. The magnesium hydroxide was completely re-dissolved after deflocculation, whereas some calcium carbonate still remained undissolved. This is in good agreement with the previous deflocculation test results (see deflocculation test in Chapter 4 and 5) that showed that pH adjustment using CO<sub>2</sub> effectively dissolved the Mg(OH)<sub>2(S)</sub> precipitates formed during flocculation but precipitated CaCO<sub>3(S)</sub> solids did not completely redissolve. The performance of the pilot-scale algae harvesting process using pH-induced flocculation/ deflocculation method confirms that the baseline jar test results were well reflected in the continuous flow system.

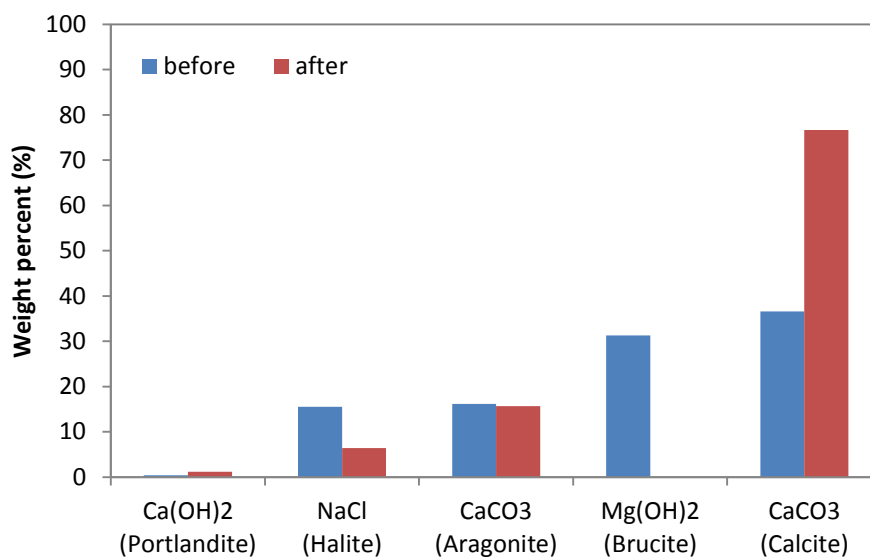


Figure 6-9 X-ray diffraction analysis to determine the chemical composition of precipitated solids before (algae-laden flocculated solids) and after deflocculation (inorganic solid residue) for source water G. CO<sub>2</sub> was bubbled through the flocculated solids until the target pH (6.0 – 6.5) was reached.

#### 6.4. CONCLUSIONS

In this chapter, baseline jar test and pilot-scale test data collected at the initial stage of this entire research study were reexamined based on the underlying science elucidated in Chapters 4 and 5 to establish strategies for optimizing the algae harvesting process for a range of algae source water. Retrospective examination revealed that baseline test results are consistent with the findings in the previous chapters. The examination suggests that the algae harvesting process can be optimized depending on the algae source water characteristics with respect to calcium, magnesium, and alkalinity.

For the source waters with low calcium and magnesium levels, the use of lime and the addition of magnesium salts are effective options to induce effective algae removal via heterogeneous nucleation of  $\text{CaCO}_{3(s)}$  and adsorption of  $\text{Mg}^{2+}$  and/or precipitation ( $\text{Mg}(\text{OH})_{2(s)}$ ) enhanced coagulation while maintaining a low pH level and minimal inorganic solid production. For source waters with high initial alkalinity, the use of lime would be of limited utility due to excessive  $\text{CaCO}_{3(s)}$  production via the higher likelihood of homogeneous nucleation of  $\text{CaCO}_{3(s)}$ . One potential option would be to employ a dealkalization pretreatment process (e.g., nanofiltration,  $\text{Cl}^-$  anion exchanged, or strong acid addition). For source waters with high ionic strength and high concentrations of calcium and magnesium, the onset of precipitation of  $\text{Mg}(\text{OH})_{2(s)}$  is responsible for the effective algae removal even though the system conditions are favorable for precipitation of  $\text{CaCO}_{3(s)}$  via homogeneous nucleation. Controlled jar tests allow optimization of the process conditions which appear to scale appropriately to continuous flow systems. However, further research is required to optimize the concentration and deflocculation stages of the pH induced flocculation/deflocculation process.

## Chapter 7: Conclusions

The primary goal of this research was to investigate the algae removal mechanisms associated with alkaline earth metals, calcium and magnesium, in a pH-induced flocculation and deflocculation harvesting process. Microalgae, *Scenedesmus* sp., was used as a model species in the synthetic water studies; however, a second species, *Chlorella* sp., was selected to validate the extensibility of findings for a different algae system. The role of magnesium and calcium in this process was studied independently (Phase I and II of the research plan). A series of controlled bench-scale experiments were designed to isolate the potential mechanisms of algae destabilization associated with each of these cations and microscopic analyses were performed to characterize the flocculated algae/precipitate mixtures and deflocculated algae. Batch and pilot scale testing with field waters of varying composition (algae speciation and water chemistry) were conducted to determine whether the underlying science elucidated in the previous chapters was consistent with algae removal in natural waters (Phase III).

In chapter 4, the specific algae removal mechanisms associated with the dissolved  $Mg^{2+}$  ion and  $Mg(OH)_{2(s)}$  in the algae harvesting process were evaluated. bench-scale experiments were designed to isolate the possible algae destabilization mechanisms of heterocoagulation, adsorption/charge neutralization and precipitation-enhanced coagulation. The main findings of this phase of research examining algae removal with Mg were:

- Heterocoagulation of algae with  $\text{Mg}(\text{OH})_{2(\text{s})}$  particles is effective, but equivalent algae removal was achieved at lower magnesium concentrations via adsorption and/or *in situ* precipitation-enhanced coagulation.
- The dominant algae removal mechanism shifts from adsorption/charge neutralization to precipitation-enhanced coagulation with increasing pH.
- A "transition zone" between the two mechanisms was apparent at approximately pH 10.
- Adsorption/charge neutralization can achieve high algae removal efficiency (e.g., 85 %) while minimizing precipitated inorganic solids.
- The overall process that includes deflocculation yielded a homogeneous and deflocculated algae concentrate suitable for downstream processing.

In chapter 5, a series of batch reactor tests were conducted to investigate the role of calcium in the algae harvesting process. Tests were conducted in the presence and absence of carbonate, and the presence and absence of Mg provided additional mechanistic understanding of the systems. The main findings of this phase of the research were:

- The modes of nucleation (heterogeneous and homogeneous nucleation) for  $\text{CaCO}_{3(\text{s})}$  control algae removal efficiency.
- Effective algae coagulation (e.g., up to 82 % algae removal efficiency) can be achieved via heterogeneous nucleation of  $\text{CaCO}_{3(\text{s})}$  at moderate supersaturation and low ionic strength.

- Algae removal can be attributed to adsorption of  $\text{Ca}^{2+}$  onto the algae cell surface which provides nucleation sites for  $\text{CaCO}_{3(s)}$  precipitation. Bridging of calcite particles between the cells leads to more rapid aggregation and formation of larger flocs in the presence of algae.
- The heterogeneous nucleation process is favored in solutions containing higher ratios of  $\text{Ca}^{2+}/\text{CO}_3^{-2}$ .
- Algae removal is diminished at high supersaturation due to the occurrence of homogeneous nucleation even for higher algae cell densities for which better collision efficiency would be expected.
- Algae-laden flocculated solids can be acidified by  $\text{CO}_2$  injection for deflocculation, but the effectiveness of the deflocculation process is a function of initial water composition.
- Water chemistry, pH, ionic strength, alkalinity and  $\text{Ca}^{2+}$  concentration can be optimized for algae harvesting operations.
- The presence of Mg was shown to inhibit  $\text{CaCO}_{3(s)}$  precipitation, but at higher pH algae removal was achieved via  $\text{Mg}(\text{OH})_{2(s)}$  precipitation-enhanced coagulation.

In chapter 6, a series of source waters were characterized based on the composition of water: calcium, magnesium, and alkalinity and jar tests were performed to determine the extent of algae removal as a function of pH. Algae removal was evaluated in pilot scale tests for several of these waters. The major conclusions of this research are:

- Results from jar tests with natural source waters were consistent with the results and mechanisms postulated for the different water chemistries studied.
- For source waters with low calcium and magnesium concentrations, the use of lime and the addition of magnesium salts can induce effective algae removal via heterogeneous nucleation of  $\text{CaCO}_{3(s)}$  and adsorption and/or precipitation-enhanced coagulation with Mg.
- For source waters with high initial alkalinity, the use of lime is of limited utility due to excessive production of  $\text{CaCO}_{3(s)}$  via homogeneous nucleation. One potential option would be to employ a dealkalization pretreatment process (e.g., nanofiltration, Cl<sup>-</sup> anion exchange, or acid addition with CO<sub>2</sub> stripping).
- For source waters with high calcium and magnesium concentrations and high ionic strength, the onset of precipitation of  $\text{Mg}(\text{OH})_{2(s)}$  is responsible for algae removal; the high ionic strength of the water reduces removal of algae due to homogeneous nucleation of  $\text{CaCO}_{3(s)}$ .
- Algae removals in the pilot-scale algae harvesting tests were similar to the removals observed in the baseline jar tests, but algae concentration factors were limited under the relatively short testing periods employed.

While the findings of this research suggested that the algae harvesting process using the pH-induced flocculation and deflocculation method can be optimized for the overall end to end process from algae growth to product recovery, additional research with more complex water chemistry needs to be incorporated into the system design for

actual field applications. Indeed, the algae harvesting process can be dependent on a number of additional parameters not specifically investigated in this research (e.g., the types and concentrations of ions, the presence of other bacteria, and natural organic matter). Therefore, additional research is required to assess how the process will perform for a wider range of water sources. In addition, more information is needed in the areas of:

- Reaction kinetics for the different precipitation mechanisms and floc formation.
- Kinetics of dissolution of calcite using CO<sub>2</sub> acidification and/or air stripping.
- Extended testing of the pilot scale system to evaluate and optimize algae concentration

## References

- Adelman, M. J.; Hurst, M. W.; Weber-Shirk, M. L.; Cabrito, T. S.; Somogyi, C.; Lion, L. W. Floc roll-up and its implications for the spacing of inclined settling devices. *Environ. Eng. Sci.* **2013**, 30, 6, 302-310
- Alamdari, A.; Rahimpour, M. R.; Esfandiari, N.; Nourafkan, E. Kinetics of Magnesium Hydroxide Precipitation from Sea Bittern. *Chem. Eng. Process. Process Intensif.* **2008**, 47, 215-221
- Alexandratos, V. G.; Elzinga, E. J.; Reeder, R. J. Arsenate uptake by calcite: Macroscopic and spectroscopic characterization of adsorption and incorporation mechanisms. *Geochim. Cosmochim. Acta.* **2007**, 71, 4172-4187
- Arp, G.; Reimer, A.; Reitner, J. Calcification in cyanobacterial biofilms of alkaline salt lakes. *Eur J Phycol.* **1999**, 34, 4, 393-403
- Ayoub, G. M.; Koopman B. Algal separation by the lime–seawater process. *J. Water Pollut. Control Fed.* **1986**, 58, 924–931
- Banerjee, A.; Sharma, R.; Chisti, Y.; Banerjee, U. C. *Botryococcus braunii*: a renewable source of hydrocarbons and other chemicals. *Crit Rev Biotechnol.* **2002**, 22, 3, 245–79
- Becker, E. W. Nutritional properties of microalgae: potentials and constraints. in: A. Richmond (Ed.), *Handbook of Microalgal Mass Culture*, CRC Press, Boca Raton, FL, **1986**, p. 339–420
- Berner, R. A. The role of magnesium in the crystal growth of calcite and aragonite from seawater. *Geochim. Cosmochim. Acta.* **1975**, 39, 4, 489-504
- Bernhardt, H.; Hoyer, O.; Schell, H.; Lusse, B. Reaction mechanisms involved in the influence of algal matter on flocculation. *Z. Wasser Abwasser Forsch.* **1985**, 18, 1, 18-30
- Bernhardt, H.; Clasen, J. Flocculation of micro-organisms. *J. Water Supply Res. Technol.-AQUA.* **1991**, 40, 2, 76–87
- Bilanovic, D.; Shelef, G.; Sukenik, A. Flocculation of microalgae with cationic polymers-effects of medium salinity. *Biomass.* **1988**, 17, 1, 65–76
- Bischoff, J. L. Kinetics of calcite nucleation: magnesium ion inhibition and ionic strength catalysis. *J. Geophys Research.* **1968**, 73, 10, 3315-3322

- Black, A. P.; Christman, R. F. Electrophoretic studies of sludge particles produced in lime-soda softening. *J. Am. Water Works Assoc.* **1961**, 53, 737-747
- Bots, P.; Benning, L. G.; Rodriguez-Blanco, J. D.; Roncal-Herrero, T.; Shaw, S. Mechanistic insights into the Crystallization of Amorphous Calcium Carbonate (ACC). *Cryst. Growth Des.* **2012**, 12, 7, 3806-3814
- Brady, P. V.; Pohl, P. I.; Hewson, J. C. A coordination chemistry model of algal Autoflocculation. *Algal Research*. in press. DOI: 10.1016/j.algal.2014.02.004
- Busienberg, E.; Plummer, L. N. Thermodynamics of magnesian calcite solid-solutions at 25°C and 1 atm total pressure. *Geochem. Cosmochim. Acta.* **1989**, 53, 1189-1208
- Chen, C.; Zhang, X. J.; Zhu, L. X.; Liu, J.; He, W. J.; Han, H. D. Disinfection by products and their precursors in a water treatment plant in North China: seasonal changes and fraction analysis. *S Sci. Total Environ.* **2008**, 397, 1-3, 140-147.
- Chiaromonti, D.; Prussi, M.; Casini, D.; Tredici, M. R.; Rodolfi, L.; Bassi, N.; Zittelli, G. C.; Bondioli, P. Review of energy balance in raceway ponds for microalgae cultivation: re-thinking a traditional system is possible. *Applied Energy.* **2013**, 102, C, 101-111
- Chibowski, E.; Hotysz, L.; Szczes, A. Time dependent changes in zeta potential of freshly precipitated calcium carbonate. *Colloids and Surfaces A: Physicochem. Eng. Aspects.* **2003**, 222, 1-3, 41-54
- Chisti, Y. Biodiesel from microalgae. *Biotechnol Adv.* **2007**, 25, 294-306
- Christenson, L.; Sims, R. Production and harvesting of microalgae for wastewater treatment, biofuels, and Bioproducts. *Biotechnol Adv.* **2011**, 29, 6, 686-702
- Cicerone, D. S.; Regazzoni, A. E.; Blesa, M. A. Electrokinetic properties of the calcite/water interface in the presence of magnesium and organic matter. *J. Colloid Interface Sci.* **1992**, 154, 2, 423-433
- Clasen, J.; Mischke, U.; Drikas, M.; Chow, C. An improved method for detecting electrophoretic mobility of algae during the destabilization process of flocculation: flocculant demand of different species and the impact of DOC. *J. Wat. Supply. Res. Technol. AQUA*, **2000**, 49, 2, 89-101
- Crist, R. H.; Oberholser, K.; Schwartz, D.; Marzoff, J.; Ryder, D.; Crist, D. R. Interactions of metals and protons with algae. *Environ. Sci. Technol.* **1988**, 22, 7, 755-760

- Dabir, B.; Peters, R. W.; Stevens, J. D. Precipitation kinetics of magnesium hydroxide in a scaling system. *Ind. Eng. Chem. Fundamen.* **1982**, 21, 3, 298–305
- Dabrowski, W.; Buchta, R.; Dabrowska, B.; Mackie, R. I. Calcium carbonate equilibria in water supply systems. *Environ. Prot. Eng.* **2010**, 36, 2, 75-94
- Danquah, M. K.; Ang, L.; Uduman, N.; Moheimani, N.; Forde, G. M. Dewatering of microalgal culture for biodiesel production: exploring polymer flocculation and tangential flow filtration. *J. Chem Technol Biotechnol.* **2009**, 84, 1078–1083
- Davis, K. J.; Dove, P. M.; De Yoreo, J. J. The role of  $Mg^{2+}$  as an impurity in calcite growth. *Science*, **2000**, 290, 1134–1137
- Davis, K. J.; Dove, P. M.; Wasylenki, L. E.; De Yoreo, J. J. Morphological consequences of differential  $Mg^{2+}$  incorporation at structurally distinct steps on calcite. *Am. Mineral.* **2004**, 89, 5-6, 714-720
- Del Campo, J. A.; Garcia-Gonzalez, M.; Guerrero, M. G. Outdoor cultivation of microalgae for carotenoid production: current state and perspectives. *Appl Microbiol Biotechnol.* **2007**, 74, 1163-1174.
- Dittrich, M.; Sibling, S. Influence of  $H^+$  and calcium ions on surface functional groups of *Synechococcus* PCC 7942 cells. *Langmuir*, **2006**, 22, 12, 5435-5442
- Divakaran, R.; Pillai, V. N. S. Flocculation of algae using chitosan. *J. Appl. Phycol.* **2002**, 14, 419–422
- D'Souza, F. M. L.; Knuckey, R. M.; Hohmann, S.; Pendrey, R. C. Flocculated microalgae concentrates as diets for larvae of the tiger prawn *Penaeus monodon* Fabricius. *Aquacult Nutr.* **2002**, 8, 113–120
- Duan, J.; Gregory, J. Coagulation by Hydrolysing Metal Salts. *Adv. Colloid Interface Sci.* **2003**, 100-102, 475–502
- Dziubek, A.M.; Kowal, A.L. Effect of magnesium hydroxide on chemical treatment of secondary effluent under alkaline conditions. Proceedings of Water Reuse Symposium III, American Waterworks Association Research Foundation, **1984**, San Diego.
- Edward, E. B. Water Treatment Plant Design; 4th ed.; American Society of Civil Engineers, American Water Works Association, **1990**.
- Edzwald, J. K. Coagulation in drinking water treatment: Particles, organics and coagulants. *Wat. Sci. Tech.* **1993**, 27, 10, 67-81

Edzwald, J. K.; Wingler, B. J. Chemical and physical aspects of dissolved air flotation for the removal of algae. *Aqua*. **1990**, 39, 24-35

Elmaleh, S.; Yahi, H.; Coma, J. Suspended solids abatement by pH increase: upgrading of an oxidation pond effluent. *Water Res*. **1996**, 30, 2357–2362

Faust, S.D.; Aly, O. M. Chemistry of Water Treatment”, Ann Arbor Press, Chelsea, MI, **1998**, p. 329

Folk, R. L. The Natural History of Crystalline Calcium Carbonate: Effect of Magnesium Contents and Salinity. *J. Sedimentary Petrology*. **1974**, 44, 1, 40-53

Folkman, Y.; Wachs, A.M. Removal of algae from stabilization pond effluent by lime treatment Water. *Water Res*. **1973**, 7, 3, 419-428

Folsom, B.R.; Popescue, N. A.; Wood, J. M. Comparative study of aluminum and copper transport and toxicity in an acid-tolerant freshwater green alga. *Environ. Sci. Technol*. **1986**, 20, 6, 616-620

Fourest, E.; Volesky, b. Alginate properties and heavy metal biosorption by marine algae. *Appl. Biochem. Biotech*. **1997**, 67, 33-44

Friedman, A. A.; Peaks, D. A.; Nichols, R. L. Algae Separation from Oxidation Pond Effluents. *J. Water Pollut. Control Fed*. **1977**, 49, 1, 111-119

Gao, S.; Yang, J.; Tian, J.; Ma, F.; Tu, G.; Du, M. Electro-coagulation flotation process for algae removal. *J. Hazard Mater*. **2010**, 177, 1–3, 336–343

Gebrehiwet, T.A.; Redden, G. D.; Fujita, Y.; Beig, M. S.; Smith, R.W. The Effect of the  $\text{CO}_3^{2-}$  to  $\text{Ca}^{2+}$  Ion activity ratio on calcite precipitation kinetics and  $\text{Sr}^{2+}$  partitioning. *Geochem Trans*. **2012**, 13, 1, 1 doi: 10.1186/1467-4866-13-1.

Giannimaras, E. K.; Koutsoukos, P. G. The crystallization of calcite in the presence of orthophosphate. *J. Colloid Interface Sci*. **1987**, 116, 2, 423-430

Gilbert, P.; Abrecht, M.; Frazer, B. H. The organic-mineral interface in biominerals. *Rev Mineral Geochem*. **2005**, 59, 1, 157-185

Golueke, C. G.; Oswald, W. J. Surface properties and ion exchange in algae removal. *J Water Pollut Control Fed*. **1970**, 42, 8, 304-314

Gratz, A. J.; Hillner, P. E.; Hansma, P. K. Step dynamics and spiral growth on calcite. *Geochem. Cosmochim. Acta.* **1993**, 57, 2, 491-495

Grima, M. E.; Belarbi, E. H.; Acién Fernández, F. G.; Robles Medina, A.; Chisti, Y. Recovery of microalgal biomass and metabolites: process options and economics. *Biotechnol Adv.* **2003**, 20, 491-515

Greenwell, H. C.; Laurens, L. M. L.; Shields, R. J.; Lovitt, R. W.; Flynn, K. J. Placing Microalgae on the Biofuels Priority List: A Review of the Technological Challenges. *J. R. Soc. Interface.* **2010**, 7, 46, 703-726

Gutjahr, A.; Dabringhaus, H.; Lacmann, R. Studies of the growth and dissolution kinetics of the CaCO<sub>3</sub> polymorphs calcite and aragonite I. Growth and dissolution rates in water. *J. Crystal growth.* **1996**, 158, 296-309

Harith, Z. T.; Yusoff, F. M.; Mohamed, M. S.; Din, M. S. M.; Ariff, A. B. Effect of different flocculants on the flocculation performance of microalgae, *Chaetoceros calcitrans*, cells. *J. Biotechnol.* **2009**, 8, 21, 5971-5978

Henderson, R. K.; Parsons, S. A.; Jefferson, B. Successful removal of algae through the control of zeta potential. *Separation Sci. Technol.* **2008**, 43, 1653-1666

Henderson, R.; Parsons, S.A.; Jefferson, B. 2010. The impact of differing cell and algogenic organic matter (AOM) characteristics on the coagulation and flotation of algae. *Water Res.* **2010**, 44, 12, 3617-3624.

Henrist, C.; Mathieu, J. P.; Vogels, C.; Rulmont, A.; Cloots, R. Morphological study of magnesium hydroxide nanoparticles precipitated in dilute aqueous solution. *J. Crystal Growth.* **2003**, 249, 321-330

Higgins, M. J.; Novak, J. T. Characterization of exocellular protein and its role in bioflocculation. *J. Environ. Eng.*, **1997**, 123, 5, 479-485

Ives, K.J. The significance of surface electric charge on algae in water purification. *J. Biochem. Microbiol. Tech. Engineer.* **1959**, 1, 1, 37-47

Jiang, J.; Graham, N. J. D.; Harward, C. Comparison of polyferric sulphate with other coagulants for the removal of algae-derived organic matter. *Water Sci. Technol.* **1993**, 27, 11, 221-230

John, D. M.; Whitton, B. A.; Brook, A. J. Freshwater Algal Flora of the British Isles: A Guide to Freshwater and Terrestrial Algae. Cambridge University Press, **2002**, Cambridge.

Jun, H. B.; Lee, Y. J.; Lee, B. D.; Knappe, D. R. U. Effectiveness of coagulants and coagulant aids for the removal of filter-clogging *Synedra*. *J. Wat. Supply. Res. Technol. AQUA*. **2001**, 50, 3, 135-148

Kashchiev, D.; Van Rosmalen, G. M. Review: Nucleation in Solutions Revisited”, *Crystal Research and Technology*, **2003**, 38, 7-8, 555-574

Katz, L. E. Surface complexation modeling of cobalt ion sorption at the alpha-aluminum oxide-water interface: Monomer, polymer, and precipitation reactions. Ph.D. Dissertation, University of Michigan, Ann Arbor, MI, **1993**.

Kawaguchi, T.; Decho, A. W. A laboratory investigation of cyanobacterial extracellular polymeric secretions (EPS) in influencing CaCO<sub>3</sub> polymorphism. *J. Crystal Growth*. **2002**, 240, 230-235

Khan, Z.; Bhadouria, P.; Bisen, P. S. Nutritional and therapeutic potential of Spirulina. *Curr Pharma Biotechnol*. **2005**, 6, 5, 373–379

Knuckey, R. M.; Brown, M. R.; Robert, R.; Frampton, D. M. F. Production of microalgal concentrates by flocculation and their assessment as aquaculture feeds. *Aquacult Eng*. **2006**, 35, 300–313

Konno, H. Settling and coagulation of slender type diatoms. *Wat. Sci. Tech.*, **1993**, 27, 11, 231

Langelier, W. F. The analytical control of anticorrosion water treatment. *J. AWWA*, **1936**, 28, 1500-1521

Larsen, K.; Bechgaard, K.; Stipp, S. L. S. The Effect of the Ca<sup>2+</sup>:CO<sub>3</sub><sup>2-</sup> Activity Ratio on Spiral Growth at the Calcite {10-14} Surface. *Geochem. Cosmochim. Acta*. **2010**, 74, 7, 2099-2109

Lawrence, C. H. Lime-soda sludge recirculation experiments at Vandenberg air force base. *J. Am. Water Works Assoc*. **1963**, 55, 2, 177

Lebron, I.; Suarez, D. L. Calcite Nucleation and Precipitation Kinetics as Affected by Dissolved Organic Matter at 25°C and pH>7.5. *Geochem. Cosmochim. Acta*. **1996**, 60, 15, 2765-2776

Lee, A.; Lewis, D.; Ashman, P. Microbial flocculation, a potentially low-cost harvesting technique for marine microalgae for the production of biodiesel. *J Appl Phycol* 2009, 21, 5, 559-567

- Lee, S.; Kim, S.; Kim, J.; Kwon, G.; Yoon, B.; Oh, H. Effects of harvesting method and growth stage on the flocculation of the green alga *Botryococcus braunii*. *Lett Appl Microbiol.* **1998**, 27, 14–28
- Leentvaar, J.; Rebhun, M. Effect of magnesium and calcium precipitation on coagulation-flocculation with lime. *Water Res.* **1982**, 16, 5, 665-662
- Lehninger, A. L. Biochemistry: The Molecular Basis of cell structure and Function. The John Hopkins University, Worth Publishers, Inc. New York, **1970**, 67-75
- Li, H. B.; Chen, F.; Zhang, T. Y.; Yang, F. Q.; Xu, G. Q. Preparative isolation and purification of lutein from the microalga *Chlorella vulgaris* by high-speed counter-current chromatography. *J. Chromatogr A.* **2001**, 905, 151–155.
- Liao, M. Y.; Randtke, S. J. Removing fulvic acid by lime softening. *J. Am. Water Works Assoc.* **1985**, 77, 8, 78-88
- Lin, Y. P.; Singer, P. C.; Aiken, G. R. Inhibition of calcite precipitation by natural organic material: Kinetics, mechanism, and thermodynamics. *Environ. Sci. Technol.* **2005**, 39, 17, 6420-6428
- Liu, S. T.; Nancollas, G. H. The crystallization of magnesium hydroxide. *Desalination.* **1973**, 12, 75–84
- Lopez, O.; Zuddas, P.; Faivre, D. The influence of temperature and seawater composition on calcite crystals growth mechanisms and kinetics: implications for Mg incorporation in calcite lattice. *Geochim. Cosmochim. Acta.* **2009**, 73, 2, 337-347
- Lowenstam, H. A. Minerals formed by organisms. *Science.* **1981**, 11, 4487, 1126-1131
- Mandal, S.; Mallick, N. Microalga *Scenedesmus obliquus* as a potential source for biodiesel production. *Appl. Microbiol. Biotechnol.* **2009**, 84, 2, 281-291
- McCausland, M. A.; Brown, M. R.; Barrett, S. M.; Diemar, J. A.; Heasman, M. P. Evaluation of live microalgae and microbial pastes as supplementary food for juvenile Pacific oyster (*Crassostrea gigas*). *Aquaculture.* **1999**, 174, 323–342
- McLaughlin, W. J.; White, J. L.; Hem, S. L. Heterocoagulation in magnesium hydroxide and aluminum hydroxycarbonate suspensions. *J. Colloid Interface Sci.* **1993**, 157, 113-123

- Mercer, K. L.; Lin, Y. P.; Singer, P. C. Enhancing Calcium Carbonate Precipitation by Heterogeneous Nucleation during Chemical Softening. *J. Am. Water Works Assoc.* **2005**, 97, 12, 116-125
- Myasnikov, S. K.; Chipryakova, A. P.; Kulov, N. N. Kinetics, Energy Characteristics, and Intensification of Crystallization Processes in Chemical Precipitation of Hardness Ions. *Theor. Found. Chem. Eng.* **2013**, 47, 5, 505–523
- Myklestad, S. M. Release of extracellular products by phytoplankton with special emphasis on polysaccharides. *Sci. Total Environ.* **1995**, 165, 1-3, 155–164
- Nancollas, G. H.; Reddy, M. M. The Crystallization of Calcium Carbonate II. Calcite Growth Mechanism. *Journal of Colloid and Interface Science*, **1971**, 37, 4, 824-830
- Nehrke, G.; Reichart, G.J.; Van Cappellen, P.; Meile, C. Bijma, J. Dependence of calcite growth rate and Sr partitioning on solution stoichiometry: non-Kossel crystal growth. *Geochim. Cosmochim. Acta.* **2007**, 71, 9, 2240–2249
- Nielsen, A. E. Electrolyte Crystal Growth. *J. Crystal Growth.* **1984**, 67, 2, 289–310.
- Nilsson, O.; Sternbeck, J. A mechanistic model for calcite crystal growth using surface speciation. *Geochim. Cosmochim. Acta.* **1999**, 63, 2, 217-225
- Northcote, D.; Goulding, K.; Horne, R. The composition and structure of the cell wall of *Chlorella pyrenoidosa*. *Biochem. J.* **1958**, 70, 391-397
- Obst, M.; Wehrli, B.; Dittrich, M. CaCO<sub>3</sub> nucleation by cyanobacteria: laboratory evidence for a passive, surface-induced mechanism. *Geobiology.* **2009**, 7, 3, 324-347
- Ogino, T.; Suzuki, T.; Sawada, K. The Formation and Transformation Mechanism of Calcium Carbonate in Water. *Geochim. Cosmochim. Acta.* **1987**, 51, 10, 2757-2767
- Ogino, T.; Suzuki, T.; Sawada, K. The rate and mechanism of polymorphic transformation of calcium carbonate in water. *J. Cryst. Growth*, **1990**, 100, 1-2, 159-167
- Ometto, F.; Pozza, C.; Whitton, R.; Smyth, B.; Torres, A. G.; Henderson, R. K.; Jarvis, P.; Jefferson, B.; Villa, R. The impacts of replacing air bubbles with microspheres for the clarification of algae from low cell-density culture. *Water res.* **2014**, 53, 15, 168-179.
- Pagnanelli, F.; Papini, M. P.; Trifoni, M.; Toro, L.; Veglio, F. Biosorption of metals ions on *Arthrobacter* sp.: biomass characterization and biosorption modeling. *Environ Sci. Technol.* **2000**, 34, 2773-2778

- Papazi, A.; Makridis, P.; Divanach, P. Harvesting *Chlorella minutissima* using cell coagulants. *J. Appl Phycol.* **2010**, 22, 3, 349–355
- Parks, G. A. Aqueous surface chemistry of oxides and complex oxide minerals. Isoelectric point and zero point of charge: in Equilibrium Concepts in Natural Water Systems. *Adv. Chem. Ser.* **1967**, 67, 121-160
- Phoochinda, W.; White, D. A. Removal of algae using froth flotation. *Environ. Technol.* **2003**, 24, 1, 87–96.
- Pieterse, A. J. H.; Cloot, A. Algal cells and coagulation, flocculation and sedimentation processes. *Water Sci. and Technol.* **1997**, 36, 4, 111-118
- Pivokonsky, M.; Kloucek, O.; Pivokonska, L. Evaluation of the production, composition and aluminium and iron complexation of algogenic organic matter. *Water Res.* **2006**, 40, 2, 3045-3052
- Plant, L. J.; House, W. A. Precipitation of calcite in the presence of inorganic phosphate. *Colloids Surf. A: Physicochem. Eng. Aspects.* **2002**, 203, 1-3, 143-153
- Plummer, J. D.; Edzwald, J. K. Effect of ozone on algae as precursors for trihalomethane and haloacetic acid production. *Environ. Sci. Technol.* **2001**, 35, 18, 3661–3668.
- Pontoni, D.; Bolze, J.; Dingenouts, N.; Narayanan, T.; Ballauff, M. Crystallization of Calcium Carbonate Observed In-situ by Combined Small- and Wide-angle X-ray Scattering. *J. Phys. Chem. B.* **2003**, 107, 22, 5123–5125
- Radha, A. V.; Forbes, T. Z.; Killian, C.E.; Gilbert, P. U. P. A.; Navrotsky, A. Transformation and crystallization energetics of synthetic and biogenic amorphous calcium carbonate. *Proc Natl Acad Sci USA.* **2010**, 107, 16438-16443
- Reddy, M. M.; Nancollas, G. H. The crystallization of calcium carbonate. IV. The effect of magnesium, strontium and sulfate ions. *J. Crystal Growth.* **1976**, 35, 33-38
- Reddy, M. M. Carbonate precipitation in Pyramid Lake, Nevada. In: Amjad Z, ed. Mineral Scale Formation and Inhibition, New York: Plenum, **1995**, p.21-32
- Reeder, R. J. Crystal chemistry of the rhombohedral carbonates. *Rev. Mineral.* **1983**, 11, 1-47

- Rodriguez-Blanco, J. D.; Shaw, S.; Benning, L. G. The Kinetics and Mechanisms of Amorphous Calcium Carbonate (ACC) Crystallization to Calcite, via Vaterite. *Nanoscale*. **2011**, 3, 1, 265-271
- Ruiz-Agudo, E.; Putnis, C. V.; Rodriguez-Navarro, C.; Putnis, A. Effect of pH on Calcite Growth at Constant  $a_{\text{Ca}^{2+}}/a_{\text{CO}_3^{2-}}$  Ratio and Supersaturation. *Geochim. Cosmochim. Acta*. **2011**, 75, 1, 284-296
- Russell, C. G.; Lawler, D. F.; Speitel, G. E. Jr.; Katz, L. E. Effect of softening precipitate composition and surface characteristics on natural organic matter adsorption. *Environ Sci Technol*. **2009**, 43, 20, 7837-7842
- Salim, S.; Bosma, R.; Vermuë, M. H. Harvesting of microalgae by bio-flocculation. *J. Appl Phycol*. **2011**, 23, 5, 849–855
- Schlomach, J.; Quarch, K.; Kind, M. Investigation of precipitation of calcium carbonate at high supersaturations. *Chem Eng Technol*. **2006**, 29, 2, 215-220
- Schmidt, W.; Hamsch, B.; Petzoldt, H. Classification of algogenic organic matter concerning its contribution to the bacterial regrowth potential and byproducts formation. *Water Sci. Technol*. **1998**, 37, 2, 91–96
- Selck, H.; Decho, A. W.; Forbes, V. E. Effects of chronic metal exposure and sediment organic matter on digestive absorption efficiency of cadmium by the deposit-feeding polychaete *Capitella species* I. *Environ. Toxicol. Chem*. **1999**, 18, 6, 1289-97
- Semerjian, L.; Ayoub, G. M. High pH-magnesium coagulation-flocculation in wastewater treatment. *Adv Environ Res*. **2003**, 7, 389-403
- Shelef, G.; Sukenik, A.; Green, M. Microalgae harvesting and processing: a literature review. Technion Research and Development Foundation Ltd. Haifa, Israel, **1984**.
- Smyth, J. R.; Ahrens, T. J. The crystal structure of calcite (III). *Geophys. Res. Lett*. **1997**, 24, 1595-1598
- Spilling, K.; Seppälä, J.; Tamminen, T. Inducing autoflocculation in the diatom *Phaeodactylum tricornutum* through CO<sub>2</sub> regulation. *J Appl Phycol*. **2011**, 23, 959-966
- Stabel H. H. Calcite precipitation in Lake Constance: Chemical equilibrium, sedimentation, and nucleation by algae. *Limnol. Oceanogr*. **1986**, 31, 5, 1081-1093
- Stipp, S. L. S. Toward a conceptual model of the calcite surface: hydration, hydrolysis, and surface potential. *Geochim. Cosmochim. Acta*. **1999**, 63, 19-20, 3121-3131

Stumm, W.; Morgan, J. J. Aquatic Chemistry: Chemical equilibrium and rates in natural waters. 3rd Ed.; John Wiley & Sons, New York, **1996**.

Stumm, W.; O'Melia, C. R. Stoichiometry of coagulation. *Amer. Water Works Assoc.* **1968**, 60, 5, 514-539

Suffet, I. H.; Mallevalle, J.; Kawczynski, E. Advances in Taste-and-Odor Treatment and Control. Cooperative Research Reports, AWWA Research Foundation, **1995**, Denver, CO, USA.

Sverjensky, D. A. Prediction of the speciation of alkaline earths adsorbed on mineral surfaces in salt solutions. *Geochim. Cosmochim. Acta.* **2006**, 70, 10, 2427–2453

Tai, C. Y.; Chen, F. B. Polymorphism of CaCO<sub>3</sub>, Precipitated in a constant-composition environment, *AIChE Journal*, **1998**, 44, 8, 1790-1798

Teng, H. H.; Dove, P. M.; DeYoreo, J. J. Kinetics of calcite growth: surface processes and relationships to macroscopic rate laws. *Geochim. Cosmochim. Acta.* **2000**, 64, 13, 2255–2266

Tenney, M. W.; Echelberger, W. F. Jr.; Schuessler, R. G.; Pavoni, J. L. Algae flocculation with synthetic organic polyelectrolytes. *J. Appl. Microb.* **1969**, 18, 965-971

Tenney, M. W.; Stumm, W. Chemical flocculation of microorganisms in biological waste treatment. *J. Water Pollut. Control Fed.* **1965**, 37, 10, 1370-1388

Thompson, J. B.; Ferris, F. G. Cyanobacterial precipitation of gypsum, calcite, and magnesite from natural alkaline lake water. *Geology*, **1990**, 18, 995–998

Toms, I. P.; Owens, M.; Hall, J. A. Observations on the performance of polishing lagoons at a large regional works. *Wat. Pollut. Contr.* **1975**, 74, 4, 383-401

Trujillo, E. M.; Jeffers, T. H.; Ferguson, C.; Stevenson, H. Q. Mathematically modeling the removal of heavy metals from wastewater using immobilized biomass. *Environ. Sci. Technol.* **1991**, 25, 9, 1559-1565

Tsezos, M.; Noh, S. H.; Baird, M. H. I. A batch reactor mass transfer kinetic model for immobilized biomass biosorption. *Biotechnol Bioeng.* **1988**, 32, 4, 545-553

Turek, M.; Gnot, W. Precipitation of magnesium hydroxide from brine. *Ind. Eng. Chem. Res.* **1995**, 34, 1, 244–250

Uduman, N.; Qi, Y.; Danquah, M. K.; Forde, G. M.; Hoadley, A. Dewatering of microalgal cultures: a major bottleneck to algae-based fuels. *J. Renew Sustain Energy*. **2010**, 2, 012701

Vandamme, D.; Pontes, S. C.; Goiris, K.; Foubert, I.; Pinoy, L. J.; Muylaert, K. Evaluation of electro-coagulation-flocculation for harvesting marine and freshwater”, *Biotechnol Bioeng*. **2011**, 108 10, 2320-2329

Vandamme, D.; Foubert, I.; Fraeye, I.; Meesschaert, B.; Muylaert, K. Flocculation of *Chlorella vulgaris* induced by high pH: role of magnesium and calcium and practical implications. *Bioresour Technol*. **2012**, 105, 114-119

Vandamme, D.; Foubert, I.; Muylaert, K. Flocculation as a Low-Cost Method for Harvesting Microalgae for Bulk Biomass Production. *Trends Biotechnol*. **2013**, 31, 4, 233-239

Van Lith, Y.; Warthmann, R.; Vasconcelos, C.; McKenzie, J. A. Microbial fossilization in carbonate sediments: A result of the bacterial surface involvement in carbonate precipitation. *Sedimentology*, **2003**, 50, 2, 237-245

Van Vuuren, L. R. J.; Stander, G. J.; Henzen, M. R.; Meiring, P. G. J.; van Blerk, S. H. V. Advanced purification of sewage works effluent using a combined system of lime softening and flotation. *Water res*. **1967**, 1, 7, 463-466

Vasudevan, V.; Stratton, R. W.; Pearlson, M. N.; Jersey, G. R.; Beyene, A. G.; Weissman, J. C. Environmental Performance of Algal Biofuel Technology Options. *Environ. Sci. Technol*. **2012**, 46, 2451-2459

Verwey, E. J. W.; Overbeek, J. Th. G. Theory of the stability of lyophobic colloids. Elsevier, New York, **1947**

Wang, P.; Li, C.; Gong, H.; Wang, H.; Liu, J. Morphology control and growth mechanism of magnesium hydroxide nanoparticles via a simple wet precipitation method. *Ceramics International*. **2011**, 37, 3365-3370

Wiechers, H. N. S.; Sturrock, P.; Marais, G. V. R. Calcium Carbonate Crystallization Kinetics. *Water Research*. **1975**, 9, 9, 835-845

Wolthers, M.; Charlet, L.; Van Cappellen, P. V. The surface chemistry of divalent metal carbonate minerals; a critical assessment of surface charge and potential data using the charge distribution multi-site ion complexation model. *Am. J. Sci*. **2008**, 308, 905-941

Wu, Z.; Zhu, Y.; Huang, W.; Zhang, C.; Li, T.; Zhang, Y.; Li, A. Evaluation of flocculation induced by pH increase for harvesting microalgae and reuse of flocculated medium. *Biosource Tech.* **2012**, 110, 496-502

Wyatt, N. B.; Gloe, L. M.; Brady, P. V.; Hewson, J. C.; Grillet, A. M.; Hankins, M. G.; Pohl, P. I. Critical conditions for ferric chloride-induced flocculation of freshwater algae. *Biotechnol Bioeng.* **2012**, 109, 2, 493-501

Xu, M.; Higgins, S. R. Effect of magnesium ions on near equilibrium calcite dissolution: step kinetics and morphology. *Geochim. Cosmochim. Acta.* **2011**, 75, 719-733

Yun, Y. S.; Lee, S. B.; Park, J. M.; Lee, C. I.; Yang, J. W. Carbon dioxide fixation by algal cultivation using wastewater. *J. Chem. Technol. Biotechnol.* **1997**, 69, 451-455

Zeppenfeld, K. Calcite Precipitation from Aqueous Solutions with Different Calcium and Hydrogen Carbonate Concentrations. *J. Water Supply Res. Technol.* **2010**, 59, 482-491.

Zhang, Y.P.; Dawe, R. The kinetics of calcite precipitation from a high salinity. *Water. Appl. Geochem.* **1998**, 13, 177-184

Zamalloa, C.; Vulstekeb, E.; Albrechtb, E.; Verstraete, W. The techno-economic potential of renewable energy through the anaerobic digestion of microalgae. *Bioresource Tech.* **2011**, 102, 2, 1149-1158

Zuddas, P.; Mucci, A. Kinetics of calcite precipitation from seawater: II. The influence of the ionic strength. *Geochem. Cosmochim. Acta.* **1998**, 62, 5, 757-766

Zuddas, P.; Pachana, K.; Faivre, D. The influence of dissolved humic acids on the kinetics of calcite precipitation from seawater solutions. *Chemical Geology.* **2003**, 201, 1-2, 91-101

## **Vita**

JIN-YONG CHOI was born in Seoul, Republic of Korea, the son of Dr. Sikyung Choi and Hosook Oh. He finished his military service as an Artillery M.O.S. in Chulwon, Korea in February 2003 and graduated from INHA University in Incheon, Korea in August 2006 as an Environmental Engineer. In December 2009, he received a Master of Science in Engineering degree in Environmental and Water Resources Engineering at The University of Texas at Austin. He continued his education in the doctoral program in the department of Civil, Architectural and Environmental Engineering at The University of Texas at Austin.

Permanent Email Address: [jinyong.choi80@gmail.com](mailto:jinyong.choi80@gmail.com)

This dissertation was typed by the author.